ISSN Print: 2518-4245
ISSN Online: 2518-4253
Vol. 55(3), September 2018

PROCEEDINGS
OF THE PAKISTAN ACADEMY OF SCIENCES:
A. Physical and Computational Sciences

PAKISTAN ACADEMY OF SCIENCES
ISLAMABAD, PAKISTAN

PAKISTAN ACADEMY OF SCIENCES

Founded 1953

Proceedings of the Pakistan Academy of Sciences, published since 1964, is quarterly journal of the Academy. It publishes original research papers and reviews in basic and applied sciences. All papers are peer reviewed. Authors are not required to be Fellows or Members of the Academy, or citizens of Pakistan.

Annual Subscription: **Pakistan:** Institutions, Rupees 2000/- ; Individuals, Rupees 1000/-
Other Countries: US$ 100.00 (includes air-lifted overseas delivery)

HEC Recognized, Category Y; PM&DC Recognized

Published by **Pakistan Academy of Sciences**, 3 Constitution Avenue, G-5/2, Islamabad, Pakistan
Tel: 92-5 1-920 7140 & 921 5478; **Fax:** 92-51-920 6770; **Website: www.paspk.org**

Printed at **PanGraphics (Pvt) Ltd.,** No. 1, I & T Centre, G-7/l, Islamabad, Pakistan
Tel: 92-51-220 2272, 220 2449 Fax: 92-51-220 2450 E-mail: pangraph@gmail.com

PROCEEDINGS
OF THE PAKISTAN ACADEMY OF SCIENCES:
A. Physical and Computational Sciences

CONTENTS

Volume 55, No. 3, September 2018 **Page**

Submission of Manuscripts: Manuscripts may be submitted as E-mail attachment at editor@paspk.org. Authors must consult the ***Instructions for Authors*** at the end of this issue or at the Website: www.paspk.org

Proceedings of the Pakistan Academy of Sciences:
A. Physical and Computational Sciences 55 (3): 01–09 (2018)

ISSN: 2518-4245 (print), 2518-4253 (online)

Pakistan Academy of Sciences

Case Study

Case Study of Detailed Settlement Analysis of an Old Residential Building within Lahore Fort, Pakistan

Ehtesham Mehmood[1], Khawaja Adeel Tariq[2*], Safeer Ullah Khan[1], and Ammar Raza[1]

[1]Department of Civil Engineering, University of Engineering & Technology, Lahore
[2]Department of Civil Engineering, Chenab College of Engineering and Technology, Gujranwala

Abstract: This study deals with settlement analysis of a single story old residential building constructed inside the Lahore fort, Pakistan. It was constructed on non-engineering fill and it exhibited major differential settlement. The building started to exhibit cracking and was rendered unserviceable in 2009. The building has to be demolished for the new proposed structure. Crack mapping was performed to get an idea about the prevailing structural condition of the building. Precise leveling was carried out to determine the exact amount of differential settlement in various parts of the building and its surrounding area. Soil investigation was carried out to determine the depth of the non-engineering fill and any other factors that contributed to the excessive settlement of the building. The engineering properties of the associated soil samples were determined. Finite element analysis was carried out using computer aided software to suggest different foundation solutions for the site. A cost analysis was also carried out for the decided remedy.

Keywords: Settlement, Soil investigation, Non-engineering fill, Foundation, Shear cracks, Lahore Fort-Pakistan

1. INTRODUCTION

The work presented in this research paper originates from an investigation of a building undergoing excessive settlement and being rendered unserviceable. This building is situated inside a historical fort, located in the most elevated region in the city of Lahore, Pakistan. The reason for its elevation is due to the succeeding empires which were building their strongholds right above the ruins of their predecessors without clearing the area. It has resulted in construction of buildings over a non-engineering fill. The investigated building exhibits numerous shear cracks and visible deformations. Similarly, a considerable number of buildings in the region have undergone significant differential settlement, and some of these even had to be demolished.

An early assessment made during the initial visual inspection at the site has concluded that the underlying soil and drainage issues were the primary causes of settlement in the building. This assessment was further supported by the fact that the massive structure surrounding the building, the Lahore Fort, had not undergone any similar settlement or deformations due to having deep foundations that are beyond the depth of the non-engineering fill. Researchers have proposed methods for assessment of vertical deformation of the structures. The settlement can be estimated using probabilistic approach [1], laboratory experiments [2] or by using numerical approaches. The settlement data obtained from the leveling equipments can be used to plot 2D or 3D displacement maps [3]. Geodetic leveling is considered as one of the techniques for investigationg the vertical deformation of the structures. This technique was used for monitoting of vertical deformation at Arenoso dam [4]. The subsidence of Cathedral and the Ghirlandina Tower at UNESCO site of Modena was also monitored with conventional leveling techniques [5]. The procedure used in this study was based on the actual measurement of settlement using survey equipments.

The scope of this study is to determine the extent of settlement throughout the building by leveling and ascertain the causes of said settlement by drilling three boreholes at strategic locations.

Received: November 2017; Accepted: September 2018
* Corresponding Author: Khawaja Adeel Tariq; khawajaadeel@hotmail.com

The field and laboratory tests were performed to propose the most viable solution of the site for future construction.

2. MATERIALS AND METHODS

2.1 Project Description

The residential building is a single story masonry structure of dimensions 64 x 11m, with an additional 3m of verandas going along the length of the building on both sides. The building has been constructed using standard 229 x 114 x 75mm bricks. The layout of the building, as well as the location of each borehole drilled for the investigation, is given in Fig. 1.

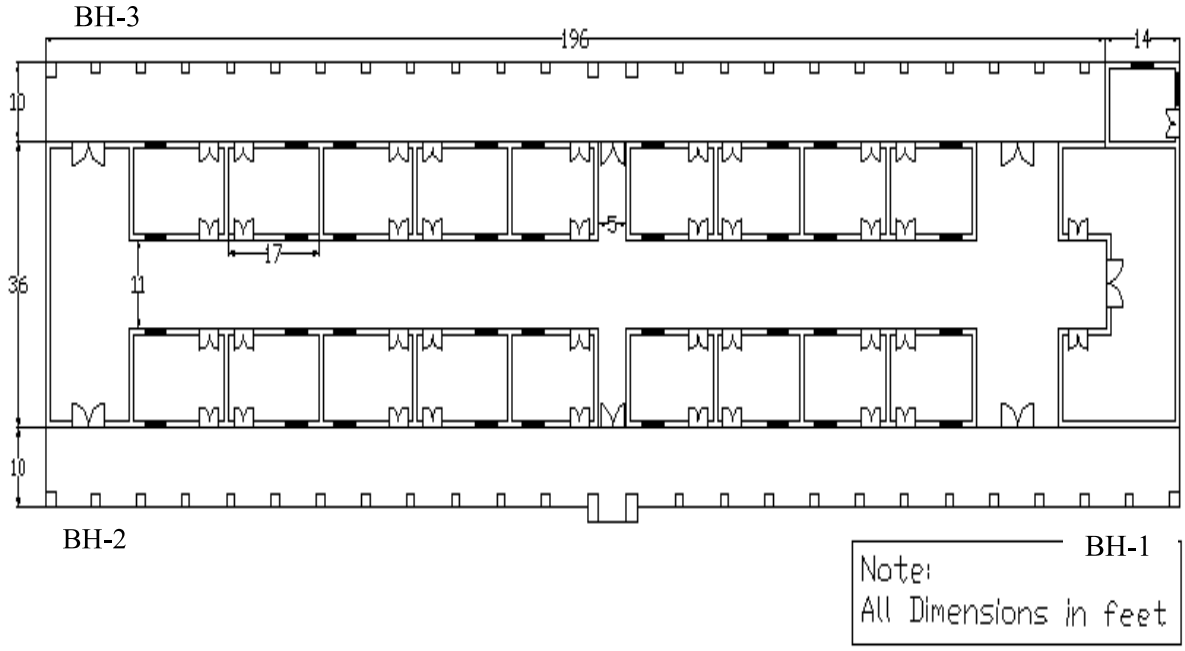

Fig. 1. Building layout

Very little information about the building in question could be found and it was discovered that 1.2m wide and 1.2m deep stepped brick foundation with the concrete slab at the base of the foundation was used. The building was constructed in 1994. Cracking started to be observed in 2001, however it was ignored until 2005, when a huge Earthquake struck Pakistan. After that, the North East half of the building was abandoned but the remaining portion of the building was in use. By 2009, the severe cracking and deformations in the building resulted in jamming of the doors, and the entire building was rendered unserviceable.

2.2 Crack Measurements

Initially, the numerous shear cracks in walls across the building were examined and their features were noted as shown in Fig. 2 and Fig. 3. The cracks on the inside face of the walls were of greater severity as compared to those on the exterior face. The width of the cracks on the exterior side was observed as less than 25mm, whereas majority of the interior cracks easily fall within the range of 50-75mm width.

Fig. 2. View of Exterior cracks

Fig. 3. View of Interior cracks

Fig. 4. View of Brick column

Additionally, the cracks angles were in the ranges between 45-60°. The residents of the building had erected several brick columns throughout the structure in order to prevent it from collapse or further damage. None of these columns served any structural purpose as they were not rigidly connected to the building and no loads or moments were being transferred to them from the building. Such actions of the residents only resulted in additional loads acting on the foundation. One of the columns mentioned above can be seen in Fig. 4.

2.3 Settlement Measurements

Leveling was performed on the site throughout a grid comprising of nearly two hundred points, as shown in Fig. 5. The precise leveling staff offers a least count of 0.1mm in comparison to the 5mm least count of an ordinary leveling staff. Therefore, it was intended to perform precise leveling throughout the grid in order to obtain more accurate results. Unfortunately, the ceiling height of the roofed porches, also known as verandas, on both sides of the building was 2.5m, which was not sufficient enough for the 3m precise leveling staff to be vertically fit. Due to this limitation in the equipment, precise leveling was only performed on the exterior perimeter of the building, while ordinary leveling was done in the verandas.

The rise and fall method was employed throughout the entire grid. In this method, the difference in elevation is determined by comparing each forward staff reading with each preceding staff reading. A rise is said to have occurred if the forward reading is lesser in value than the preceding reading, and a fall occurs if the forward reading is greater in value than the preceding reading. These rises and falls are then added to a Reduced Level (RL). The results obtained from the leveling of the building site were then entered into MATLAB to create a 3-D model of the settlement the building, that can be seen in Fig. 6. It can be seen that the building has undergone massive differential settlement.

The results of the leveling confirmed the initial estimation of the building's settlement lying within the range of 0.3m. However, one portion in the corner of the building had undergone excessive settlement to about 0.6m. The reason for such an anomaly was discovered to be a running cracked sewer line beneath that portion. The seeping water has washed away soil particles, resulted in collapse of the soil beneath the structure. The settlement problem resulting from groundwater extraction in city of Bologna was also reported [6]

2.4 Soil Investigation

Standard Penetration Test was performed into the drilled boreholes according to ASTM specifications [7]. Standard Penetration Test is the most practiced soil investigation method in Pakistan because it is the most economical method. Furthermore, the number of blows (N) against standard penetration can be used in empirical relations [8] to estimate soil properties such as expected settlement and bearing capacity.

Three boreholdes were drilled at selective areas. The first hole was drilled in area having noticeable

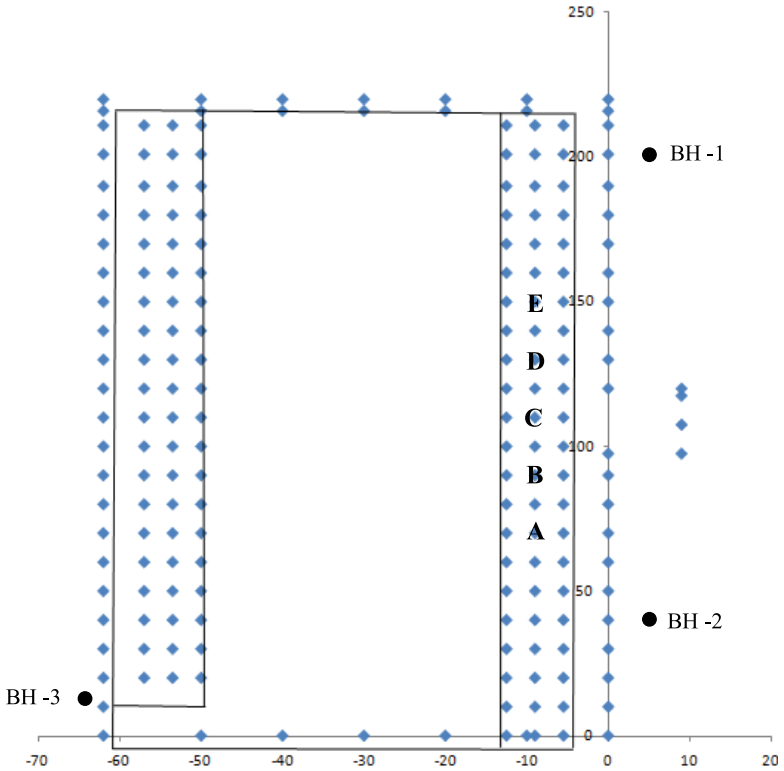

Fig. 5. Surveying grid (ft) showing location of Bore Holes (BH)

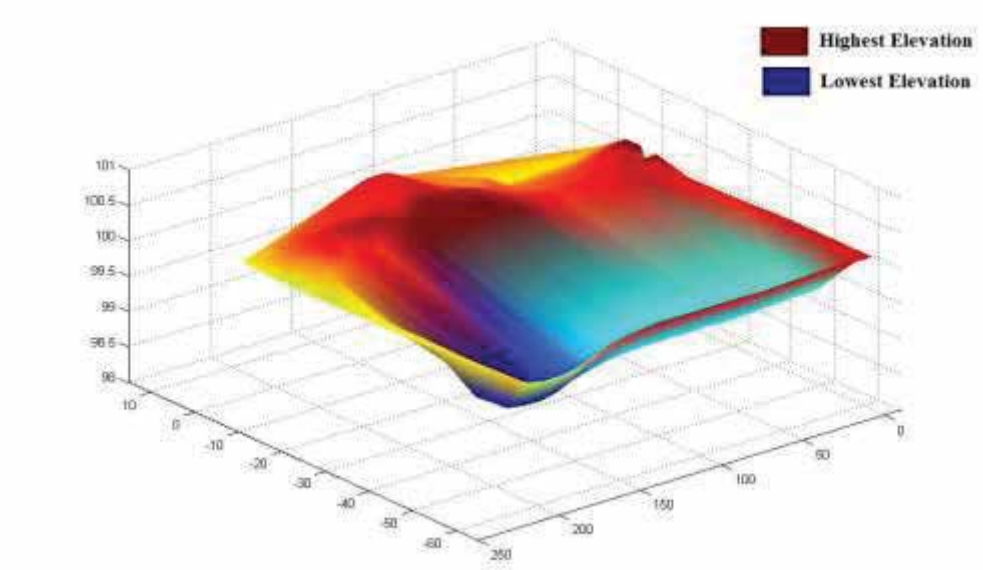

Fig. 6. 3-D Settlement model (ft)

average settlement, and the second where the soil seemed to have heaved outwards. The third borehole was drilled in area where execessive settlement had occurred. Each borehole was drilled up to a depth of 9m, and the number of blows (N) was recorded and soil samples were also collected. The N values obtained by the Standard Penetration Test had to be discarded as false values were obtained due to the interference of the non-engineering fill. The presence of multiple layers of brick ballast in the soil strata resulted in an outrageous number of blows. Images of the samples obtained from bore holes can be seen in Fig. 7. The borehole log of BH-3 is shown in Fig. 8.

(a) (b)

Fig. 7. Soil Sample obtained from BH-3 at (a) 1.8m and (b) 7.6m depth

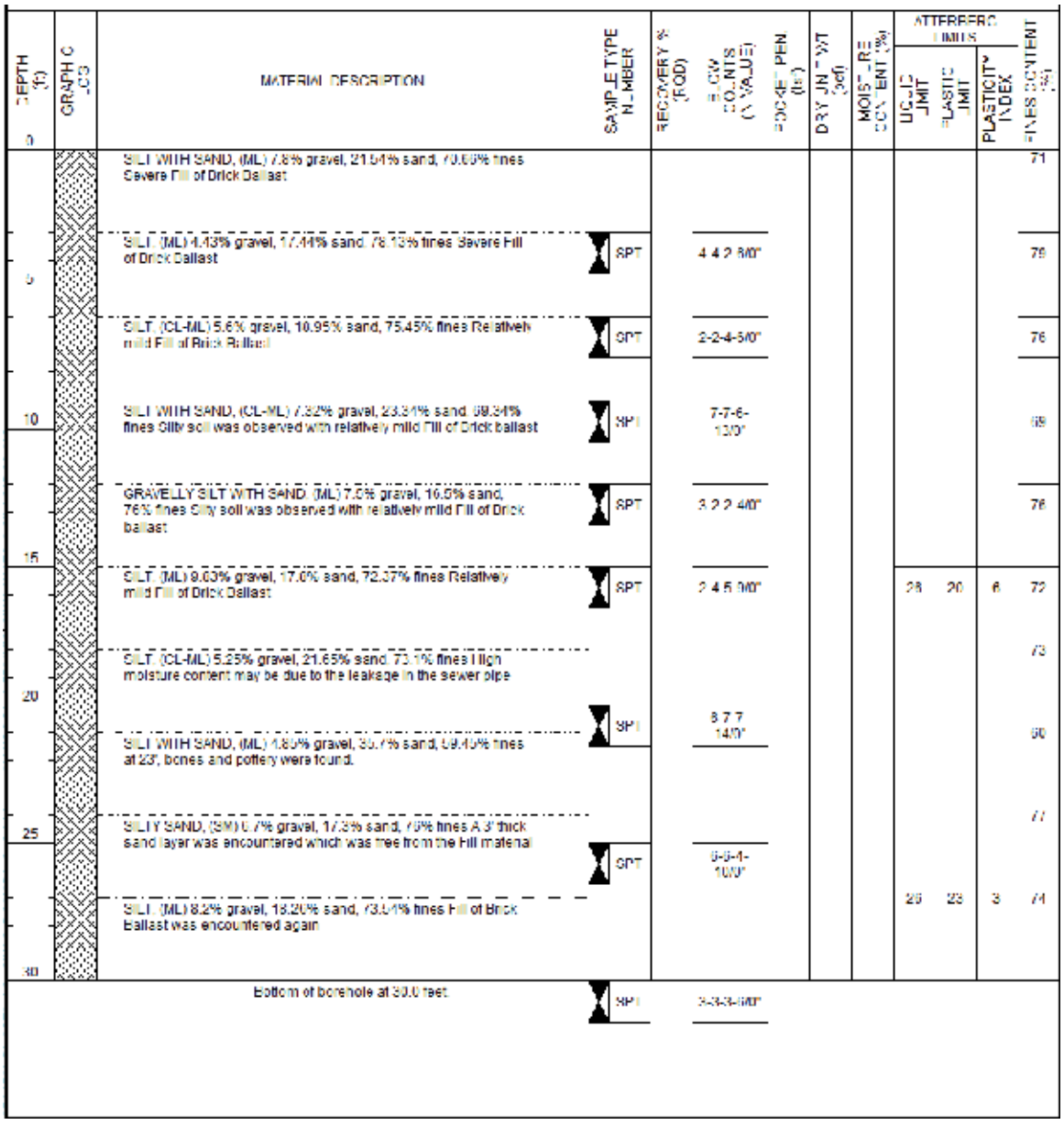

Fig. 8. Borehole log, BH-3

2.5 Soil Testing

The soil samples obtained from the boreholes were taken to the laboratory for testing. From each borehole, samples were used from the depths of 4.5m and 9.0m. The soil samples taken to the laboratory were pulverized, dried and then placed in separate containers for the different types of testing, such as particle size analysis, Atterburg limits [10], shear strength parameters First of all, each of the soil samples was put through sieve analysis to ascertain the particle size distribution. This was carried out according to ASTM procedure [9] as shown in Fig. 9. The Atterberg limits [10] of the soil (the Liquid Limits and Plastic Limits) of the soil were measured using ASTM- D4381 method and samples are given in Table 1. Increasing trend with depth was in general observed in laboaratory estimated values for liquid limit, plastic limit and plasticity index. The collected soil samples were classified in accordance with the [11] specifications and are shown in Table 2. Th soil samples are mostly classified as low plastic clay and silty sand.

Direct Shear test was performed on the soil samples in both saturated and dry conditions in order to determine their shear strength parameters (soil cohesion 'C' and their angle of internal friction 'f'). This test was also performed according to standard [12] specifications and the results are given in Table 3. The soil samples exhibits little to no cohesion with average angle of internal friction as 31 degrees.

Table 1. Atterberg limits (ASTM-D4381 Method)

Borehole	Depth m	Liquid Limit %	Plastic Limit %	Plasticity Index %
1	4.5	24.99	9.75	15.24
	9	33.27	10.1	23.17
2	4.5	29.78	13	16.78
	9	31.77	12.5	19.27
3	4.5	26.29	20	6.29
	9	25.56	22.98	2.58

Table 2. USCS Soil Classification (ASTM-D2487 Method)

Borehole	Depth m	USCS Classification
1	4.5	CL
	9	CL
2	4.5	CL
	9	CL
3	4.5	CL-ML
	9	ML

3. RESULTS

The finite element analysis was carried out on GeoStudio. The non-engineering fill was a heterogeneous material and the soil properties were not evenly distributed throughout it. Therefore, the average of the determined soil parameters were used. The empirical relations based on modulus elasticity were used for determination of unknown parameters. Linear Elastic model is used to model the soil behavior. The parameters used for analysis of original soil consist of C = 0, $\phi = 30°$, $\gamma = 14$ kN/m^3 and Elastic Modulus = 5MPa The simulations were run on the software to recreate the settlement in the range of what the building had undergone. For a building load of 25kPa, a settlement of 180mm was produced when an elastic modulus of 5MPa was used. The details of the settlement analysis can be seen in Fig. 10.

It was concluded that the existing soil conditions beneath the surface were insufficient for any form of

Table 3. Soil shear strength analysis (ASTM-D3080 Method)

Borehole	Depth m	Soil Condition	C (kPa)	ϕ (degrees)
1	6	Dry	5.84	30.17
	6	Saturated	0	33.1
	9	Dry	0	42
	9	Saturated	0	32.95
2	4.5	Dry	0	32.8
	4.5	Saturated	3.13	20.26
	9	Dry	0	34.52
	9	Saturated	3.97	12.54
3	4.5	Dry	0	32.28
	4.5	Saturated	0	31.69
	9	Dry	6.90	31.23
	9	Saturated	0	30.8

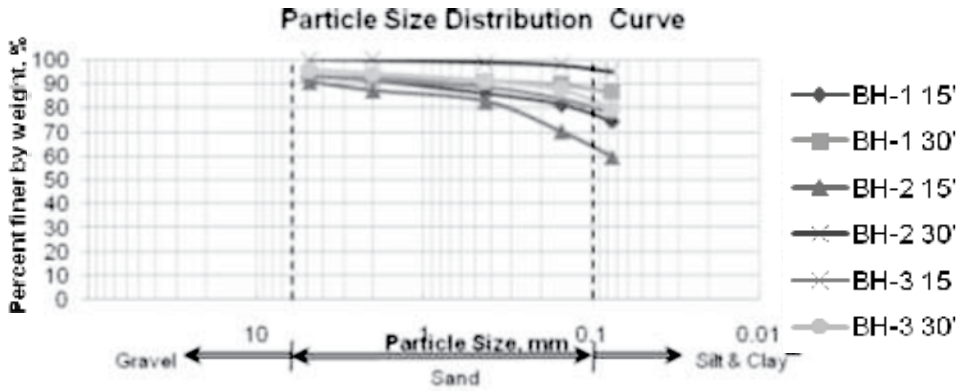

Fig. 9. Sieve analysis of soil samples recovered from boreholes (ASTM-D422-63 method)

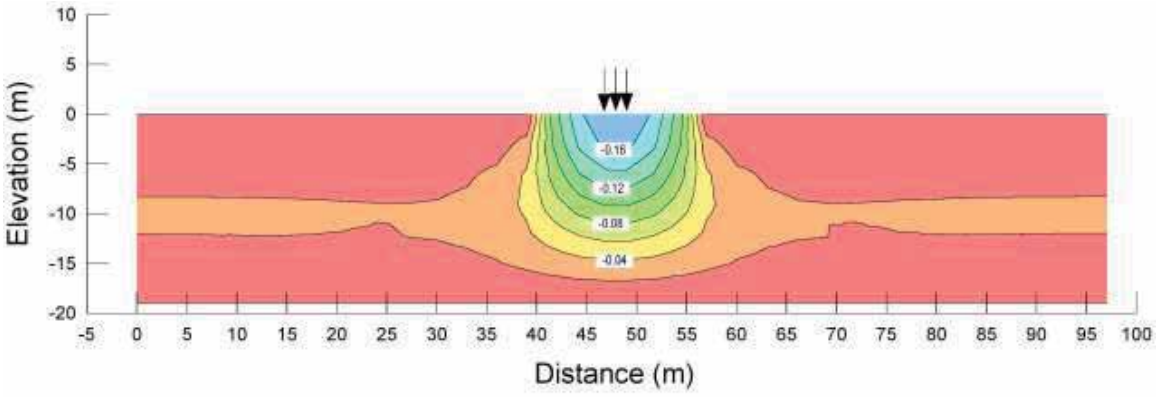

Fig. 10. Settlement analysis for existing soil beneath building

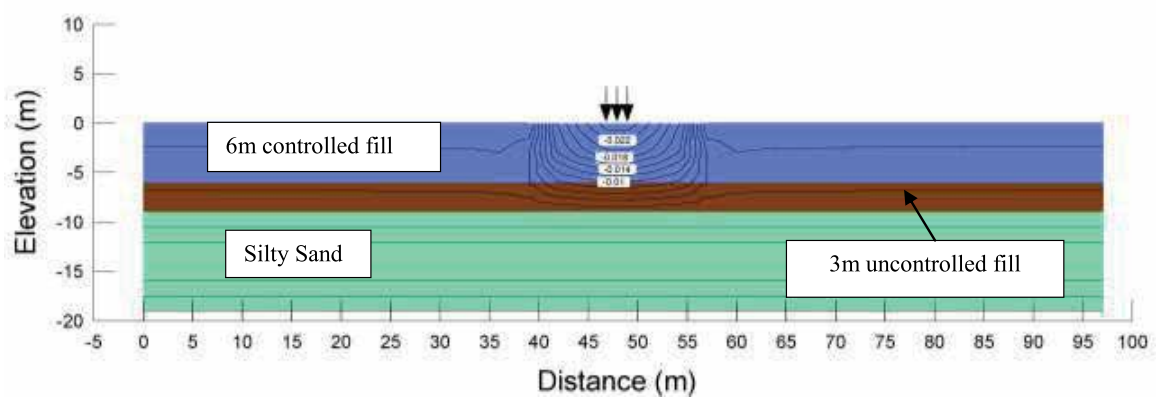

Fig. 11. Settlement analysis with recommended soil replacement of 6 m

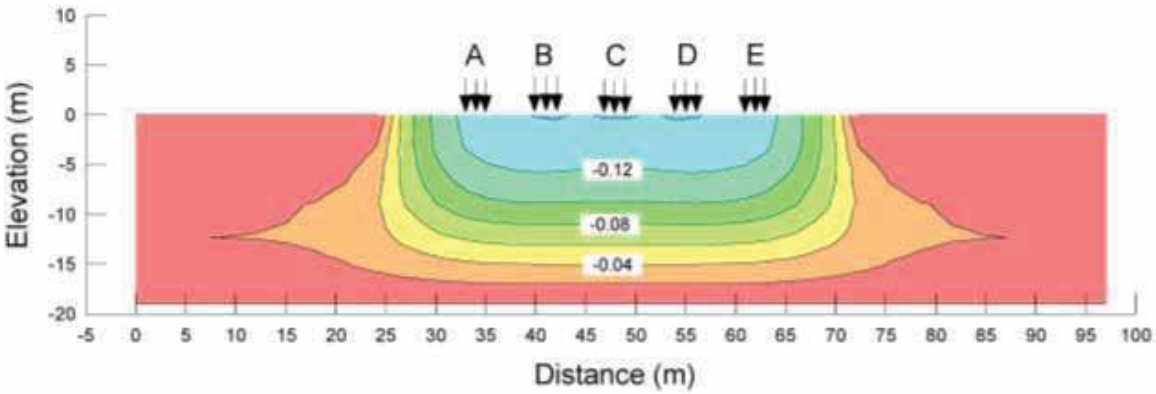

Fig. 12. Settlement analysis of five (5) footings with recommended soil replacement of 6 m

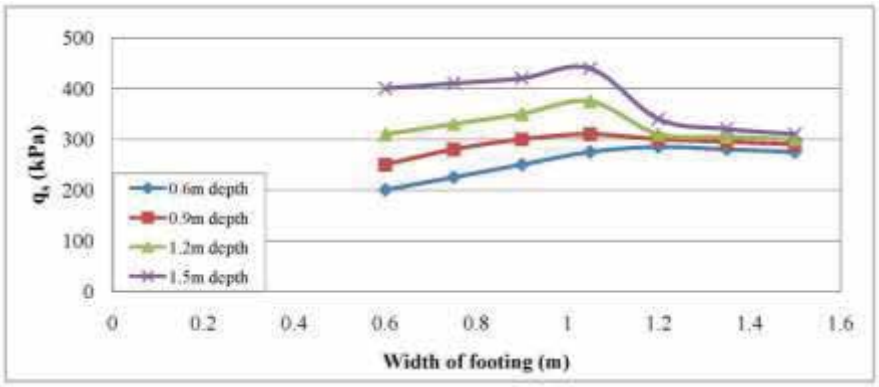

Fig. 13. Bearing capacity curves for soil

Table 5. Settlement comparison (Actual measured and by GeoStudio)

Location*	Settlement (mm)	
	Actual measured	GeoStudio
A	150	132
B	200	129
C	240	125
D	180	130
E	200	131

future construction. The (MRS) market rate systems rates [13] were used to evaluate the economically viable solution (and 1USD = 100PKR). The most economical solution (Table 4) would be to replace the soil beneath its zone of influence having more suitable properties. It would be suitable to use A-3 [14] soil with the properties of C = 0, $\phi = 33°$, $\gamma = 16$ kN/m^3, Elastic Modulus = 8MPa, Permeability = 10^{-5}m/s. The replaced soil should be compacted to 95% according to [15] specifications. The depth of replacement was decided by using GeoStudio, by replacing depths in trial and error until the settlement produced was within an acceptable range of 25mm. In the end, a settlement of 25mm was achieved with soil replacement of 6m as shown in Fig. 11. Buidling has undergone differential settlement. The settlement analysis considering the affect of 5 footings is shown in Fig. 12 and results are compared with actual measured settlement in Table 5. The difference in result is due to hydrogeneity of the problem. Furthermore, detailed manual calculations were also done for development of bearing capacity curves with regards to both shear and settlement [17]. The influence zone of each footing was taken to be four times its width. The bearing capacity curves are given in Fig. 13.

4. CONCLUSION

The historic site are very sensitive for new building construction. The situation becomes critical when excavation has to done adjacent to building of histroical nature. The 6m replacement can be achieved by first constructing soldier piles/ diaphragm wall with tie back anchors along the perimeter of the building to a sufficient depth. Instrumentation and other measures must be used to measure the reponse of the adjacent historic building to vibration, settlement, etc. during construction [16]. It is recommended to use a strip foundation for better and more uniform distribution of the building loads.

5. REFERENCES

1. Bungenstab, F. C. & K.V. Bicalho. Settlement predictions of footings on sands using probabilistic analysis. *Journal of Rock Mechancis and Geotechnical Engineeirng*: doi: 10.1016/j. jrmge.2015.08.009 (2016).
2. Hayashi, H., S. Nishimoto. & T. Yamanashi. Applicability of settlement prediction method to peaty ground. *Soils and Foundations*. doi: 10.1016/j. sandf.2016.01.012 (2016).
3. Jaramillo, R. J., Albea, M. E. & A. M. Morilla. Proposed methodology for measurement, survey and assessment of vertical deformation of structures. *Structural Survey*. doi:10.1108/SS-02-2016-0006 (2016).
4. Lacy, C. M., Ramos, I. M., Gil, J. A., Franco, D. O., Herrera, M. A., Aviles, M., Dominguez, A. & J. C. Chica. Monitoring of vertical deformations by means high-precision geodetic levelling. Test case: The Arenoso dam (South of Spain). *Journal of Applied Geodesy*. doi:10.1515/jag-2016-0034

(2017).
5. Castagnettic, C., Cosentini, M. R., Lancellotta, R. & A. Capra. Geodetic monitoring and geotechnical analyses of subsidence induced settlements of historic structures. *Structual Control Health Monitoring*. doi:10.1002/stc.2030 (2017).
6. Spacagna, L. R., Rasulo, A. & G. Modoni. Geostatistical analysis of settlements induced by groundwater extraction. *International Conference on Computational Science and Its Applications*. doi:10.1007/978-3-319-62401-3_26 (2017).
7. ASTM D1586-11. Standard test method for Standard penetration test (SPT) and Split-Barrel sampling of soils. *American Society for Testing and Materials*, West Conshohocken, Pennsylvania, USA (2011).
8. Bowles, J. *Foundation Analysis and Design*. *5th ed*. McGraw Hill, New York, NY, USA, 1997.
9. ASTM D422-63. Standard method for Particle size analysis of soils. *American Society for Testing and Materials*, West Conshohocken, Pennsylvania, USA (2007).
10. ASTM D4318. Standard test methods for Liquid limit, Plasic limit and Plasticity index of soils. *American Society for Testing and Materials*, West Conshohocken, Pennsylvania, USA (2010).
11. ASTM D2487. Standard Practice for Classification of Soils for Engineering Purposes (Unified Soil Classification System). *American Society for Testing and Materials*, West Conshohocken, Pennsylvania, USA (2011).
12. ASTM D3080. Standard test method for Direct Shear Test of soils under consolidated drained conditions. *American Society for Testing and Materials*, West Conshohocken, Pennsylvania, USA (2011).
13. Market rates system (MRS) bi-annual period. Government of the Punjab Finance Department, Pakistan.
14. ASTM D3282. Standard Practice for Classification of Soils and Soil-Aggregate Mixtures for Highway Construction Purposes. *American Society for Testing and Materials*, West Conshohocken, Pennsylvania, USA (2015).
15. AASHTO T99. Standard Method of Test for Moisture-Density Relations of Soils Using a 2.5-kg (5.5-lb) Rammer and a 305-mm (12-in.) Drop. *American Association of State Highway and Transportation Officials*, Washington, USA (2015).
16. Randl, C. Protecting a historic structure during adjacent construction. *Temporary Protection Number 3*. U.S. Department of the Interior, Hertiage Preservation Services (2001).
17. Meyerhof, G.G. Penetration Test and Bearing Capacity of Cohesionless Soils. *Journal of the Soil Mechanics and Foundation Division*, ASCE, Volume 82, No. SM1, pp. 1-19, (1956).

Proceedings of the Pakistan Academy of Sciences:
A. Physical and Computational Sciences 55 (3): 11–20 (2018)

ISSN: 2518-4245 (print), 2518-4253 (online)

Pakistan Academy of Sciences

Research Article

5G – The Expectations and Enablers

Bushra Naeem[1*], Raza Ali[1], Bilal Shabbir[1], Faisal Khan[1], and Kamran Ali[2]

[1]Department of Telecommunication Engineering, BUITEMS,
Takatu Campus, Quetta
[2]Department of Computer Science, BUITEMS, Takatu Campus, Quetta

Abstract: 5G the fifth generation of mobile communication technology relies on a new network architecture that will be used to overcome the challenges faced in 4G technology. The current 4G Network architecture is unable to cater the increasing data traffic demand with very low latency rate. It is also not able to provide 100% network coverage. 5G technology will enable mobile users to experience the network with almost 100X better network capacity and coverage, very low latency and increased data traffic rates with new multiple radio access technology, improved radio network optimization and resource sharing. This paper provides an overview of key technology enablers that are imperative to ensure the promises of 5G.

Keywords: 5G mobile communication, Wireless communications, Massive MIMO, Heterogeneous networks.

1. INTRODUCTION

While the time is passing at the fastest stride, the newly introduced technologies in recent era have driven a developing consensus that information technologies are affecting the way humans live, work, connect, and establish the routine life together with the working culture [1]. Numerous technologies have modernized the lifestyle of humans in the past decades. The technologies including the manual hand tools, mechanical devices, powered machineries, and automated robotic maneuvers have indeed made the standard of living much on ease. However, among these developments, wireless communications stand out as vital contribution in the global transformation [2]. As the telecom network is evolving rapidly due to the rising needs of data rates, capacity and bandwidth, the continuous evolution in number of customers and data traffic is also increasing worldwide. Considering all this, 5G network is designed to provide splendid features including, high data rates, high capacity, compatibility with different data types, support of third-party applications energy efficient and flexible to spectrum utilization.

Small cells have turned 5G to be one of the feasible options to cater the increased traffic, i.e. inclusion of small cells leads to the increased capacity [3, 4]. Thus, the future deployment of wireless mobile networks includes small cells in conjunction with traditional macro-cells to increase the capacity and coverage in future generation networks. To Cope with the random deployment of small cells into the heterogeneous network architecture, dynamic on-off of cells and flat system architecture have been proposed [5, 6]. These requirements pose many challenges for the wireless communication industry to comply with the requirements of future mobile users.

IoT is another main segment for 5G networks and it will be prerequisite for industry 4.0 [7]. Industrial IoT (IIoT) [8] is envisioned to work in a way that the data is obtained from sensors and feedback systems and automatically transferred to cloud-based data centers for processing and ultimately updating the configuration of industry system based on the result of processed data. Wireless sensor networks are the core part of IIoT and a research area is focused for virtual WSN to bring the discussed advantages of virtualization in IIoT.

Received: August 2016; Accepted: September 2018
* Corresponding Author: Bushra Naeem; bushra.naeem@buitms.edu.pk

The emerging 5G wireless standard is expected to provide great advancements to the society and consumers. The benefits of the 5G technology include lower battery consumption, multiple paths for duplex data transmissions, data of multiple Gbps, software defined processing, greater system level spectral efficiency, no harming effects for human health, intelligent wearable devices cheaper charges as a result to less costs in infrastructure development, antenna systems with smart beams, and many more [9,10]. 5G is predicted to connect the globe as never before, using a communication infrastructure with ultra-reliable links, much lower latencies, massive traffic, instant information and greater spectrum [11]. The major developments that 5G will bring using various techniques are described in the Table 1 [12].

Thus, the key enabling technologies of 5G will include network cooperation along with a greater interference mitigation among the neighboring cells, massive MIMO, context awareness, both transmission and reception at the same time and use of various technologies to provide high speed connections that were never expected before [13].

This paper aims to address the expectations from 5G and the key enablers of 5G technology. The paper is organized as follows: Section 1 Introduction about 5G. Section 2 explains the enablers of 5G networks in terms of requirements of 5G technology, architecture of 5G networks, details of network challenges in 5G, and explicates the network slicing in 5G technology; the section 3 finally concludes the paper.

2. ENABLERS OF 5G NETWORKS

The requirement of upcoming 5G mobile networks is to achieve a higher spectral efficiency. The three major factors that may lead to higher spectral efficiency are: Interference reduction, addition of small cells to densify the network and massive multiple-input multiple-output (MIMO), which refers to a great increase in the number of antennas at base stations as well as the mobile stations [2]. The fifth generation of Mobile networks is anticipated to provide a better area spectral and energy efficiency alongside improved and uniform user experience. Moreover, a peak data rate of more than 10Gb/s is predicted [14]. A capacity growth through network densification comes with a great challenge of severe inter-cell interference [15]. In order to meet the network requirements of 5G, the networks over 5G slices, NFV and SDN technologies are broadly considered as the key enablers in network architecture and design. The trailing sections explain about these enablers.

2.1 Network Architecture for 5G

In a heterogeneous network scenario, the channel and traffic variations will be rapid and there is no central node to perform the radio resource allocation, thus the system architecture becomes flat. Thus, as a result of random deployment and flat system architecture, it is critical to develop efficient algorithms based on cooperation and self-organization networks for load distribution synchronization, inter-cell power control, and so on [3, 14]. Due to the challenge of random deployment,

Table 1. The Key aims of 5G and the methods to achieve them

The aims of 5G	Technologies to provide these developments
20 times increased data rate	Using Massive MIMO and Millimeter Wave Spectrum
A triple times spectral efficiency in the downlink	Device to Device Communication(D2D), full duplex systems and massive MIMO
Data processing increased to 100 times in a given radius	Using Radio-access network, D2D, small cells and Millimeter wavelength
Per square KM, about 900 000 more devices will be connected	Small cells and D2D
Increase the mobile devices speed from about 350km/h to 500km/h	Heterogeneous network architecture
Reduce the latency to one tenth	D2D, and content catching close to the users
Provide 100 times greater efficiency	Massive MIMO

dynamic on-off and flat system architecture, there is a need for cooperative algorithms that can enable random deployment and improve the performance in next generation hyper-dense small cell networks. The 5G networks is enabled through Network slicing technology which works with Network Function Virtualization (NFV) and Software Defined Networking. These technologies are briefly discussed in the following sections.

2.1.1 Network Slicing in 5G Technology

It is a concept in which a physical network allows to open several logical self-contained networks for the requirement of several specific services on its physical infrastructure. These network slices are given on lease for a specific period and the lessee has access to physical, service and virtualization layers of 5G networks and this concept integrate the network vertically. Using slicing concept different network services specific to requirement may be offered using virtual network functions using a single network infrastructure making it cost effective and using network efficiently [16]. As network slicing is a recent concept [17] so it needs to be standardized. 3GPP is working on requirement definition [18], and NGMN identified network sharing among slices as one of the key 5G issues [19]. A network slice is set of network function and resources required to run the function as per NGMN, it contains three layers:

i) Service instance layer, which represent the operator or 3rd party service provider
ii) Network slice instance provides network functions with the help of resource layer
iii) Resource layer contains physical resources such as computers, storage and memory etc.

Network slicing will make 5G network architecture more complex and challenging as different slices are deployed and managed at each level and data and traffic management will be more complex. To overcome these challenges some rules may be defined which are as follows:

i) Flexible and seamless management of resources (physical and virtual) across all three layers.
ii) End to end service management for each network slice.
iii) End-to-end programmable connectivity for each service.

Network function virtualization (NFV) and Software Defined Networking (SDN), are the key technologies that can overcome the above-mentioned requirements. NFV is designed to cater the flexibility and scalability requirements where SDN can make the networking requirement programmable in 5G networks. But there are still many challenges in making these two technologies deployable [20].

2.1.2 Software Defined Networking

SDN is used as a reference model for an extended version of SDN which is Software Defined Mobile Network (SDMN) and there are many integration issues in SDMN which needs to be discussed [21].

Architecture Issues: Since SDMN is an extension to SDN as SDMN will work in wireless domain which is more challenging due to complexity of mobile radio networks, Radio link reliability and quality is a challenge while designing SDMN.

Controller Placement: is an issue in addition to deciding the optimal number of controllers, as it will affect network performance [22]. Network controller optimal placement and optimal quantity van minimize the latency and improve the reliability and SDMN architecture will introduce additional constraints and requirements in the controller placement problem.

Cognitive radio integration to SDMN: Cognitive radio can monitor and dynamically reconfigure physical radio characteristics based on the environment variability and we can have centralized intelligence of network by integrating cognitive radio to SDMN [23].

Mobility Management: It ensures reliable data delivery without and disruptions while the user is moving. Future mobile networks will complicate things more as we can have extremely fast-moving users or apps (e.g. high speed trains) [24].

2.1.3 Network and function virtualization

In C-RAN BBU is shifted from physical to virtual machine, but virtual machine is using the same

physical resource, there are following challenges that needs to be addressed to minimize overhead and improve performance:

2.1.3.1 Optimized Performance
Due to increase in overhead network performance is facing degradation. Some means needs to be explored to minimize latency and overhead.

2.1.3.2 Isolated Network
Virtual networks should be isolated from each other; this requirement in mobile networks is a major challenge due to the broadcast nature of wireless medium [25].

2.1.3.3 Resource Allocation
It is also a major challenge in wireless medium due to wide availability of spectrum, mobile nature of devices and separate uplink and downlink channel.

2.1.3.4 Slice Management
Network slices should be scalable as per requirement and dynamic nature of 5G network makes it a challenging task [26].

2.2. Enabling Interoperability to Deploy Flat Network for 5G

The current communication networks rely on the traditional IP based protocol stack, which cannot be completely isolated to attain flat architectures, however the cross-layer approach enables information exchange to attain the flat architecture since it allows direct access between all the layers.

The traditional OSI and TCP/IP support only upward approach because of physical and networks constraints. This causes difficulty in catering the downward user demands. Thus, there is a disagreement of opinion about the layered architectures suitability for the wireless access networks. A protocol which is designed by violating reference layered communication architecture is called cross-layer protocol.

A cross-layer design can help capture these concerns by arranging a uniform framework at different semantic levels. Moreover, the layered architecture makes the information dependent on other layers and may produce delays in the information exchange. On the contrary, the cross-layer approach allows different layers of protocol stack to communicate with each other directly. In this approach, one layer may access data from another, thus enabling information exchange between various layers. Hence, a cross-layer approach has a vital role in the next-generation of Mobile networks which are featured by IP-based protocol stack [27, 28, 29].

A further study at the University of Surrey has envisaged some important requirements for 5G architecture [30]. The primarily requirement of flat architecture is to provide distributed cloud based services and architecture flexibility on time. The architecture must also provide content centric networking and support Internet of Things and various kinds of nodes involved in these services. The network resources should be optimally used providing context aware networking to both user and network. A low latency must be achieved through direct interactions, supporting cloud computing and quick access to the nodes and devices associated with the Internet of Things. Flat network architecture is based on the distributed mobility management whereas the previous generations had been working on centralized mobility management. The section below provides a brief discussion on both types of network architectures to comprehend the transition from centralized to the distributed/flat network.

2.2.1 Flat Network architecture VS Centralized Mobility Management

The Mobile Network Operators (MNO's) are attracted towards complete IP-based networks to provide maximum capacity for voice data as well as video data. There are various standard mobility management protocols including MIPv6 and PMIPv6. These protocols are implemented through a central anchor node, and are known as Centralized Mobility Management (CMM) protocols. The problem with centralized mobility architecture is that they include single point of failure, they require redundant mobility functions and they suffer with traffic congestion [31, 32]. Therefore, a re-design of network architecture is required that must consider the following features:

i) Flexibility: The new architecture must enable the network to upgrade the software's, provide

new services whenever required and allow variations in traffic management systems and strategies.

ii) Performance: The architecture should be scalable and should ease the traffic management

iii) Complexity: Must be simple and easy to deploy, implement and manage the costs [33].

The above concerns can be sought by the flat architecture that is based on distributed mobility management. The systems that are built on a centralized/hierarchical structure, connect multiple access networks to a central core. The important network functionalities such as controlling charging and managing traffic all take place at the mobility anchors. These problems may be solved by the Distributed Mobility Management (DMM) architecture, where the centralized anchor is removed [34]. Figure 1 depicts a typical CMM architecture.

2.2.2 Distributed Mobility Management

The purpose of DMM architecture is to realize such a network that communicates without a centralized entity. This allows the IP flows to be routed in a more flexible way. The key entities in a DMM are mobility-enabled access routers that are located at the edge of the operator's network, i.e. in the vicinity of the users, and they are enabled to communicate with the external IP networks. The Figure 2 provides a diagram of DMM approach [35]. A cloud based and virtualization concept new RAN architecture is being introduced that will minimize operators CAPEX and OPEX by minimizing the needs of base stations deployment requirement. [36, 37, 38]. Cloud computing will enable the user to access shared resources for computing and virtualization will enable the network to be programmable through SDN and all network functions to be virtualized through network function virtualization (NFV) [39, 40, 41, 42]. Cloud-RAN (C-RAN) can be deployed on the same infrastructure with reduced cost of deployment and also reduced OPEX [43, 44, 45]. The Technologies that Complement C-RAN include C-RAN, SDN, NFV, Network virtualization and slicing, and Common public radio interface CPRI [46].

2.3 The 5G Radio Perspective

The promise of higher data rates and anytime anywhere connectivity by 5G has to be kept while also knowing that the limited radio spectrum has to be fully and intelligently utilized to deliver the promise. The following subsections provide important discussion about 5G radio.

2.3.1 Massive MIMO Antenna

To provide Gigabits of speed to end users, it is imperative to use the massive MIMO antennas. Some of the drawbacks faced by this technology include: High costs, difficult installation in high-rise sights and very High Complexity.

2.3.2 Better Signal to Noise Ratio

5G systems also require better SNR to guarantee the quality of service. Some of the practical methods to achieve an improved SNR include: Cell densification through addition of micro, pico and femto cells, usage of steerable beam antennas and application of Interference reduction techniques.

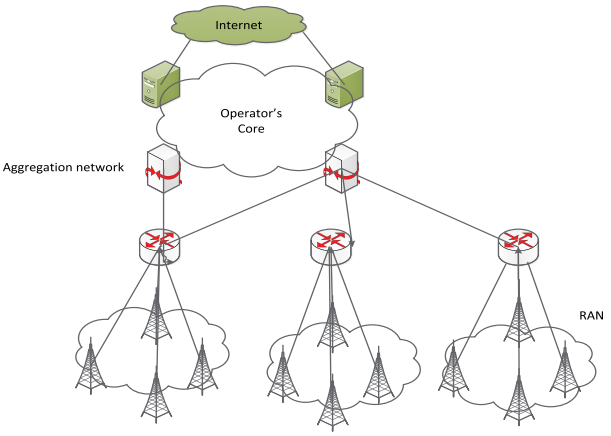

Fig. 1. Centralized Mobility Management Architecture

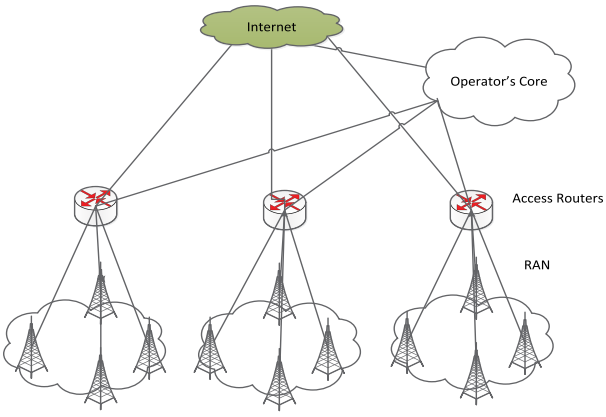

Fig. 2. Distributed Mobility Management Architecture/Flat Architecture

2.3.3 Spectrum for 5G

The spectrum scarcity of frequency bands currently utilized has resulted in discovery of new spectrum spaces that can be used to 5G. It is vital to identify the spectrum range that than enable the vision of 5G. The Millimeter wave spectrum is being considered for communication. It has the range of frequencies starting at 30 GHz to 300 GHz and correspondingly have a wavelength between 10 mm and 1 mm. Millimeter-wave bands offer substantially wider bandwidth and Provide dramatically higher data capacity than the current cellular bands. Thus, they are suitable to equip the 5G systems with the core requirements. The initial experimentation on 28GHz frequency has acceded that these frequencies can be used for 5G coverage. However, the initial stage of 5G deployment is believed to start with 3300-4200 MHz, 4400-5000 MHz and 700 MHz. These bands are particularly suitable for machine type applications in 5G. Whereas, the usage of higher mmWave frequencies with an extensive RF range is anticipated to help global ecosystems and deployments below building rooftops in urban/ suburban environments with directional beams towards targeted coverage areas [47, 48, 49, 50].

2.3.4 Capacity VS Spectrum Crunch

The ever-growing demand in network capacity is inevitable due to increasing user demands and inventions of vast range of mobile applications. However, the dilemma is that there is only a fixed amount of spectrum that may be used by wireless communications. The section *1)* give details on the developments and concerns regarding network capacity and followed by that, section *2)* describes the problem of having fixed spectrum availability and proposes few potential solutions.

2.3.5 Network Capacity

During recent years, a sudden shift of mobile subscribers to the smart phone devices has resulted in a great increase of mobile data usage. Subscribers need high speed connectivity at every instant and location. A well-known quote by Plato is that, necessity is the mother of invention. This applies to the network capacity too. Cooper's Law establishes that "Capacity has doubled every two-and-a-half year for last 104 years. This has resulted in a cumulative improvement of spectrum utilization to one million times! Thus, it may be inferred that the need for mobile data have led to the significant increase in the wireless network capacity, which is witnessed today. There are various reasons that have directed towards this development. Some of the reasons include: increase in the number of wireless nodes, increased use of radio spectrum and improvement in the link efficiency [15]. Fig.3 shows the rate of improvement in the spectrum utilization, owing to various technological techniques during past 45 years [51].

According to Fig.3, a five times increase is experienced because of using various frequency division schemes as well as modulations and spread spectrum techniques. A 25x rise is a result of being able to use greater amount of spectrum. Finally, a huge increase of 1600x is obtained by spectrum re-use, which is achieved using small cells.

2.3.6 Addition of Small Cells

In order to support 1000 times mobile data traffic increases by 2020, the new generation 5G network technologies are under development to provide high data rates and increased network capacity. A number of industry activities and organizations have been established to define and develop 5G standards, one of the solutions to cater the need higher capacity and network densification is the deployment of small cells. Small cell for residential is saturated but keep growth for enterprise and public area scenario and the main purpose is shifted from coverage extension to capacity improvement.

In future it is anticipated that the small cells such as micro cells, picocells and femtocells will be compactly integrated to the macrocell networks creating cooperation based heterogeneous networks. Deployment of such access points provides additional benefits other than providing extra capacity to the current marcrocell infrastructure. They have lower transmitter powers. Further, the co-ordination with the small cells is quicker for the reason that they are mostly not directly linked to the macro base stations. The mobile operators have also been attracted towards small cells to improve indoor and local area system capacity along with service coverage [52]. However, reception of high power macrocells yields most of user devices staying connected to them, which results in the under-

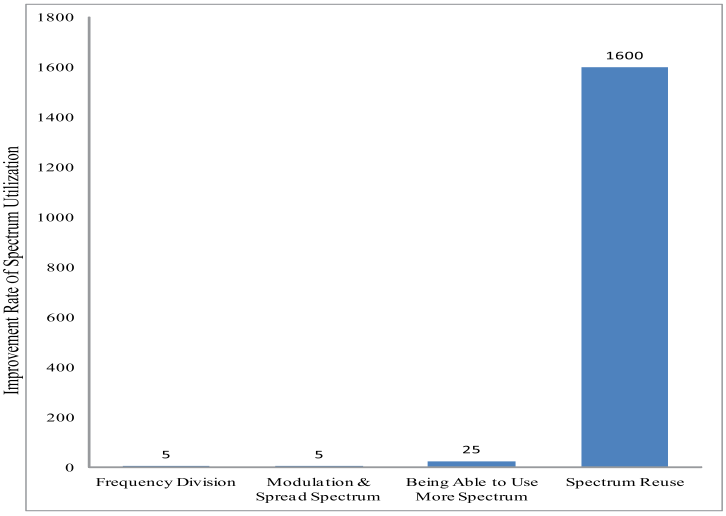

Fig. 3. Rate of improvement in the spectrum utilization in last 45 years

utilization of small cells

2.3.7 Carrier Aggregation

To increase capacity carrier aggregation is the key factor for doing this, some types of carrier aggregation include LTE and WiFi aggregation, LTE and licensed and unlicensed bands.

2.3.8 Multi-cell Coordination

The resource and management allocation will be a challenge in densely deploying small cell for 5G network. Multi cell joint transmission, channel prediction technique, channel reciprocity, channel state info feedback scheme, multi cell synchronization are the challenges [53]. Multi cell will require multiple antennas, distributed antenna or massive antenna arrays, for this some kind of pre-coding or post-coding techniques will be required to manage antenna beams. For switching of transmission modes adaptive algorithm will be required. This multi-cell coordination also known as network MIMO will play a key factor in 5G network.

Spectrum efficiency can improve the system capacity by using massive MIMO i.e. by deploying large number of antennas which will serve more users in parallel with low interference. Higher order modulation scheme and new multiple access schemes will be required to increase system capacity.

It is suggested by most of the researchers and from the statistics that the key method to achieve requirements of 5G networks will be network densification. However, serious concerns have been raised on the limit of densification of wireless network in [54]. It is argued that there are some fundamental limits to the amount of densification that may be done to increase network capacity.

3. CONCLUSION

It is expected that cellular communications industry will facilitate multiples of user demands expected in coming decades. This work has explored the methods that are expected to provide a platform for competing with the needs of fifth generation of mobile networks. As discussed in preceding sections, the emerging 5G wireless standard is expected to provide great advancements to the society and consumers. The benefits of the 5G technology include lower battery consumption, multiple paths for duplex data transmissions, data of multiple Gbps, software defined processing, greater system level spectral efficiency, no harming effects for human health, intelligent wearable devices cheaper charges as a result to less costs in infrastructure development, antenna systems with smart beams, and many more. The challenges faced by the wireless industry currently have also been explored in this work. To achieve a higher spectral with affordable complexity, some of the solutions have been envisaged. These include advanced

interference mitigation techniques, massive MIMO and network densification. It is observed that a diversity of methods has been suggested and will be deployed to increase the many-fold network capacity. In the light of discussion carried out in preceding sections, it is concluded that 5G although is a very heavy investment but it opens many prospects for the betterment of the society, may it be any social class, the people can take advantage of automated facilities, given that the government and industries collaborate to provide these services to the public at easily affordable rates for all social categories including the upper, middle and lower classes.

The current architecture will be modified extensively as the need for high speed data traffic and low latency mobile network is arising and with the advent of 5G concepts such as SDN and NFV as well as advancements in optical and wireless technologies are shaping the way mobile networks are designed and deployed, ultimately enabling operators to provide more diverse, flexible, and cost-effective services to users.

4. REFERENCES

1. Orlikowski, W. J., & Barley, S. R., "Technology and institutions: What can research on information technology and research on organizations learn from each other?", *MIS quarterly*, (5): 145-165(2001)
2. Viswanathan, H. & M. Weldon, "The past, present, and future of mobile communications," in *Bell Labs Technical Journal,* 19: 8-21(2014)
3. Osseiran A, F. Boccardi, V. Braun, K. Kusume, P.Marsch, M. Maternia, & M. Fallgren, "Scenarios for 5G mobile and wireless communications: the vision of the METIS project.," *Communications Magazine*, *IEEE ,* 52(5): 26-35 (2014)
4. Jungnickel V., K. Manolakis, W. Zirwas, B. Panzner, V.Braun, M. Lossow, & T. Svensson, "The role of small cells, coordinated multipoint, and massive MIMO in 5G," in *Communications Magazine, IEEE*, 52(5): 44-51, (2014)
5. Zhang H., X. Chu, W. Guo, & S. Wang, "Coexistence of Wi-Fi and heterogeneous small cell networks sharing unlicensed spectrum*,"in Communications Magazine*, *IEEE* , 53(3):158-164, (2015)
6. Fortes S., A. Aguilar-García, R. Barco, F. Barba, J., Fernández-luque & A. Fernández-Durán, , "Management architecture for location-aware self-organizing LTE/LTE-a small cell networks*,"* in *Communications Magazine, IEEE*, 53:294-302, (2015)
7. Wollschlaeger M., T. Sauter & J. Jasperneite, "The future of industrial communication: automation networks in the era of the internet of things and industry 4.0," in *IEEE Industrial Electronics Magazine*, 11(1):17-27, (2017)
8. Palattella M. R. *et al*., "Internet of Things in the 5G Era: enablers, architecture, and business models," in *IEEE Journal on Selected Areas in Communications*, 34(3):510-527, (2016).
9. Albreem, M. A., "5G wireless communication systems: vision and challenges", in *IEEE Computer*, *Communications, and Control Technology (I4CT), International Conference,* 493-497, (2015)
10. Ericsson white paper, "5G systems enabling industry and society transformation Ericsson", (2015)
11. Keysight technologies, inc., A, "Autonomous vehicles navigating through traffic. Handsfree", in *IEEE Spectrum*, (2016)
12. Young, L.J., "Telecom experts plot a path to 5G*",*in *IEEE Spectrum*, 52(10):14-15, (2015)
13. Sood, R. & Garg, A., "Digital Society from 1G to 5G: A Comparative Study", in *International Journal of Application or Innovation in Engineering & Management (IJAIEM)*, 3(2):186-193, (2014)
14. Xu J., J.Wang, Y. Zhu, Y. Yang, X. Zheng, S. Wang, L Liu, K. Horneman, & Y. Teng, "Cooperative distributed optimization for the hyper-dense small cell deployment," in *Communications Magazine*, *IEEE , 52(5):61-67, (2014)*
15. Bhushan N., J. Li, D. Malladi, R. Gilmore, D. Brenner, A. Damnjanovic & S. Geirhofer, "Network densification: the dominant theme for wireless evolution into 5G," in *Communications Magazine*, *IEEE*, 52(2):82-89, (2014)
16. Yousaf F. Z., M. Bredel, S. Schaller & F. Schneider, "NFV and SDN—Key Technology Enablers for 5G Networks," in *IEEE Journal on Selected Areas in Communications*, 35(11):2468-2478, (2017)
17. NGMN Alliance, "Description of Network Slicing Concept, NGMN 5G P1, Requirements & Architecture", in v1.0.8. Accessed: Nov. 2, 2017. [Online]. Available: https://www.ngmn.org/uploads/media/161010_NGMN_Network_Slicing_framework_v1.0.8.pdf, (2016)
18. 3rd Generat. Partnership Project ,"Study on architecture for next generation system", in *Tech. Rep. TR 23.799*, accessed: Nov. 2, 2017. [Online]. Available: http://www.3gpp.org/ftp/Specs/html-

info/23799.htm, (2016)
19. Alliance, N. G. M. N, "5G white paper", in *Next generation mobile networks, white paper*, 1-125, (2015)
20. Taleb T., "Toward carrier cloud: Potential, challenges, and solutions", in *IEEE Wireless Communications*, 21(3): 80-91, (2014)
21. Pentikousis K., Y. Wang & W. Hu, "Mobileflow: Toward software-defined mobile networks," in *IEEE Communications Magazine*, 51(7): 44-53, (2013)
22. Hu B., Y. Wu ,C. Wang & Y., "The controller placement problem for software-defined networks," in *2nd IEEE International Conference on Computer and Communications (ICCC)*, 2435-2439, (2016)
23. Liang Y. C., K. C. Chen, G. Y. Li & P. Mahonen, "Cognitive radio networking and communications: an overview," in *IEEE Transactions on Vehicular Technology*, 60(7): 3386-3407, (2011)
24. Wu J. & P. Fan, "A Survey on High Mobility Wireless Communications: Challenges, Opportunities and Solutions," in *IEEE Access*, 4:450-476, (2016)
25. Pliatsios, D., P. Sarigiannidis, S. Goudos, & G. K. Karagiannidis, "Realizing 5G vision through cloud RAN: technologies, challenges, and trends", in *EURASIP Journal on Wireless Communications and Networking*, (1):136, (2018)
26. Zhang H., N. Liu, X. Chu, K. Long, A. H. Aghvami & V. C. M. Leung, "Network Slicing Based 5G and Future Mobile Networks: Mobility, Resource Management, and Challenges," in *IEEE communications magazine*, 55(8): 138-145, (2017)
27. Srivastava V., & M. Motani, "Cross-layer design: a survey and the road ahead,"in *IEEE communications magazine*, vol. 43, no. 12, pp. 112-119, (2005)
28. Bin-Salem A., & T. C. Wan, "Survey of cross-layer designs for video transmission over wireless networks", in *IETE Technical Review*, 29(3):229-247, (2012)
29. Raisinghani V.T. & S.Iyer, "Cross-layer design optimizations in wireless protocol stacks*"*,in *Computer Communications,* 27(8):720-724, (2004)
30. "The Flat Distributed Cloud (FDC) 5G Architecture Revolution",in University of Surrey,5G Whitepaper, (2016)
31. Johnsn D., C.Perkins, , & J. Arkko, "Mobility support" in *IPv6 (No. RFC 3775),* (2004)
32. Chan H., D. Liu, P. Seite, H.Yokota, & J. Korhonen, "Requirements for distributed mobility management" in RFC (No. RFC 7333), (2014)
33. Jaber M., M. A. Imran, Tafazolli, R., & A. Tukmanov, "5G backhaul challenges and emerging research directions: A survey*"*, in *IEEE Access*, 4:1743-1766, (2016)
34. Murtadha M. K., N. K. Noordin, , B. M. Ali, & F. Hashim, "Design and evaluation of distributed and dynamic mobility management approach based on PMIPv6 and MIH protocols", in *Wireless Networks*,21(8):2747-2763, (2015)
35. Agiwal, M., Roy, A., & Saxena, N. "Next generation 5G wireless networks: A comprehensive survey", in *IEEE Communications Surveys & Tutorials*, 18(3):1617-1655, (2016).
36. CV Forecast, "Cisco Visual Networking Index: Global Mobile Data Traffic Forecast Update, 2016–2021", in *White Paper Cisco Public Information* https://www.cisco.com/c/en/us/solutions/collateral/service-provider/visual-networking-index-vni/mobile-white-paper-c11-520862.pdf, (2017)
37. Sarigiannidis P., T. Lagkas, S. Bibi, A. Ampatzoglou & P. Bellavista, "Hybrid 5G optical-wireless SDN-based networks, challenges and open issues," in *IET Networks*, 6(6):141-148, (2017)
38. Rost P. *et al*., "Cloud technologies for flexible 5G radio access networks," in *IEEE Communications Magazine*, 52(5): 68-76, (2014)
39. Han B., V. Gopalakrishnan, L. Ji & S. Lee, "Network function virtualization: Challenges and opportunities for innovations," in *IEEE Communications Magazine*, 53:(2):90-97, (2015)
40. Chiosi, M., D. Clarke, & P. Willis, "Network functions virtualisation", in *introductory white paper*, SDN and OpenFlow World Congress, (2012)
41. Xia W., Y. Wen, C. H. Foh, D. Niyato & H. Xie, "A Survey on Software-Defined Networking," in *IEEE Communications Surveys & Tutorials*, 17(1):27-51, (2015)
42. Kreutz D., F. M. V. Ramos, P. E. Veríssimo, C. E. Rothenberg, S. Azodolmolky & S. Uhlig, "Software-Defined Networking: a comprehensive survey," in *Proceedings of the IEEE*, 103(1):14-76, (2015)
43. Hadzialic M., B. Dosenovic, M. Dzaferagic & J. Musovic, "Cloud-RAN: Innovative radio access network architecture," in *Proceedings ELMAR-2013*, 115-120, (2013)
44. Wu J., Z. Zhang, Y. Hong & Y. Wen, "Cloud radio access network (C-RAN): a primer," in *IEEE Network*, 29(1): 35-41, (2015)
45. Checko, A, H. L. Christiansen, & Y. Yan, & L. Scolari, et, al. Cloud RAN for Mobile Networks—A Technology Overview. *in IEEE communications*

surveys & tutorials, 17:405-426, (2015)

46. AB Ericsson, Huawei Technologies Co. Ltd, NEC Corporation, Alcatel Lucent, Nokia Networks,in Common public radio interface (cpri); interface specification. CPRI Specification. 5:1–119, [Online] Available: http://www.cpri.info/ downloads/ CPRI_v_7_0_2015-10-09.pdf, (2015)
47. "Cisco Visual Networking Index: Forecast and Methodology 2012-2017", in *White paper Cisco VNI Repor*t, [online] Available: http://www.cisco.com/en/US/solutions/collateral/ns341/ns525/ns537/ns705/ns827/white_paper_c11-481360.pdf., 2013
48. Kim. T, J. Park, J. Seol, S. Jeong, J. Cho & W. Roh, "Tens of Gbps support with mmWave beamforming systems for next generation communications,"in *EEE Global Communications Conference (GLOBECOM)*, Atlanta, GA, 3685-3690, (2013)
49. Murdock J. N., E. Ben-Dor, Y. Qiao, J. I. Tamir & T. S. Rappaport, "A 38 GHz cellular outage study for an urban outdoor campus environment," *in IEEE Wireless Communications and Networking Conference (WCNC)*, Shanghai, 3085-3090, (2012)
50. Lee J., *et al*., "Spectrum for 5G: Global Status, Challenges, and Enabling Technologies," in *IEEE CommunicationsMagazine*,56(3):12-18,(2018)
51. Cooper M., "Cooper's Law," [online available: Arraycomm, http://www. arraycomm. com/ technology/coopers-law], (2009)
52. Zhang H., X. Chu, W. Guo, & S. Wang, "Coexistence of Wi-Fi and heterogeneous small cell networks sharing unlicensed spectrum," in *Communications Magazine*, *IEEE , 53(3):158-164, (2015)*
53. Zhang H., Y. Qiu, K. Long, G. K. Karagiannidis, X. Wang & A. Nallanathan, "Resource Allocation in NOMA-Based Fog Radio Access Networks," in *IEEE Wireless Communications*, 25(3):110-115, (2018)
54. Ersue M, "ETSI NFV management and orchestration—an overview", in *Presentation at the IETF# 88Meeting* (2013).

Proceedings of the Pakistan Academy of Sciences:
A. Physical and Computational Sciences 55 (3): 21–33 (2018)

ISSN: 2518-4245 (print), 2518-4253 (online)

Pakistan Academy of Sciences

Research Article

Broadband Reflectarray Antenna with High Gain for X Band (8 to 12GHz) Applications

Najvia, and Shahid Bashir*

Department of Electrical Engineering, University of Engineering & Technology, Peshawar, Pakistan

Abstract: In this paper high gain reflectarray antenna for broadband applications is proposed. The proposed design, based on a novel hexagonal unit cell shows a large reflection phase range of 1000° with smooth linear phase slope. A center horn fed 11 x 11 reflectarray antenna with the proposed unit cell is designed for X Band (8 to 12 GHz) applications. It is simulated for different f/D (focus point to largest dimension of antenna) ratios to evaluate its effect. For optimum results, only two f/D ratios 1.0 and 1.96 are chosen. The simulated results show that a wide operational bandwidth of 39.6% for 3dB gain dropping is obtained over the frequency band of 8 to 12 GHz which is much improved than the previously reported results. Simulations for the f/D ratio of 1.96 shows improvement in the aperture efficiency with 3 dB gain bandwidth of 29%. This single layer, low profile reflectarray antenna can be a useful candidate for high gain broadband applications.

Keywords: Broadband reflectarray, High Gain, X-Band, Compact antennas.

1. INTRODUCTION

In the age of radio communication, antennas play an active role in making the overall mobile communications systems viable. For this purpose continued advancement and investigation in the domain of antennas is done to further improve the performance and effectiveness of antenna specification while keeping in view the issue of antenna miniaturization. Usually high-gain parabolic reflectors are employed in navigational devices and long range communications. But they are massive, rigid, spacious and hard to be fixed also having inefficiency in beam scanning. These weaknesses of parabolic radiators were covered by a highly directive group of antennas called as phased-array antennas. They are driven with steerable phase shifters, to electronically achieve large beam scanning angle, having slim and portable design. Regardless of these benefits, it is having certain drawbacks such as its intricate design, use of expensive phase shifters and amplifier units to obtain required phase response and beam angle. To overwhelm the inadequacies of the former antennas, an innovative antenna design was presented in 1960's known as "reflect array antenna" [1, 2].

Reflect array antenna is a planar structure consisting of smart radiative units. These units (or antennas) are devised in such a manner that it reradiates the incoming wave in the aimed path with the precise phase adjustment. It is a simple structure with horn antenna acting as a source for the whole setup rather than having individual sources for each and every unit of the structure as in phased array antennas thus minimizing the system intricacy. It has gained popularity and replaced the parabolic reflectors because it combines the intelligent attributes of high directivity and desired pattern configuration from parabolic reflectors and phased array antennas respectively along with its own adaptability in beam shaping. Despite of these favors, main drawback of reflectarray antennas is limited bandwidth [3]. To overcome this deficiency, different approaches are presented by researchers. These techniques include multi-layer approach in which multiple layers are stacked together thus making it heavy and inflexible and only 10% to

Received: May 2018; Accepted: September 2018
* Corresponding Author: Shahid Bashir; Shahid.bashir@uetpeshawar.edu.pk

20% bandwidth was achieved [4, 5]. Similarly nested conductive loops with thick substrates [6], double crossed loops structures with changeable lengths showed radiation efficiency of 55% and 10% bandwidth [7]. Resonating module's structure and shape has notable impact on the performance of the antenna. So in this context new shape elements such as ridge, dog bone were introduced with 13% gain-bandwidth [8]. In [9] a circularly polarized RA antenna was represented with loop elements having variable rotations resulting in improved gain but narrow band.

In the same manner varactor diodes are used in the array modules for the purpose of phase adjustment. Required phase shifts and phase correction is done by changing the electrical length of the patches. High gain and wide beam contouring

Table 1. Performance characteristics of different Reflectarray Antennas

Methodology	unit cell geometry	Phase range (degrees)	Centre frequency (GHz)	Bandwidth (%)
Multi layer structure [4,5]	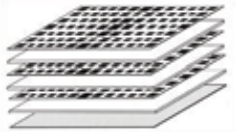	360	12	10-20
Double loop structure with thick substrate [6]		330	10	10
Dual cross loop structure with adjustable dimensions [7]		500	22	10
Comparison of Dogbone shaped resonating element with existing shapes [8]	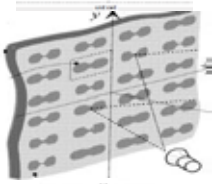	>360	12	13
Circularly polarized with loop elements [9]		------	7.1	4
Electronically tunable antenna [12]	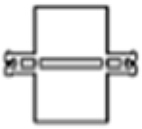	≈360	5.8	-----
Single layer [15]	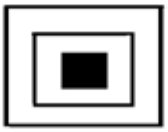	360	5	30.8
Analysis of S-Shaped phasing curves [16]		150 -- 177	10	1-10
Optimization of reflection curve [22]		≈420	5.8	7
Double hexagonal ring structured cell [26]		>360	10.5	28.5

ability is examined from the results [10-13].

Factors such as intermediate gap between the radiating elements and the mutual coupling also play an active role in the improvement of bandwidth as in [14] and [15]. 3-dB bandwidth of 30.8 % is attained by varying these factors. Some papers [16-18] focused on s-shaped reflection phase curves to achieve phase range greater than 360° for widening the bandwidth. In [19, 20] Genetic algorithm (GA) based controller is represented to have more command over the phase adjustment to achieve desired radiation pattern in relation with the varying path lengths of the source from the reflecting surface. Other papers [21, 22] showed optimization methods to enhance the performance of reflectarray antennas. Based on available published results, maximum 30.8% bandwidth is achieved up till now at the cost of system complexity or size. Table 1 compares the performance characteristics achieved so far for reflectarray antennas.

In this paper, a novel element having hexagonal structure with open ended triangular loops on the inner side is proposed. A wide reflection phase sweep of 1000°and phase gradient of 303°/mm is achieved as a function of varying element size, thus adding freedom for further enhancement in bandwidth. An 11 x 11 elements symmetrical single layer reflectarray is designed for X-band and illuminated by a horn antenna. Simulations are carried out in CST microwave studio and 3 dB gain bandwidth of designed reflectarray reached 39.6% for this band. Thus a very good bandwidth is achieved with smaller size having approximately 9% enhancement of bandwidth as compared to other single layer reflectarray antennas.

2. METHODOLOGY

The theoretical analysis for the design of reflectarray antenna is executed using full-wave simulation tool i.e. Computer Simulated Technology (CST MWS). Fig. 1 shows the complete methodology having two main steps i.e. element design and system design. Basically three approaches are utilized in the analysis and design procedure of reflect array antennas. These three approaches include homogenous array, non-homogeneous array and resonating elements with variable angular rotations. In this paper non homogenous array approach is used because of its simplicity as other approaches require stubs, delay lines or phase shifters for the phase compensation.

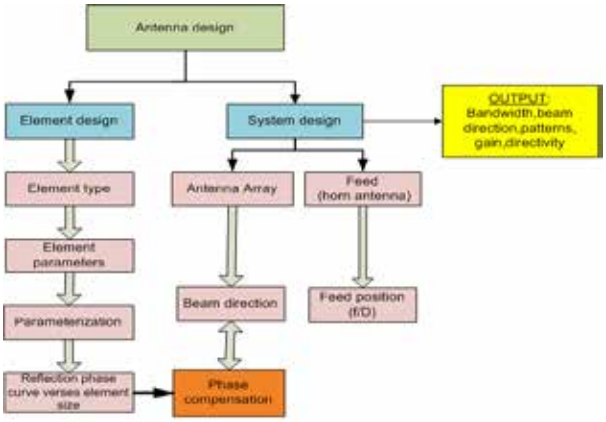

Fig. 1. Flowchart of Methodology for Reflectarray Antenna design

Unit cell design is the initial stage in which parameterization is done to obtain S-shape curves of reflection phase versus variable parameters of the resonating element. This method is known as unit cell analysis. In unit cell analysis, Floquet modes are applied to analyze the behavior of unit cell. Floquet modes compute the performance of unit cell in an infinite array environment.

Second step is the analysis of Phase distribution on the entire reflectarray using the proposed elements. Using this step phase compensation is done to achieve a sharp beam normal to the plane of reflect array antenna. After this step, whole system consisting of an array and horn antenna is designed and simulated to determine the radiation properties of that antenna.

2.1 Element Design

The proposed element of reflectarray antenna is shown in Fig.2. It is designed to function in X-band

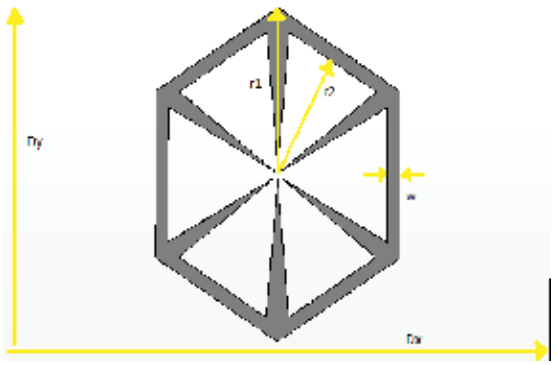

Fig. 2. Resonating Element

(i.e. from 8 to 12 GHz) with a center frequency of 10 GHz. The resonating unit is a hexagon ring structure with triangle shaped loops inside. As seen in the Fig. 2, r1 represent the radius of the hexagon ring and r2 is the height of the inner triangular loop. Whereas hexagonal ring width "w "is given a constant value of 0.1mm.

These resonating elements are arranged in a square prototype having length Dx and width Dy of 15mm respectively. Thus obtaining periodicity of 15mm (i.e. the space (S) between the adjacent cell centers).This value of periodicity helps in the reduction of the grating lobes according to the criterion given below,

$$S \leq \lambda/(1+\sin\theta) \quad (1)$$

Where θ is the reflected rays angle and wavelength (λ) is 30mm according to the center frequency of antenna.

Parameters r1 and r2 are related in accordance with the following equation i.e. r2 = r1-(0.1*r1). To attain optimization goals, distribution of phases is controlled for the whole operating range of frequencies through the process of parameterization. By alternating the variables r1 and hence r2, the resonating frequency is varied and the phase adjustment is achieved at different positions of the reflectarray antenna.

Table 2. Summary of the Unit Cell Dimension

SPECIFICATIONS	VALUE
Width of hexagonal ring, w	0.1mm
Height of triangular loop	r 2
Radius of hexagonal ring	r 1
Dielectric constant , ε_r	2.08
Substrate loss tangent , tan δ	0.0004
Dielectric material thickness , t	2mm
Air gap thickness, h	5.5mm
Relationship between r_1 & r_2	$r_2 = r_1 - (0.1*r_1)$
Periodicity, p	15mm
Resonance frequency, f	10 GHz

Table 3. Parametric Sweep

Parameters	VALUE
r1 (mm)	1.0 - 4.4
r2 (mm)	r1-(w*r1)
w (mm)	0.1

Structure of the unit cell consists of a sheet of dielectric material having relative permittivity of 2.08 and tangent loss factor of 0.0004. An air gap is inserted between the dielectric material and ground. The purpose of the accommodation of the air gap is to achieve wide range of reflection phases. Specifications of the single unit cell are summarized in Table 2.

2.2 Geometry Optimization

Variables such as hexagonal ring radius r1, hexagonal ring thickness w, triangular loop altitude r2 , and the relationship between these variables i.e. r2=r1-(0.1*r1) are introduced in the geometry of the phasing element to achieve optimization goals. These variables help in controlling the reflection phase responses over the whole working range of frequencies.

The purpose of parameterization is to get an even phase response of the phasing element. Settings for the parameter's sweep are given in Table 3. In order to compute the analysis of the phasing element for X-band, frequency domain solver (FD) is applied. Floquet modes with unit cell boundaries are used in the unit cell analysis; thus analyzing the performance of resonating element in an infinite array environment [23].

2.3 Phasing Characteristics Of Unit Cell Element

In antenna arrays design procedure, phasing properties of the resonating element play a vital role in revealing the overall response of the antenna. Whenever a wave is incident upon the reflecting surface (antenna array), it is scattered in the medium with some arbitrary angle. In order to achieve a sharp directive beam, the resonating elements must have the capability to adjust and correct the phase of the incoming wave and reradiate it as collimated beam in the particular direction. Hence the range of reflected phases versus variable dimensions of the resonating patch must be larger than 360° to offer appropriate phase adjustment.

Therefore, variation of the following two factors determines the phase characteristics of the unit cell i.e. Shape of Resonating Patch Element

and Thickness of Substrate. Reflected phase responses as a function of the variation of these two elements are plotted which are also known as S-shape curves. These S-shaped plots are helpful in giving an insight of the antenna specification [24].

2.4 Shape of Resonating Patch Element

Patch element's profile plays a very important role in passive reflectarrays to control the deviation of phases. Through variation in one of the parameter of the resonating element, one can get control on the phase changes in the arrays antenna. It acts like weights in phase array antennas which multiply to the actual phase of the incident wave to get the desired phased beam.

Fig. 3 shows three different shapes of the patch which are examined. Simple hexagonal patch is shown in Fig. 3 (a) in which radius r1 is kept variable for obtaining different phase responses. Similarly, in Fig. 3 (b), r1 is kept fixed, where height of the triangular area in hexagon r2, is varied to determine the reflection phase curve for this variation. In Fig. 3 (c) both r1 and r2 are varied, as to consider the impact of two variable parameters to get an optimum phase response.

Fig. 4 shows the reflection phases for different shaped resonating elements. It shows the combined results of all three patches. The variation of the parameter r1 from 1 to 4.4 mm of simple hexagonal shape shows variation in the reflection phase from 10° to -50°. Thus total range of 60 degrees is obtained with slope of 18.1°/mm with simple hexagon.

The Fig. 4 also shows the plot of fixed hexagon with variable triangular loops. The parameter r was varied to achieve different phases. With variation of parameter r from 1 to 4.4 mm, phase variation is from -61° to -65°. Thus total phase range of 4° is obtained with slope of 1.21°/mm.

The variation of the parameter r1 from 1 to 4.4 mm for variable hexagon having variable triangular loops is also shown. Total phase range of 1000° is achieved with a slope of 303°/mm. The result shows a drastic variation in the phase range and phase slope. The third curve which is for

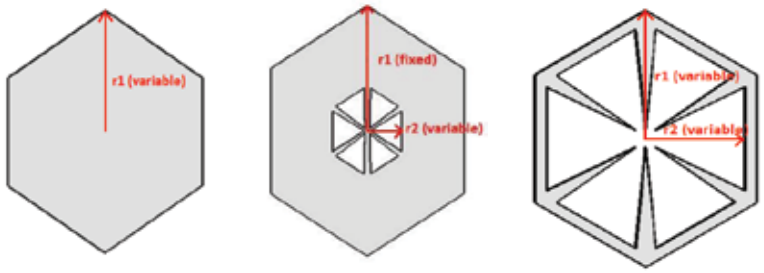

Fig. 3. Different Shapes of the Phasing Element (a) Simple Hexagonal Patch Element (b) Fix Hexagonal Patch with Variable Triangular Gaps (c) Variable Hexagonal Shape with Variable Triangular Gap

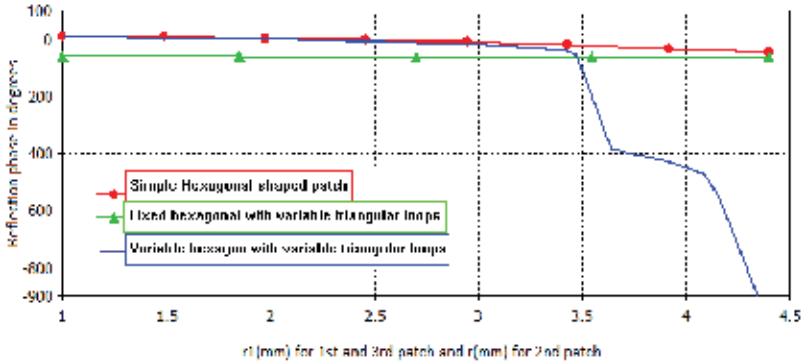

Fig. 4. Plot of Reflection Phases versus Variable Parameter of Resonating Elements

the proposed resonating element having variable hexagon with triangular loops shows very good reflection phase curve, as having wide range of 1000° for compensation of phase changes. In addition to this, the slope is also smooth, so it can tolerate fabrication errors.

2.5 Thickness of Substrate

Varying the thickness of substrate i.e. air gap has a visible effect on the phasing property of the resonating element. Suppression of surface waves becomes possible through the introduction of air gap [25, 26]. It also extends the range of reflection phase to have larger functional bandwith band of antenna. Thus to widen the bandwidth, an air-filled space is introduced.

Fig. 5 represents the plots of the reflected phase responses for variable heights of the air-filled gap. The curve with circles shows air gap height of 3.0 mm. This height gives deviation of phase from 76° to -670°, when r1 is varied from 1.50 to 4.40 mm.

The second curve for air gap height of, 4.0 mm shows a total phase range of 650°. Similarly, third curve for height of 5.0 mm shows deviation in phase response from 15° to -608°, attaining the phase range of 623°.

Second to last curve is for air gap height of 6.0 mm exhibiting the change in the reflected phase from 0° to 1072°. This curve shows leveled and an even response with extended range of 1072 degrees. But in order to get improved gain bandwidth product, an air gap height of 5.50 mm is chosen. This height of substrate gives reflected phase deflection from 0° to 1000°.Summary of the results are presented in the Table 4.

2.6 Reflection Phase Response

By investigating various shaped phasing elements, variable thickness and size of the substrate material, the most favorable response in terms of reflection phase angles is achieved with variable hexagon having variable height of the triangular area. Final plot of the reflection phase response versus the variable dimension r1 of resonating patch element is shown in Fig. 6. The finalized phasing element

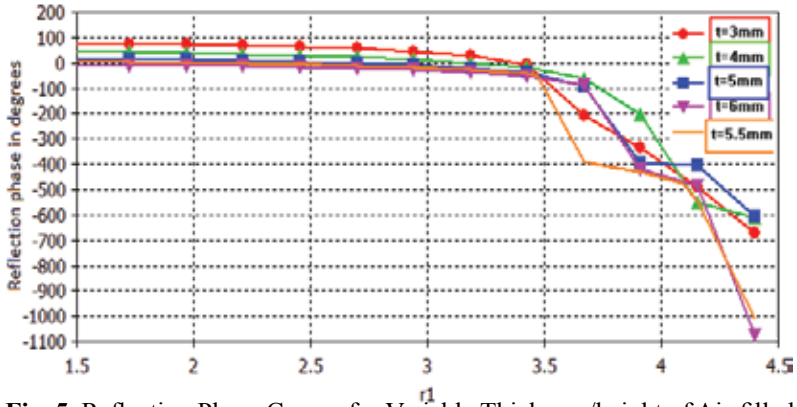

Fig. 5. Reflection Phase Curves for Variable Thickness/height of Air-filled Gap

Table 4. Summarized Results for Different Resonating Elements and Variable Air Gap Height/Thickness

Resonating Element's Patch Structure	Phase Slope	Phase Range
Plain hexagonal patch	18.1°/mm	60°
Variable radius of hexagon with variable height of triangular area	303°/mm	1000°
Fixed hexagon with variable height of triangular gap	1.21°/mm	4°
Air gap ,t=6.0 mm	369°/mm	1072°
Air gap , t=5.50 mm	303°/mm	1000°
Air gap, t=5.0 mm	214°/mm	623°
t=4.0 mm	224°/mm	650°
t=3.0 mm	257°/mm	746°

aids in attaining even and extended phase range of 1000°. Hence these characteristics support wide bandwidth and a good figure of merit.

2.7 Array Analysis

In array designing, phase tuning is an essential aspect of the whole array setup. Usually horn is used as a feed. The incident wave from the horn antenna on the patch element of the reflectarray antenna is reflected back in the medium with the necessary phase angle making a progressive phase shift distribution on the reflecting surface. This pattern of gradually increasing phases on the plane of the reflectarray is presented by;

$$\phi(x_i,y_i) = -k\sin\theta_b\,(\cos\varphi_b x_i + \sin\varphi_b y_i) \quad (2)$$

(x_i,y_i) are the coordinates of ith element,

k is the free space propagation constant,

$(\theta b,\varphi b)$ gives the direction of beam.

The resultant phase of the wave originating from every element of the reflectarray is equivalent to the phase of incoming wave from feed plus the induced phase shift by each element.

$$\phi(x_i,y_i) = -kd_i + \phi_{element\ phase}\,(x_i,y_i) \quad (3)$$

Where d_i is the distance of the ith array element from the center of the source, therefore the necessary phase for each element is obtained by,

$$\phi_{element\ phase}\,(x_i,y_i) = -kd_i\ k(x_i\cos\varphi_b + y_i\sin\varphi_b)\sin\theta_b \quad (4)$$

An array of size 11x11 having 121 radiating elements is designed using CST MW Studio at center frequency of 10 GHz for X-band as shown in Fig. 7. Proposed reflectarray antenna has square aperture with dimension of 15mm x 11mm .A

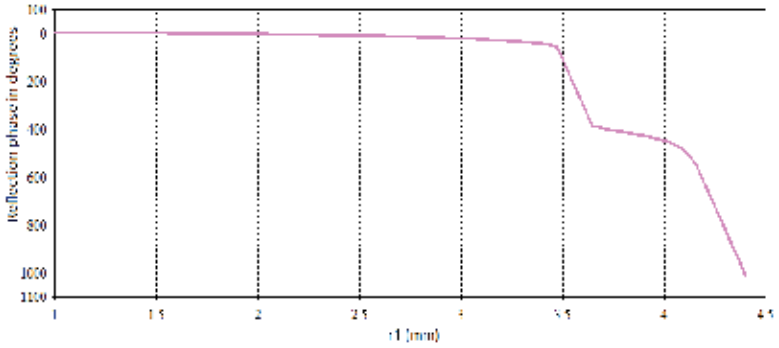

Fig. 6. Finalized Reflected Phase Response

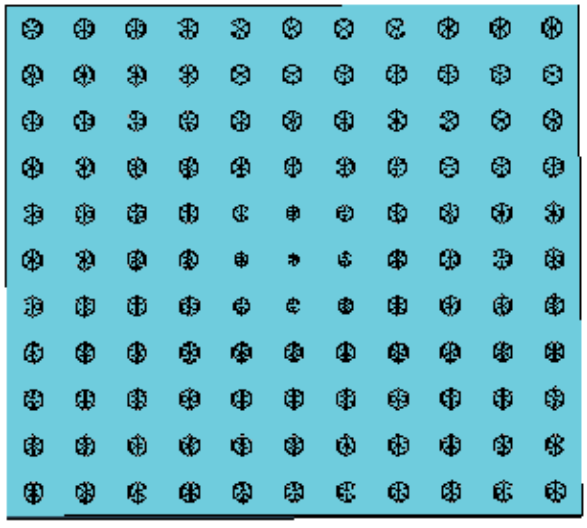

Fig. 7. 11 x 11 Reflectarray Antenna

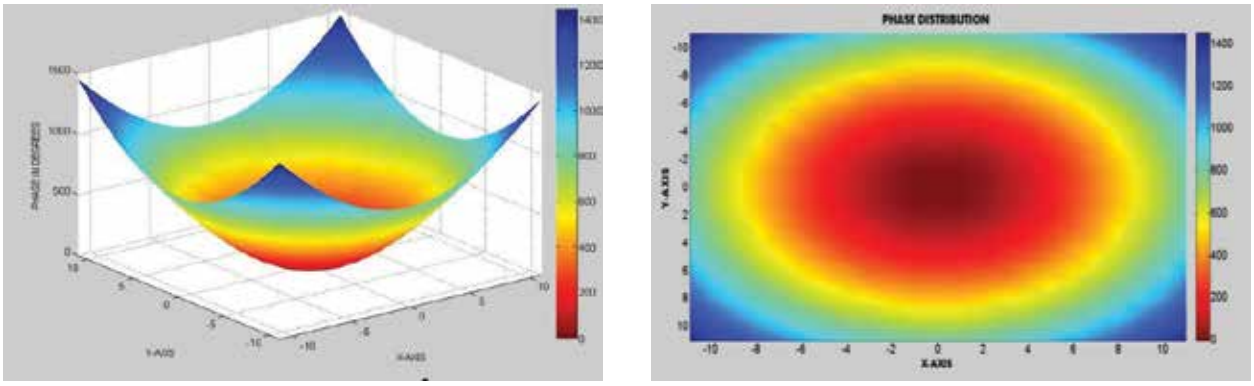

(a) (b)

Fig. 8. (a) Distribution of Phase on a Square Reflectarray Antenna with 10 GHz Centre Frequency (b) 3-D phase distribution corresponding to parabolic reflector

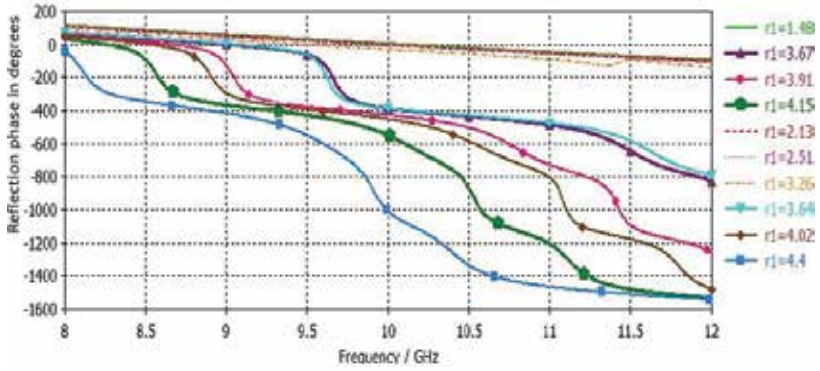

Fig. 9. Reflected Phase Response versus Frequency

normal incident center fed source is supposed for this specific antenna i.e. ϕ & $\theta = 0°$.

Using (3) and (4), one can obtain required phase distribution as depicted by Fig. 8. Hence the required weights for directive and coherent beam are achieved through this methodology.

Fig. 8 (b) shows the correspondence of the phase shifts at each element with the parabolic reflector. Thus the reflected beam from the plane reflectarray will behave in the same way as reflected from the parabolic reflector antenna.

3. RESULTS & DISCUSSIONS

To evaluate the performance of proposed reflectarray antenna, simulations are carried out in CST MW Studio. Discussions will also be made in this section on the basis of simulation results.

3.1 Reflect Array Unit Cell

Reflection phase response versus frequency range of the proposed unit cell from 8 to 12 GHz is plotted as shown in Fig. 9 to analyze the behavior of unit cell over the whole frequency range. By observing the frequency band from 8 to 12 GHz, the change in reflected phase by changing one of the dimensions of the phasing element; is quite visible.

For the analysis of unit cell, floquet modes are utilized as mentioned earlier. This approach provides the facility to test the behavior of resonating element for various angles of incidence. In this paper, angle of incidence is varied from 0° to 30° for verifying the influence of angle of incidence on the results. Reflection phase characteristics obtained in Fig. 10 shows that the performance is nearly identical for angles of incidence other than the normal incidence. Thus set of curves with good parallelism corresponding to the particular value of r1 over the entire frequency range can be achieved with the devised element as shown in Fig.10(a), Fig.10(b) and Fig.10(c) . The previously proposed unit cells had this drawback of degrading performace with changing angle of incidence [4-6].

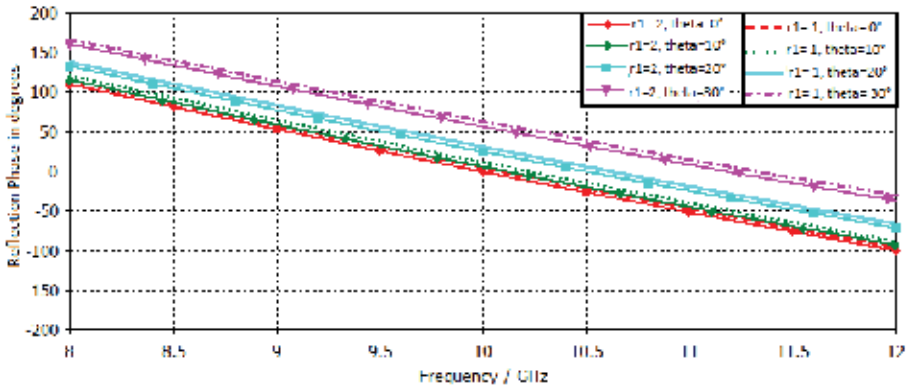

(a)

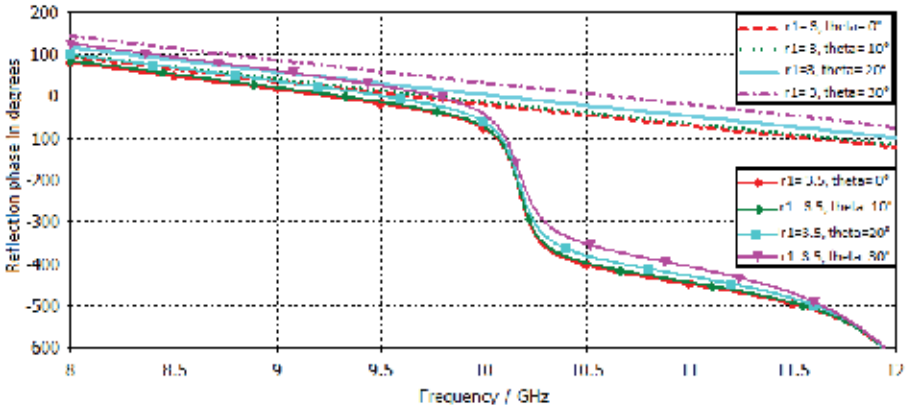

(b)

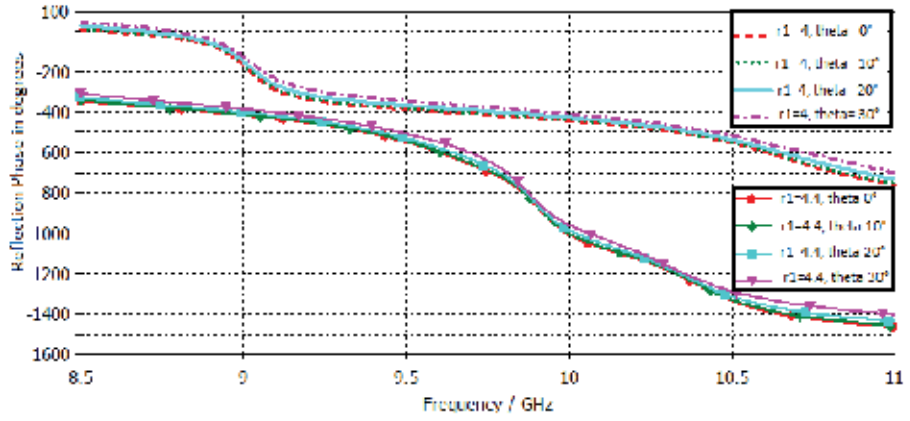

(c)

Fig. 10. Reflecd Phase Response of the Element with respect to frequency for different values of angle of incidence and r1 (mm) **(a)** r1=1 and 2 **(b)** r1=3 and 3.5 **(c)** r1=4 and 4.4

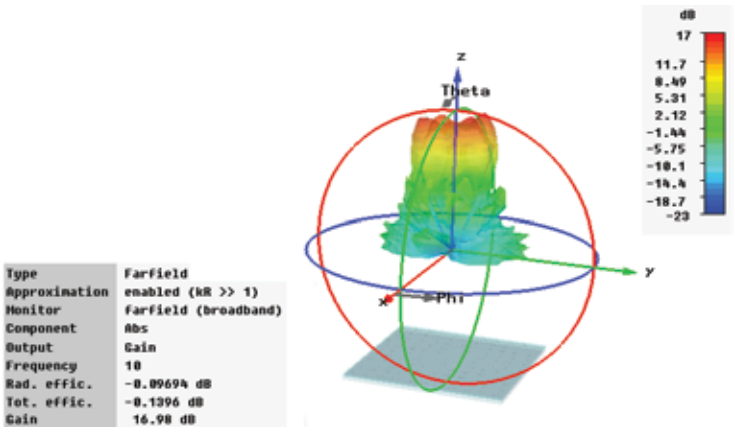

Fig. 11. Array far field Radiation Pattern at Center Frequency of 10 GHz

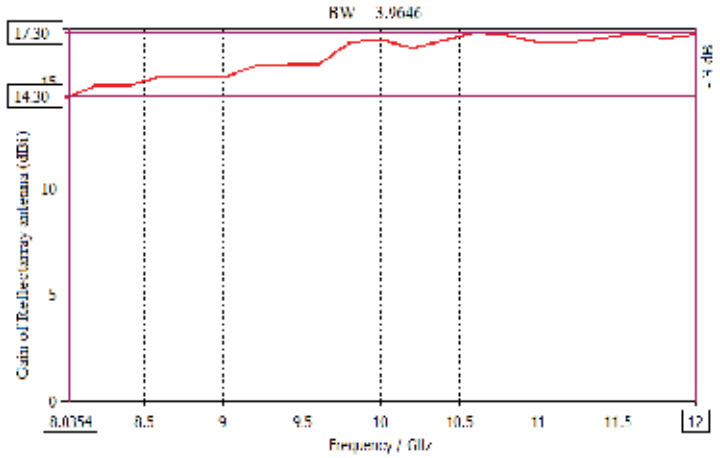

Fig. 12. 3-dB Gain-bandwidth at f/D =1

3.2 Reflectarray Antenna

Based on the proposed unit cell having optimum phase response, an array of 121 elements is designed and simulated. Array is in square pattern as shown in the Fig. 7. A center fed horn antenna operational in X-band is used as a source impinging incident wave normal to the reflecting plane. Each element's individual phase was calculated by the contour of phase distribution.

Radiation pattern in Fig. 11 proves the achievement of 97 % radiation efficiency with high gain of 16.98 dBi. The displacement between the array and horn antenna i.e. fraction of the focal length to the antenna's largest diameter (f/D) is set to a value of 1.0.

Fig. 12 shows that a simulated 3 dB Gain dropping bandwidth of 39.6% is attained, i.e. from 8.035 to 12 GHz at the mid frequency of 10 GHz. Till present, hardly any reflectarrays are able to attain 30% of the bandwidth as can be seen in Table 1. Hence the simulated results are satisfying the wide band nature of reflect array antenna.

3.3 S-Parameters for Different Position of Horn Antenna from the Array

Position of Horn antenna plays an essential role in determining the radiation and aperture efficiency of the designed array [8-9]. Fig. 13 demonstrates different curves of S-parameters which are obtained by placing the horn antenna at various lengths from the array. In this paper two lengths of d = 165mm and d = 323mm are selected for giving the most suitable results on the basis of directivity and gain. By further increasing the distance of horn

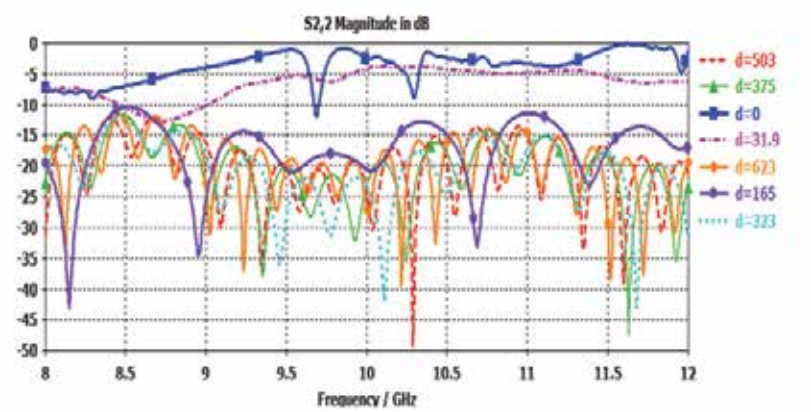

Fig. 13. S-Parameters for Different Positions 'd' of Horn Antenna from the Array

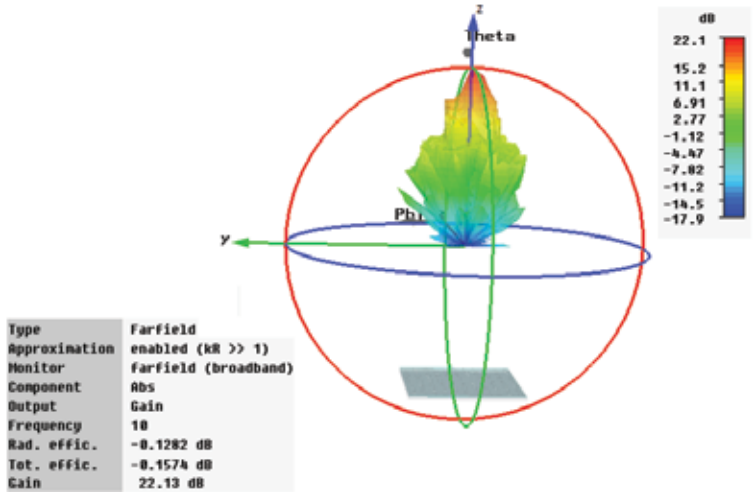

Fig. 14. Far field Radiation for F/D of 1.96 at Centre Frequency of 10 GHz

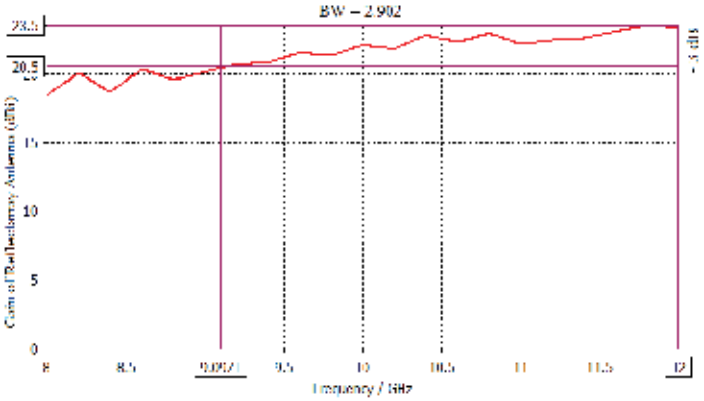

Fig. 15. 3-dB Gain Dropping Bandwidth for F/D=1.96

antenna beyond 323 mm, the effect on S-parameter becomes negligible, i.e. saturation point is reached. Hence distance of 323 mm is chosen for having less simulation time and high gain.

3.4 Simulated Results of RA Antenna at F/D =1.96

Simulated results in Fig. 14 shows that the radiation efficiency is 96% with an increased gain of 22.13 dB at center frequency of 10 GHz. Hence source positioned at 323 mm away from array antenna provides reasonable gain. At a distance larger than the saturation point, simulation time increases without any significant increase in the gain.

Fig. 15 is the gain bandwidth curve of reflectarray antenna for f/D ratio of 1.96. Satisfactory gain of 19 to 23.5 dBi is obtained in the X-band. But now, the 3-db gain-bandwidth is reduced to 29 %. Thus, by placing linearly polarized horn antenna at a distance of 323 mm from the array provides high gain but at the expense of reduced bandwidth.

Consequently, we can draw further conclusion that aperture efficiency of the reflectarray antenna increases with increasing the spacing between horn and array antenna.

4. CONCLUSION

A single layer low profile reflectarray novel element and a resultant reflectarray antenna has been designed, simulated and analyzed in this paper. This reflectarray antenna is proposed for wideband applications at X-band. Using parameterization and optimization method, desired objective of broad band reflectarray antenna design is achieved. 3-dB gain bandwidth of 39.6% is obtained. Till present hardly any reflectarrays are able to attain 30% of the bandwidth. Thus the desired goal of achieving broad band characteristic of RA antenna is validated through the simulation results.

The intended antenna has also been simulated for different f/D ratios to calculate its effect. From simulation results we can conclude that improved aperture efficiency is obtained with increasing distance of source from the reflectarray antenna plane but at the cost of reduced bandwidth and radiation efficiency.

5. REFERENCES

1. J. Huang and J. A. Encinar. *Reflectarray Antennas*. John Wiley & Sons, Inc., USA (2008).
2. Javor, R. D., Wu, X. D., & Chang, K. Design and performance of a microstrip flat reflect-array antenna. *Microwave and Optical Technology Letters 7*(7): 322-324 (1994).
3. Pozar, D. M. Bandwidth of reflectarrays. *Electronics Letters 39*(21): 1490-1491 (2003).
4. Encinar, J. A. Design of two-layer printed reflectarrays using patches of variable size. *IEEE Transactions on Antennas and Propagation 49*(10): 1403-1410 (2001).
5. Encinar, J. A., & Zornoza, J. A. Three-layer printed reflectarrays for contoured beam space applications. *IEEE Transactions on Antennas and Propagation 52*(5): 1138-1148 (2004).
6. Misran, N., Cahill, R., & Fusco, V. F. Design optimisation of ring elements for broadband reflectarray antennas. *IEE Proceedings-Microwaves, Antennas and Propagation 150*(6): 440-444 (2003).
7. Chaharmir, M. R., Shaker, J., Cuhaci, M., & Ittipiboon, A. Broadband reflectarray antenna with double cross loops. *Electronics Letters 42*(2): 65-66 (2006).
8. Bozzi, M., Germani, S., & Perregrini, L. Performance comparison of different element shapes used in printed reflectarrays. *IEEE Antennas and Wireless Propagation Letters 2*(1): 219-222 (2003).
9. Strassner, B., Han, C., & Chang, KCircularly polarized reflectarray with microstrip ring elements having variable rotation angles. *IEEE Transactions on Antennas and Propagation 52*(4): 1122-1125 (2004).
10. Gianvittorio, J. P., & Rahmat-Samii, Y. Reconfigurable patch antennas for steerable reflectarray applications. *IEEE Transactions on Antennas and Propagation 54*(5): 1388-1392 (2006).
11. Riel, M., & Laurin, J. J. Design of an electronically beam scanning reflectarray using aperture-coupled elements. *IEEE Transactions on Antennas and Propagation 55*(5): 1260-1266 (2007).
12. Hum, S. V., Okoniewski, M., & Davies, R. J. Modeling and design of electronically tunable reflectarrays. *IEEE transactions on Antennas and Propagation 55*(8): 2200-2210 (2007).
13. Zainud-Deen, S. H., Gaber, S. M., & Awadalla, K. H. Beam steering reflectarray using varactor diodes. *Japan-Egypt Conference on Electronics, Communications and Computers (JEC-ECC):* 178-181 (2012).
14. Karnati, K., Ebadi, S., & Gong, X. Effects of inter-element spacing on mutual coupling and resonant properties in reflectarray unit cell design. *Radio and Wireless Symposium (RWS)*: 83-86 (2012).
15. Zhang, K., Li, J., Wei, G., Fan, Y., Xu, J., & Gao, S. Design and optimization of broadband single-layer reflectarray. *Proceedings of the International Symposium on Antennas & Propagation (ISAP) 2*:

1226-1229 (2013).

16. Ismail, M. Y., & Shukri, M. F. M. Study of Phasing Distribution Characteristics Of Reflectarray Antenna Using Different Resonant Elements. *International Journal of Integrated Engineering 1*(3): 47–52 (2009).
17. Ismail, M. Y., & Abbasi, M. I. Analysis of design optimization of bandwidth and loss performance of reflectarray antennas based on material properties. *Modern Applied Science 4*(1): 28 (2009).
18. Ismail, M. Y., Abbasi, M. I., Zain, A. F. M., Amin, M., & Abdullah, M. F. L. Characterization of loss and bandwidth performance of reflectarray antenna based on lumped components. *Int. J. Electr. Electrocnics Informatics 2*(2): 113-122 (2010).
19. Hum, S. V., Okoniewski, M., & Davies, R. J. An evolvable antenna platform based on reconfigurable reflectarrays. *NASA/DoD Conference on Evolvable Hardware :* 139-146 (2005).
20. Gosal, G., McNamara, D., & Yagoub, M. Transmitarray Antenna Design Using Forward and Inverse Neural Network Modeling. *IEEE Antennas and Wireless Propagation Letters 15*: 1483-1486 (2016).
21. Prado, D. R., Arrebola, M., Pino, M. R., & Las-Heras, F. Improved Reflectarray Phase-Only Synthesis Using the Generalized Intersection Approach with Dielectric Frame and First Principle of Equivalence. *International Journal of Antennas and Propagation* 1: (2017).
22. Chen, X., Chen, Q., Feng, P., & Huang, K. Efficient design of the microstrip reflectarray antenna by optimizing the reflection phase curve. *International Journal of Antennas and Propagation* 1: 6–8 (2016).
23. Abbasi, M. I., & Ismail, M. Y. Reflection loss and bandwidth performance of X-band infinite reflectarrays: Simulations and measurements. *Microwave and Optical Technology Letters 53*(1): 77-80 (2011).
24. Ismail, M. Y., & Shukri, M. F. M. Study Of Phasing Distribution Characteristics Of Reflectarray Antenna Using Different Resonant Elements. *International Journal of Integrated Engineering 1*(3): 47–52 (2009).
25. Zhang, Y. S., Zhang, H., & Jin, J. A novel broadband reflect-array antenna with rectangle ring element for Ku-band application. *IEEE MTT-S International Microwave Workshop Series on Millimeter Wave Wireless Technology and Applications (IMWS)* :1-4 (2012).
26. Arshad, M. K., Tahir, F. A., & Rashid, A. Design of a single layer reflectarray unit cells based on hexagonal ring for wideband operation. *International Symposium Antennas and Propagation Society (APSURSI):*815-816 (2014).

Proceedings of the Pakistan Academy of Sciences:
A. Physical and Computational Sciences 55 (3): 35–44 (2018)

ISSN: 2518-4245 (print), 2518-4253 (online)

Pakistan Academy of Sciences

Research Article

Integrated Infrastructure Management Using Web-GIS Application

Muhammad Aqiff Abdul Wahid[1], Khairul Nizam Abdul Maulud[2*], Muhammad Amartur Rahman[3], Mohd Aizat Saiful Bahri[3], and Othman Jaafar[2,3]

[1]Earth Observation Centre (EOC), Institute of Climate Change,
Universiti Kebangsaan Malaysia, Malaysia
[2]Smart & Sustainable Township Research Centre, Faculty of Engineering & Built Environment,
Universiti Kebangsaan Malaysia, Malaysia
[3]Prasarana UKM, Universiti Kebangsaan Malaysia, Malaysia

Abstract: The aim of this research is to build a web application using Geographic Information System (GIS) Technology and at the same time can assist the university in managing infrastructure asset. Infrastructure assets information which is stored using conventional methods such as in paper form; paper maps; and drawings are not reliable anymore. However, this information can be used by converting them into a geospatial data format. Furthermore, a geodatabase is created to store all the information. Spatial data and attribute data are connected to each other in the geodatabase. ArcGIS Desktop is an application to create, manage, edit, manipulate, visualize and publish geospatial data. The publish service will be used in ArcGIS Online and act as a medium to customize a webmap application. The web-map application is capable to provide and visualize the spatial and non-spatial information of each infrastructure asset. In addition, assets information can easily be shared among the university management and with the advantage of GIS mapping, the information can be understood by everyone. The research investigates the infrastructure asset management using ArcGIS Online and how it can improve the conventional method of asset management.

Keywords: ArcGIS Online, Geospatial, Infrastructure management, Web application, UKM

1. INTRODUCTION

Universiti Kebangsaan Malaysia (UKM) is one of the oldest universities in Malaysia and it is almost 50 years old. Within the last 50 years, a lot of new development and improvement has been done to provide better services to its community and the organizations. Infrastructure management is an aspect that is very important for an organization like UKM. Such organizations which provide services and in this case education services would need a proper workflow in managing all its infrastructures. Without a proper workflow in managing infrastructure assets, the organization tends to lose profit and also the customers, in these contexts the students of the university. As mentioned by E. Too [1], L. Hardwicke [2], and Mandele et al [3], economic growth also depends on the imperative role of the infrastructure assets. Therefore, massive attention is required to have good infrastructure assets management because of the big roles its have within the organizations.

An asset is a store of value and one that creates benefit for the organizations. It is something that business possesses and deploys to create some future benefit. Cash, inventory, property, plant, and equipment are all considered business assets because they have value and can give benefit to the organizations [4]. Hastings [5] define asset management as the set of activities that are associated with identifying what type of assets are needed, identifying funding requirements, acquiring assets, providing logistic and maintenance support systems for the assets, and disposing or renewing assets. Asset management is a strategic and integrated set of processes to gain lifetime effectiveness, utilization and returns from physical

Received: April 2018; Accepted: September 2018
* Corresponding Author: Khairul Nizam Abdul Maulud; knam@ukm.edu.my

assets. In addition, infrastructure asset is a multiplex structure with extremely important and essential elements for an organization [6]. By understanding asset management, it will help organizations to manage the complexity of the infrastructure assets information.

Information Technology (IT), however, is the prime enabler of success in managing asset for organizations. This day, IT utilized for asset management is required to provide an integrated view of lifecycle information. Such an integrated view not only provides for the decentralized control of asset management tasks but also allows for holistic and informed decision support. A critical aspect of IT adoption is to find the strategic fit between the way an organization manages its assets and the technologies selected to aid in its execution [7]. This is supported by Hastings [5], IT in asset management has three major roles. IT is utilized in the collection, storage, and analysis of information spanning asset lifecycle processes. Secondly, IT provides decision support capabilities through the analytic conclusions from analysis of data. Thirdly, IT provides an integrated view of asset management through processing and communication of information and thereby allow for the basis of asset management functional integration. Generally, it means that the ultimate goal of using information systems for asset management is to create information enabled an integrated view of asset management. These inter-related components of asset management would benefit from what GIS technology can be offered nowadays [8,9].

Spatial and information system capabilities of GIS technology have been long recognized in assisting asset management. Baird [10] state that, GIS has become an obvious choice of the solution in asset management because of the extended use of asset information with spatial information. Spatial information capable answering all the questions about locations, patterns, trends, and condition [11]. This is supported by Campbell et al [12], taking the point of knowing what and where the location of the assets is where GIS comes to be acknowledged. A system with spatial integration is capable to analyses a complex data structure based on spatial location, such as visualize data using a map using various relation to show the proximity, adjacency, and others spatial relationship. For decades, most assets information was confined to use on desktop-based PCs and could not be easily accessed or shared with other organizations. Nowadays, GIS technology also capable to host the asset information and shared the information across not only computers but in any mobile devices at anywhere and anytime. This is possible because of the new emerging technology, science and mathematics which influencing the approaches and understanding of the importance of asset management.

Nevertheless, the traditional method is still widely used in asset management, many organizations required their staffs to record down all the information in a paper form and later transferring the information into the digital database in tabular format. Meanwhile, human errors might happen during the process of transferring data of non-digital format as handwriting in a report form, it can get smudged or unrecognizable, typos and unintentional mismatches among data can occur as well [13]. This is very common mistakes when transferring information between different formats. However, this issue cannot be overlooked, technical staffs may not see the problem when such an incident occurred, but this kind of information is very important for the management. Management of an organization needs a lot of information and details in order for them to make decisions. Small errors in the information might produce a big impact on their decisions. Other than that, management also need to get the information in a very simple way but precise and the information need to be easy to understand, also the information can be access anywhere and anytime.

Therefore, GIS technology and its web applications technology can be a new approach for solving the issues of storing assets information using geodatabase and to make the information can be shared with other organizations. In addition, the information can be visualized with spatially related information which other asset management application does not have. GIS application will only help the organization to reduce the workload of their workers and also keep the updated data in their geodatabase. Samiullah [14] mentioned that GIS is very effective tools that can save time and resources. Besides, when the assets are linked to a geographic location and visualize it on a map, it can be a powerful decision-making tool [15]. In addition, GIS provides an efficient platform for better management of assets and outages, planning

and analysis, improving customer service, and increased the accuracy of data. This paper will briefly discuss the process of building a geodatabase that stores asset information, also how to publish the information and make it available online using web GIS application.

2. METHODOLOGY

This study was conducted to customize web applications using ArcGIS Online – WebApp Builder to visualize the information of infrastructure in UKM and also to integrate the information of all infrastructures with GIS geodatabase. The study will cover UKM, Bangi area and the focus are the buildings, roads, sewages, pipelines, and garbage bins as shown in Fig. 1.

Web GIS applications should be able to provide an informative solution to users. Combining the database that keeps all the information of the infrastructures and a geodatabase that contain the spatial information of the infrastructures and to visualize in one application would be the main task of this study. The study is divided into four phases as a guideline and each phase needs to be done according to the guideline in order to ensure the objectives can be achieved. Fig. 2 used to show the workflow of the study.

3. DATABASE DESIGN

A geodatabase is a place where all the spatial data and non-spatial data are stored. A geodatabase will be developed to occupy the needs of UKM's infrastructure management. The planning and design should take place before database development phases. This is to ensure that the databases can operate like it needs to be. Besides, a good database is important to support all operations and analysis [15].

There are three sub-phases in database design which are conceptual, logical, and physical.

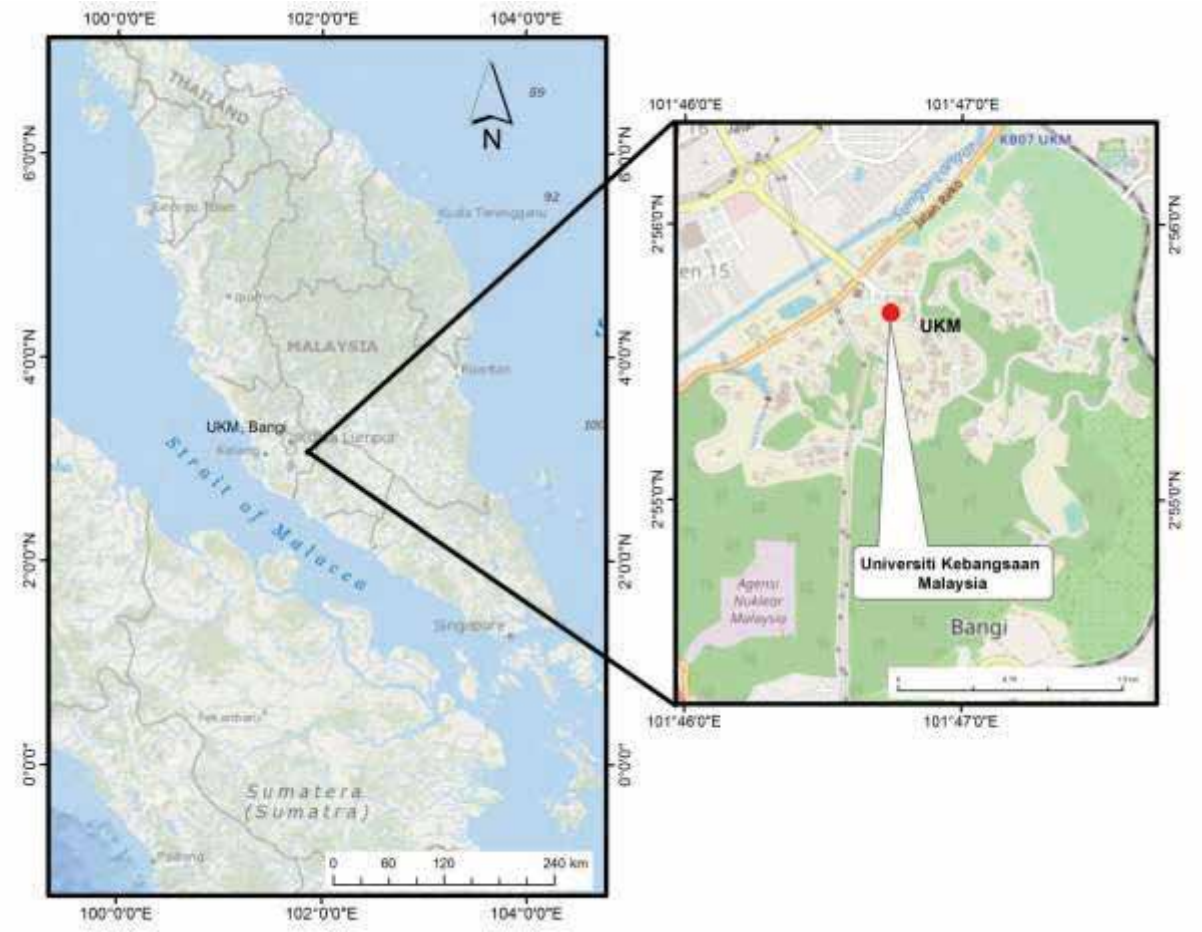

Fig. 1. Study area (UKM, Bangi)

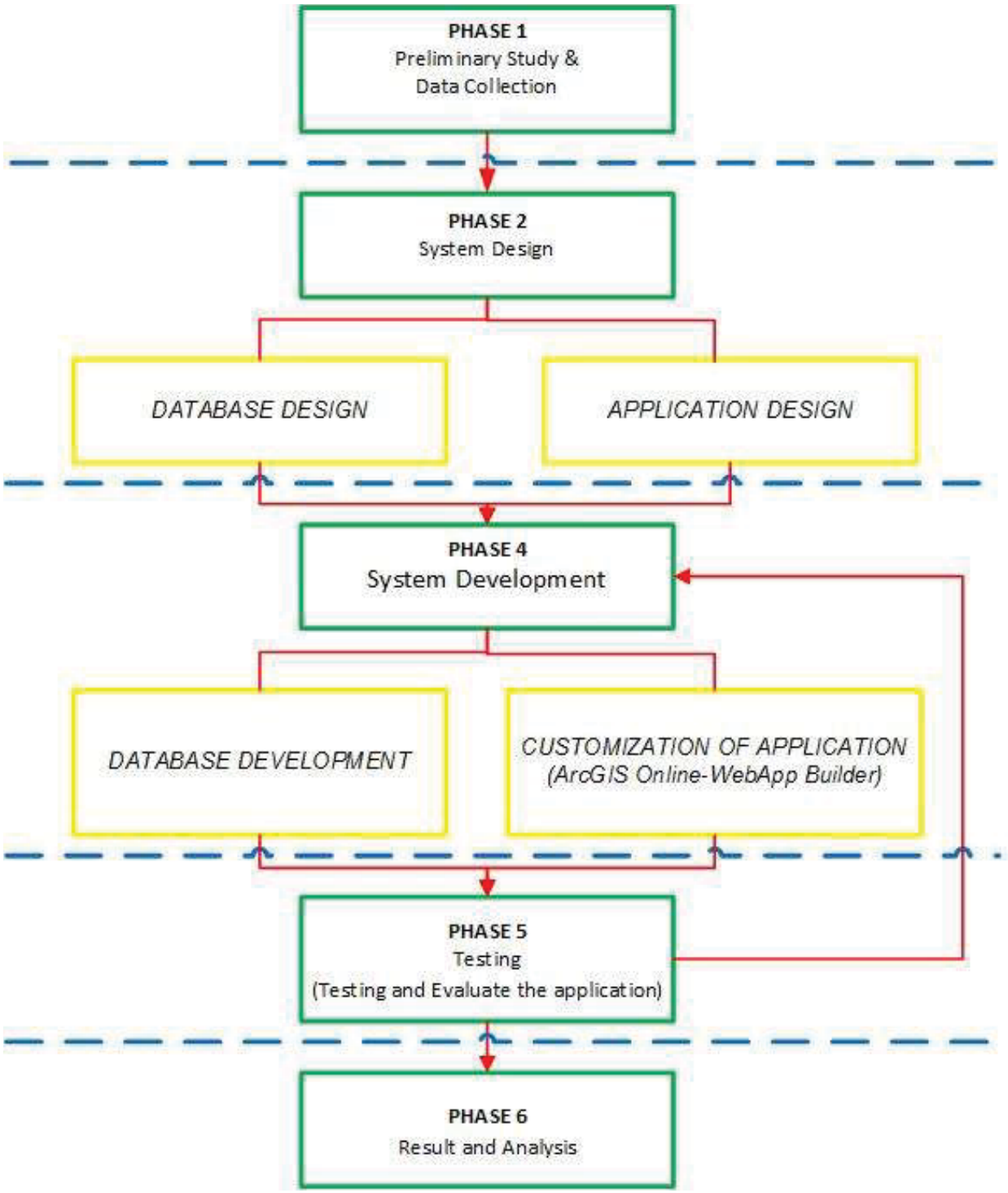

Fig. 2. Study framework

3.1 Conceptual

Conceptual design is a very important process in database design. This process will describe the data model for the application and also the overall scheme of the database. The database will be hosted in ArcGIS Online cloud service where the services will be shared to an authorized person only. This is to ensure the data security. Open Street Map (OSM) basemap is used as a basemap for this application, this is to reduce the time for data processing while loading the web applications. By using ESRI's basemap layers, the process of uploading the basemap is simpler compared to uploading user own basemap. The service hosted can be access at the same time by the multi user as shown in Fig. 3.

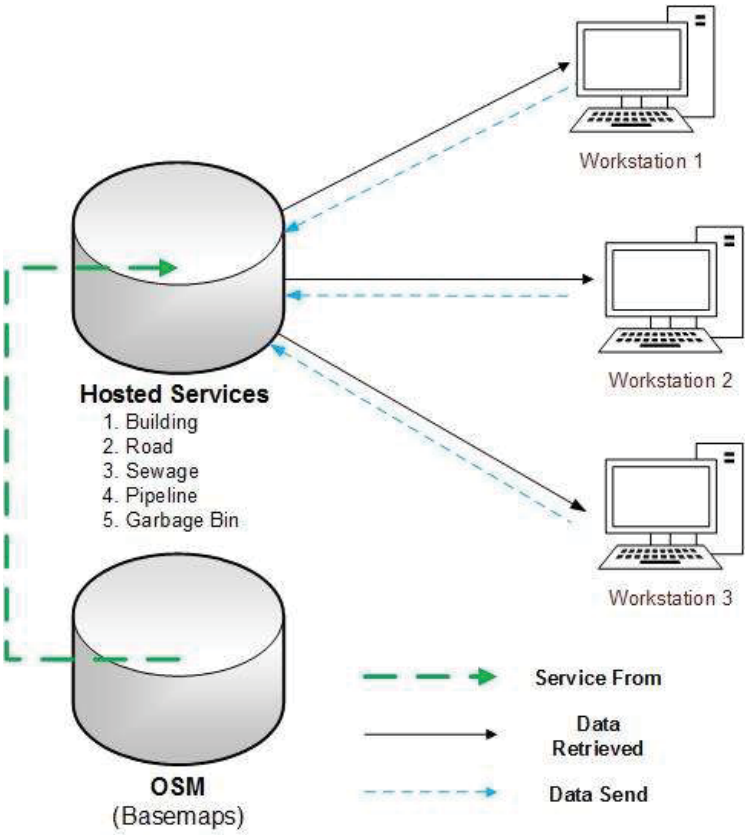

Fig. 3. Conceptual design

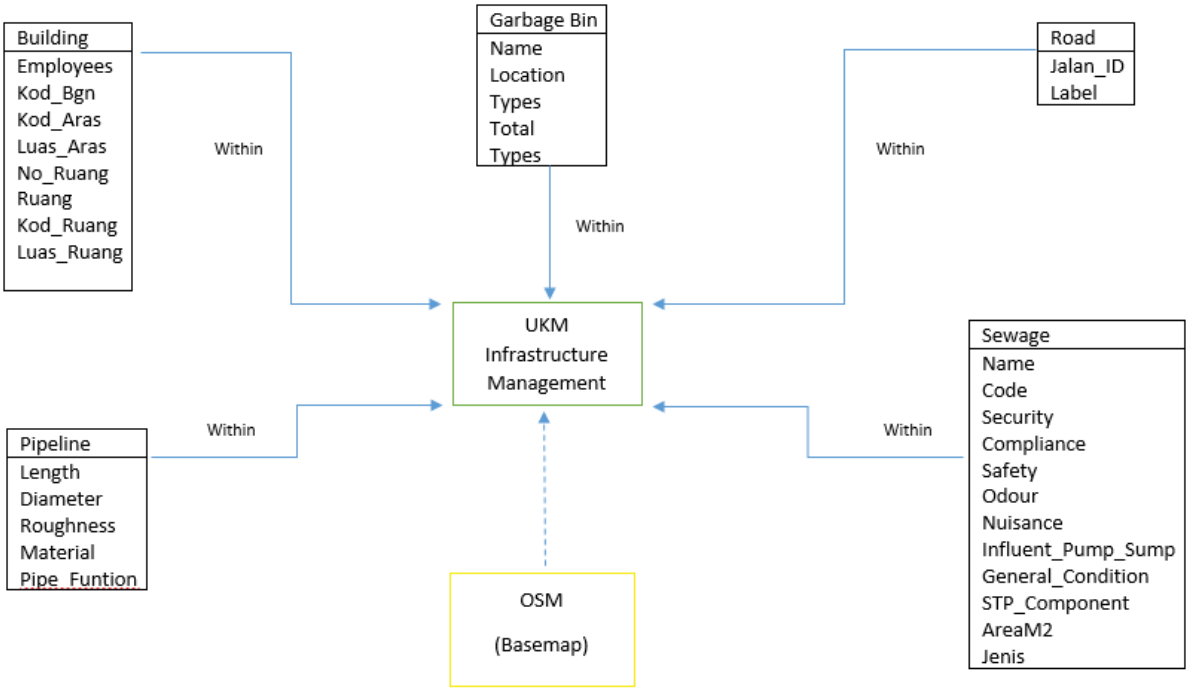

Fig. 4. ER Diagram for UKM infrastructure database

3.2 Logical

The logical design is the end users view of the data environment. End users are the people who use the application programs as well as those who designed and implemented them. The data storage is shown in the entity relationship logically as shown in Fig. 4. In logical design, the high-level data model of conceptual design is changed into a Database Management System (DBMS) data model.

3.3 Physical

The physical model requires the designer to match the conceptual model's characteristics and constraints to those of the selected hierarchical, network or relational database model. Because the physical design depends on the specific database software, it is said to be software dependent [16]. Fig. 5 shows the Geodatabase developed for UKM infrastructure management using Arc Catalog.

4. ARCGIS ONLINE

There are a lot of methods and techniques have been developed to provide a better process for infrastructure management. However, most of these applications were developed to work as a standalone system and with limited functionality such as inventory and condition data management [17]. This limitation makes the process inefficient, time-consuming and tends to produced errors when interpreting the information.

ArcGIS Online technology is a convenient method to use for publishing spatial data online [18]. It is a collaborative, cloud-based platform that allows members of an organization to use, create, and share maps, apps, and data, including authoritative basemaps published by ESRI. Through ArcGIS Online user will get access to ESRI's secure cloud, and use it to manage, create, store, and access data as published web layers, and because ArcGIS Online is an integral part of the ArcGIS system, user can use it to extend the capabilities of ArcGIS for Desktop, ArcGIS for Server, ArcGIS apps, and ArcGIS Web APIs, and ArcGIS Runtime SDKs.

4.1 Publish a Service

As mention above, geodatabases are prepared in ArcGIS Catalog and Desktop. The geodatabase or offline data such as polygon, line, point and raster need to be published to be available online. Hosted service will be published in the organization account which is "Universiti Kebangsaan Malaysia". There are two types of services are available which are tiled map and feature service.

Tiled map service work like a cache map service. The entire map will be drawn in several different scales and stores copies of the map images. As a result, each time user request for the same service

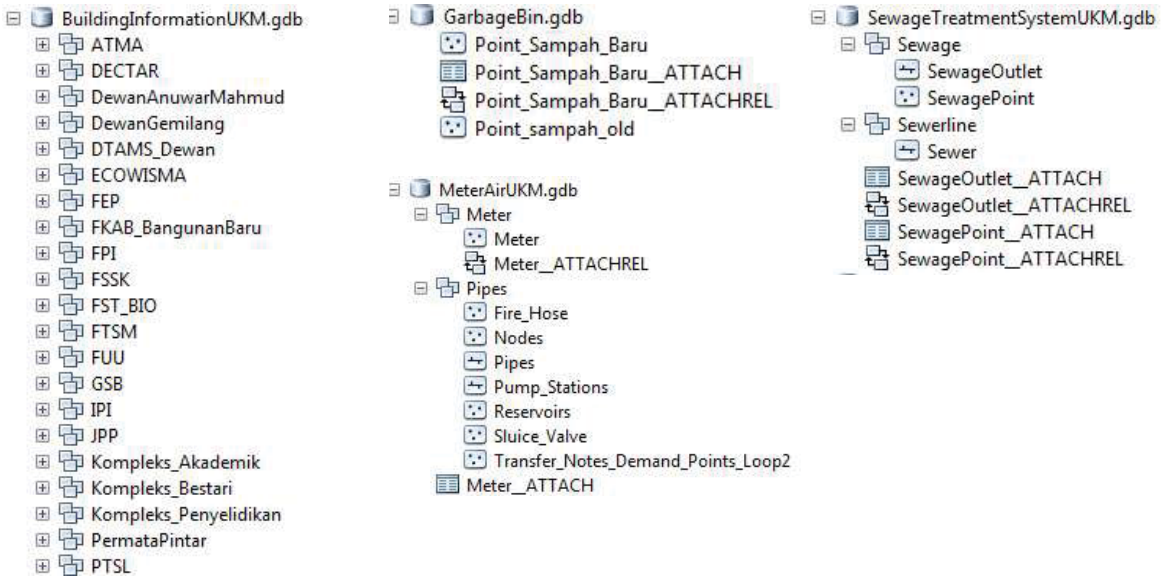

Fig. 5. Physical geodatabase of UKM infrastructure

the output will be quicker because it only needs to recall the caches rather than drawn the map again. Feature service allows the user to alter the data such as edit, add, delete, and update the data. Tiled map service does not have this service because the service is published as images of the data.

There are building, road, pipeline, sewage and garbage bin services and each has one GIS web applications. As mention above, the map of each data is prepared in ArcMap and the service will be published from ArcMap. It required an Internet connection. The user needs to sign in and use the same organization account. Once the process to publish and host feature layer in ArcGIS Online is complete user can see the services in organization account and proceed with creating a map and share it as web map and web applications.

4.1 Create and Share Map

In this phase a map will be created to be used to build a web app. Starting with a basemap, configuring the data, and customizing the application settings. Finally, all the maps information will share with all members in the group created before. The layer that published before will be added to a new map. The default basemap used were standard ArcGIS Topographic basemap. For this map, OSM maps are chosen as the basemap.

As mention above, the web applications will be created a base on the type of infrastructures. Each type will have different web map. Fig. 6 shows one of the web maps of the garbage bin. All web map will be used the same basemap. Next, the user adds the feature layer and configures the symbology and how the attributes will look to the end user.

5. RESULT AND DISCUSSION

ArcGIS Online already provides templates that can be used for the web applications and the user also can choose to build new applications using Web App Builder. Web App Builder offers a lot of choices in configuring the appearance, settings and functionality of the web application. This is more convenient methods to create a new application with a different identity from the given templates.

The web application used visual and compositional themes offer in the Web App Builder and following widgets layer list, attribute table, print, zoom slider, measurement, home, scalebar, coordinate and filter are added to provide more options for the user. Once the web applications are ready, it has an option where it can be shared among the organization members. Only an authorized member will have access to the web application because of the data security issues. The following are the results of each infrastructure asset management based on their type of infrastructures.

As shown in Fig. 7-11, each application using OSM basemap respectively. The user can view the attributes each feature by selecting the feature, and

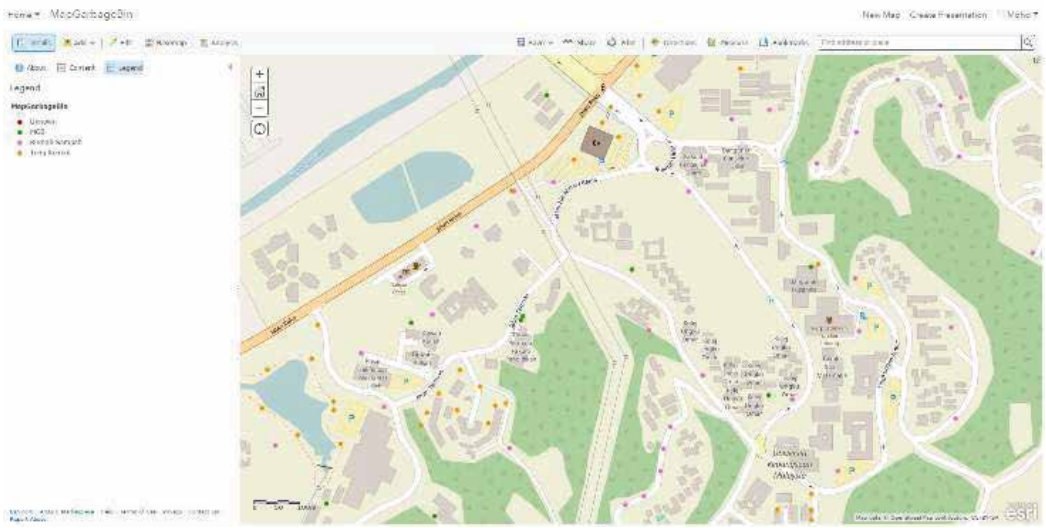

Fig. 6. Garbage bin web map

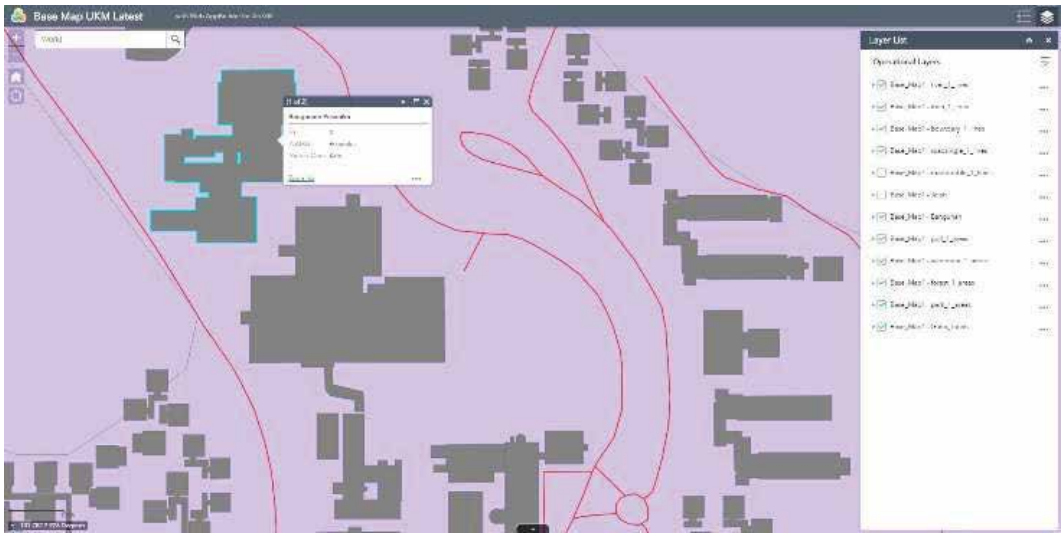

Fig. 7. Building web applications

Fig. 8. Road web applications

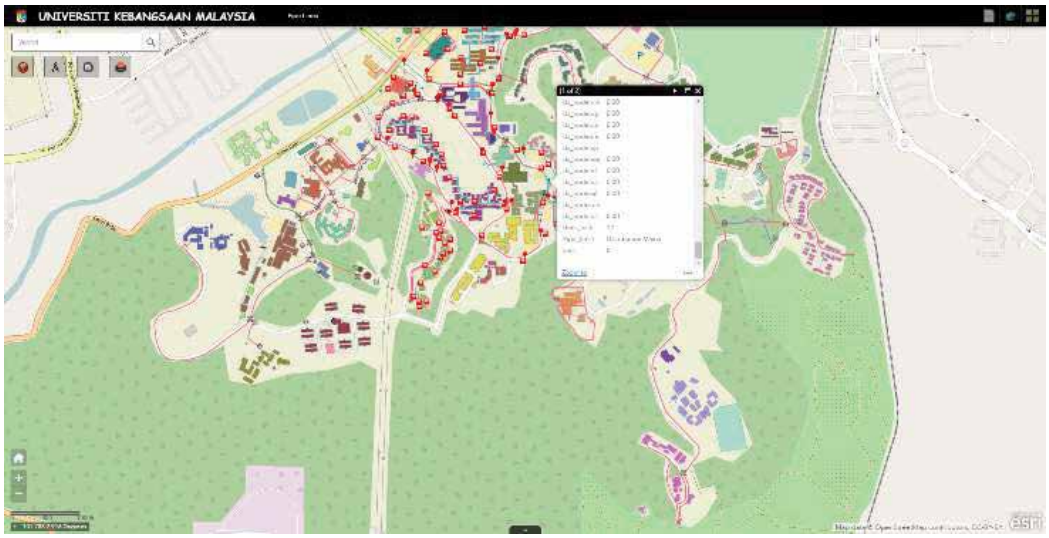

Fig. 9. Pipeline web applications

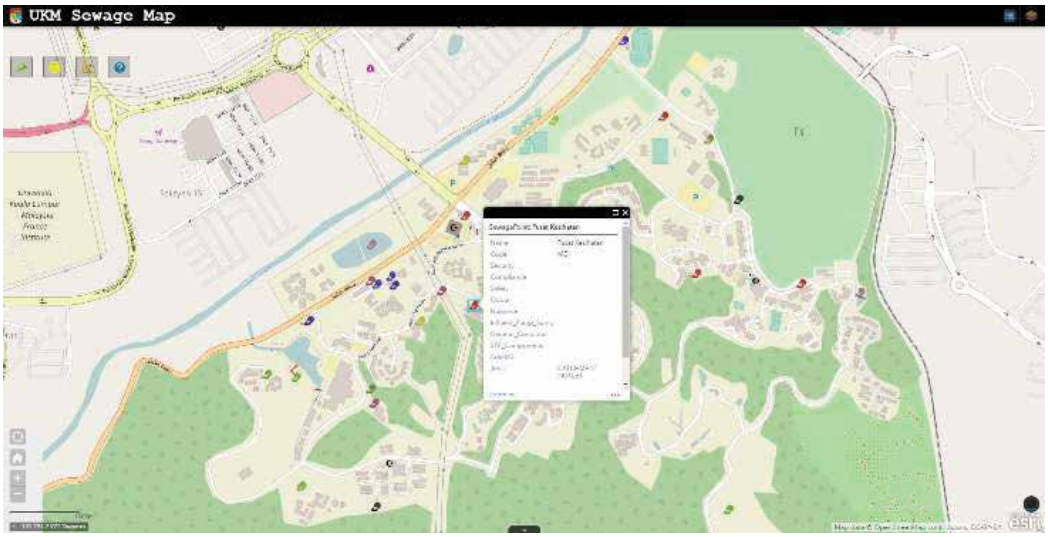

Fig. 10. Sewage web applications

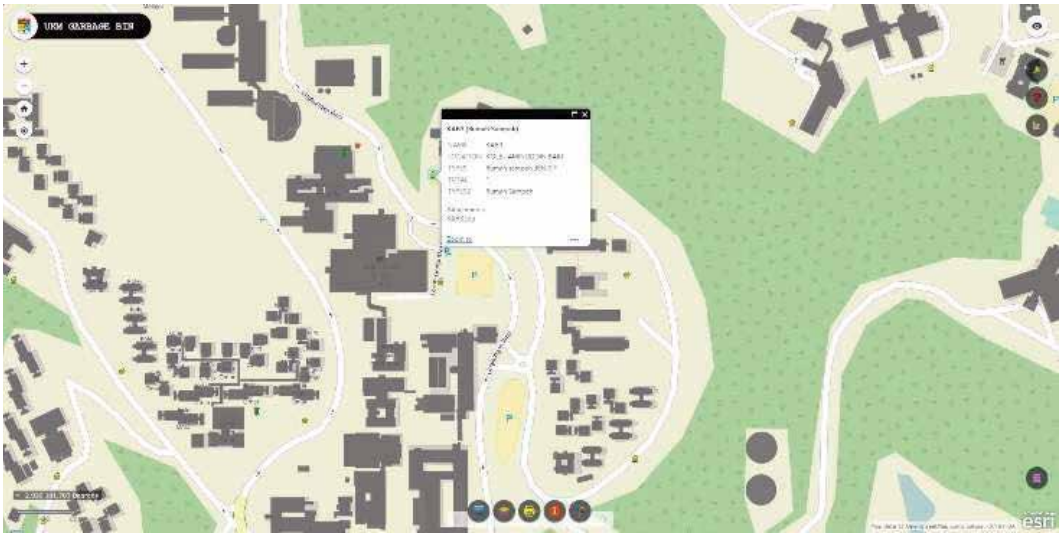

Fig. 11. Garbage bin web applications

attributes windows will come out and list out all important information. Through this application, the user will not only have the information of the asset and will be able to identify the location of the asset from the map view. The choices of the basemap also vary and the user has the option to choose which better suit the application.

Every steps and process in developing the web applications require absolute attention which starts from the data collection and preparation, second designing and developing the geodatabase, third configuration before publishing the data, fourth customization of the web applications and lastly publish the web applications. Any steps or processes that not follow the right methods will affect the next flow of the process. However, there is still a lot of improvement that can be done to maximise the effectiveness of the application but through this research hopefully will give the ideas on how GIS can aid asset manager and the university.

6. ADVANTAGES OF ARCGIS ONLINE

ArcGIS Online has proved to be a good option that quickly and user-friendly application to represents spatial data. Multi users can also access the data simultaneously from anywhere anytime. The user can also add attachments such as pictures and PDFs. The services that hosted can also be used in others

web map and web applications at the same time.

7. CONCLUSION

The present study was to introduce a new method to be used for infrastructure management of UKM using ArcGIS Online web applications. ArcGIS Online has been chosen because of the capabilities of the application in providing a good platform for the user to customize and configure the applications based on the user needs. The process of storing and visualizing the information of the infrastructure becomes more convenient and efficient. Moreover, useable to access the latest data and share it among the members of the organization.

A good infrastructure asset management will always benefit the organization in many ways. It will also be a great help to management in making better planning and decisions for the better future of the organization and its customers.

8. ACKNOWLEDGMENTS

The authors acknowledge and are thankful for the financial support given by the Universiti Kebangsaan Malaysia Top Down Grant through KRA-2018-019, TD-2016-012.

9. REFERENCES

1. Too, E. Infrastructure asset: developing maintenance management capability. Facilities30: 234–253 (2012).
2. Hardwicke, L. Australian infrastructure report card. Barton, ACT: Engineers Australia(2005).
3. Mandele, M.V.D. Walker, W. &Bexelius, S. Policy development for infrastructure networks: concepts and ideas.Journal of Infrastructure Systems12(2): 69–76 (2006).
4. Advani, R. Chapter 1: Assets, Financial Freedom: A Guide to Achieving Lifelong Wealth and Security. Springer-Verlag New York (2013).
5. Hastings, N. Physical Asset Management. Springer London (2010).
6. Lemer, A.C. Progress toward integrated infrastructure-assets-management systems: gis and beyond. APWA International Public Works Congress NRCC/CPWA Seminar Series "Innovations in Urban Infrastructure, 410: 7–24 (1998).
7. Haider, A. Information and Operational Technologies Governance Framework for Engineering Asset Management. Springer London (2012).
8. Nasir, N. A. M., Maulud, K. N. A. & Yusoff, N. I.M.Geospatial analysis of road distresses and the relationship with the slope factor. Journal of Engineering Science and Technology, Vol. 11 No. 5: 655-665 (2016).
9. Yusoff, N.M.R. Shafri, H.Z.M. &Muniandy, R.. An effective road management system using web-based GIS software. 7thIGRSM International Remote Sensing & GIS Conference and Exhibition. 1-8 (2014).
10. Baird, G.M. Leveraging your GIS, Part 1: Achieving a low-cost enterprise asset management system. Journal American Water Works Association. 102(10): 16–20. 2010.
11. Heywood, D.I. Cornelius, S. & Carver, S.An introduction to geographical information systems. Harlow, England, N.Y, Prentice Hall (2011).
12. Campbell, J. Jardine, A. & McGlynn, J. Asset Management Excellence. Boca Raton: CRC Press(2011).
13. Lemmens, M.Geo-information, Geotechnologies and the Environment 5, Springer Science+Business Media B.V. (2011).
14. Samiullah, R, A. Shah, S.A.A. Khan, S. & Khan Z.Identification of suitable sites for solid waste disposal using GIS multi-criteria analysis in Peshawar, Pakistan. Proceedings of the Pakistan academy of sciences, 53(4): 309-321(2016).
15. ESRI. GIS for utilities and communication. Retrieved on October, 23, 2013, from http://www.esri.com/industries/utilities-communication. (2013)
16. Awange, J. L. & Kyalo, J. B. Chapter 16: GIS Database, Environmental Geoinformatics. Springer Berlin Heidelberg. (2013).
17. Halfawy, M.R. Pyzoha, D. & El-Hosseiny, T. An integrated framework for GIS-based civil infrastructure management systems. In Proceedings of the Canadian Society for Civil Engineers (CSCE) Conference, Montreal, Canada. (2002)
18. Seamann, P. Web mapping application of Roman Catholic Church administration in the Czech lands in the early modern period. Geoinformatics FCE CTU 16(1), (2017).

Proceedings of the Pakistan Academy of Sciences:
A. Physical and Computational Sciences 55 (3): 45–51 (2018)

ISSN: 2518-4245 (print), 2518-4253 (online)

Pakistan Academy of Sciences

Research Article

Fabrication and Analysis of a Triple Band Patch Antenna

Gulzar Ahmad*, Asif Sultan, M. Inayatullah Khan Babar, Majid Ashraf, and Tariqullah Jan

Department of Electrical Engineering, University of Engineering and Technology, Peshawar, Pakistan

Abstract: The paper presents the design and fabrication of a patch antenna of hexagonal shape on FR-4 lossy substrate of 1.6mm thickness. To achieve multi bands an inverted C-Shaped cut was etched in the patch. The antenna has over all dimensions of $61\times48\times1.6mm^3$. Microstrip line feed has been used for the excitation purpose of the antenna. Measurements of Return Loss (RL), Voltage Standing Wave Ratio (VSWR) and Input Impedance were taken using Vector Network Analyzer (VNA) of Rohde & Schwarz Company. The antenna offered three bands with resonant frequencies of 3.36GHz, 4.06GHz and 7.01GHz lying in S and C bands. The -10dB bandwidths achieved are 60MHz (3.340GHz-3.400GHz), 76MHz (4.033GHz-4.109GHz) and 754MHz (6.391GHz-7.145GHz) with corresponding return losses of 20.23dB, 16.30dB and 25.24dB respectively. VSWR of the antenna for all the above mentioned three bands remains below 2. The antenna can be used for different military and commercial applications in S and C bands.

Keywords: Vector Network Analyzer, FR-4, Microstrip Line Feed, Triple Band, Patch Antenna

1. INTRODUCTION

Antenna plays a vital role in wireless communication. It converts the electrical energy into EM waves at the transmitter and EM waves into electrical energy at the receiver side. Modern communication devices like smart phones urge the development of smart and compact size antennas. Trends in recent development in communication show the demand of integrating many wireless systems in one single device. Demand for research on small and multiple antennas have correspondingly increased [1]. Multi band and wide band antennas are preferred instead of using multiple antennas. However,in order to design a single antenna to cover multiple bands like GSM, GPS, WiFi, WLAN, Bluetooth and LTE bands is a difficult task and is need of the hour. The Reciprocity Theorem can be applied to antenna, so if antenna is tested in the transmitting mode, the same characteristics can be used in the receiving mode as well. IEEE defines the electromagnetic spectrum of the S-band as well as C-band. S-band covers frequencies from 2 to 4 GHz. The C-band is a part of microwave band and it covers the frequency from 4 to 8GHz as given in Table-1. In this work a patch antenna has been fabricated and tested in the laboratory of one of the esteemed institutes of our homeland that gives good results in three different bands.

2. LITERATURE REVIEW

A microstrip patch antenna in its most simple form is a tri layer structure. The three layers are patch, ground and a dielectric substrate sandwiched between the two as shown in the Fig. 1 [2]. The patch and ground layers are prepared of a conducting material like Copper or Gold. The patch may be of any arbitrary shape but the most common shapes are shown in Fig. 2 [2]. The substrates used in the patch antennas have dielectric constant ranging from 2.2 to 12. Various techniques are used to excite the patch like micro strip line feed, coax feed, aperture coupling and proximity feed. The most common

Table 1. Bandwidth of S and C-Band

Designation of Band	Bandwidth
S- Band	2GHz-4GHz
C-Band	4GHz-8GHz

Received: April 2018; Accepted: September 2018
* Corresponding Author: Gulzar Ahmad; gulzar@uetpeshawar.edu.pk

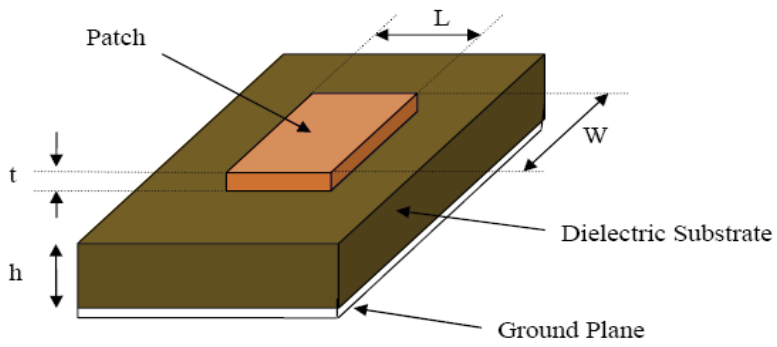

Fig. 1. Microstrip Antenna

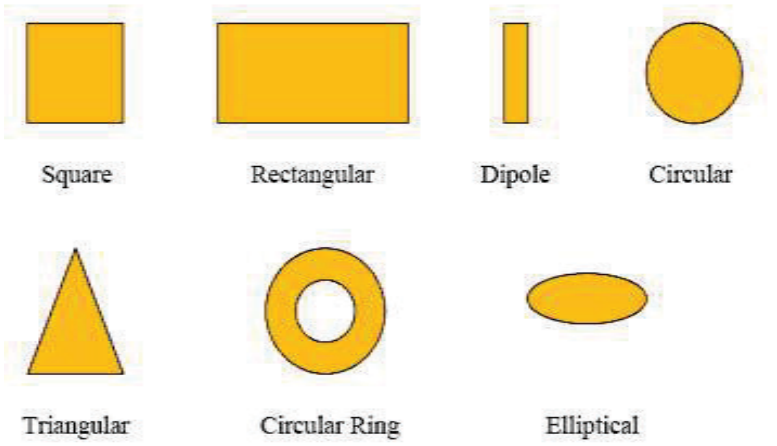

Fig. 2. Various common patch formats

method of analysis of patch antenna is transmission line model. Micro strip antenna has numerous benefits like small size, low profile, light weight, easy fabrication and conformability. The two main weaknesses associated with patch antenna are low bandwidth and reduced gain. Various studies have been conducted for finding broad banding techniques of micro strip patch antennas [3-11]. Many researchers have also focused their work on multi-banding techniques of micro strip patch antennas [12-16].

In [17] a multiband design of 42×54mm^2 have a bandwidth of 90MHz at the center frequency of 6.7GHz and the dB value of reflection coefficient(r) in this research is -17dB. In [18] a multiband design of 30×40mm^2 have a bandwidth of 190MHz at the center frequency of 6.3GHz and the dB value of r in this research is -30.56dB. In [19] a multiband design of 35×26mm^2 have the center frequency of 6.7GHz and the dB value of r in this research is -13dB, while the bandwidth has not been mentioned by the author. In [20] a multiband design of 47×50mm^2 has been elaborated which has got a bandwidth of 200MHz at the center frequency of 6.7GHz and the dB value of r at the mentioned frequency is -17.89dB [21] explains the multiband patch having length of 30mm and width of 30mm as well. The center frequency of 6.3GHz has attained a reflection coefficient of -14dB and its reported bandwidth is 200MHz.

3. DESIGN AND FABRICATION OF THE ANTENNA

The basic dimensions of the antenna were derived using formulas in [2] and [17]. To attain multiband behavior C shaped cut was employed in the hexagonal patch. The proposed antenna was practically fabricated and experimentally investigated. The complete sketch of suggested antenna is presented in Figure 3. The ground plane has same dimensions as the substrate so Lg and Wg in the following Fig.3 define the length and the

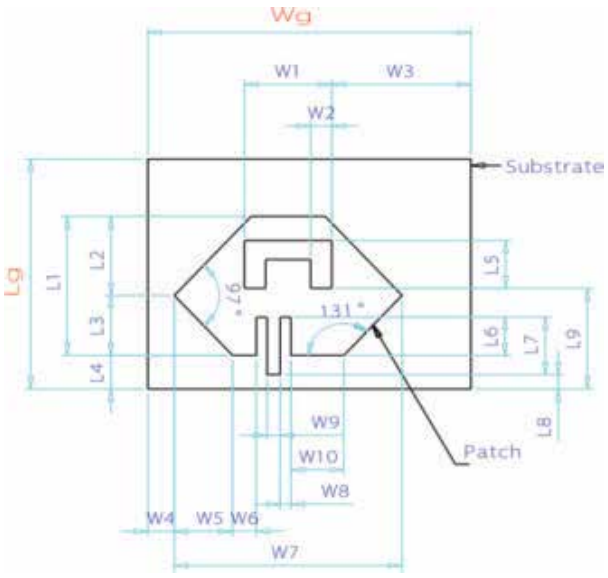

Fig. 3. Sketch of the planned antenna

Table 2. Geometrical measurements of the antenna

Parameters	Size (mm)	Parameters	Size (mm)
Wg	61	W10	10
Lg	48	L1	29
W1	16.5	L2	16.5
W2	4	L3	12.5
W3	26.3	L4	7
W4	5	L5	10
W5	11	L6	8
W6	4.5	L7	12
W7	43	L8	3
W8	2	L9	21
W9	2.5		

width of the ground. The geometrical dimensions are given in Table 2. FR-4 material is used for substrate and it has a thickness of 1.6mm. FR-4 has been selected for the substrate of this design as the antenna has been fabricated indigenously and this material is readily available in the local market and gives good results. The thickness of patch and ground conductor is 0.035mm. The patch is hexagonal shaped with a C-shaped cut as in Fig. 3.

4. RESULTS AND DISCUSSION

The fabricated indigenous antenna was experimentally tested for important performance parameters using vector network analyzer of Rohde & Schwarz, Model FSH20 as shown in Fig. 15.This vector network analyzer has the capacity to measure the bandwidth, return loss, antenna impedance under resonance condition and the voltage standing wave ratio. The measuring capacity of this analyzer is from 1KHz to 8GHz. The obtained results for Return loss, Voltage Standing Wave Ratio, Antenna impedance are briefed in Table 3.

The three resonant frequencies are 3.36GHz, 4.06GHz and 7.01GHz and these three central resonant frequencies are denoted by M_1, M_2 and M_3 in Fig. 4. The three frequency bands are

Table 3. Summary of the results of the fabricated structure

Resonance frequency	3.36 GHz	4.06 GHz	7.01 GHz
Bandwidth	60 MHz	76 MHz	754 MHz
Bandwidth	1.78 %	1.87 %	10.75 %
Return Loss	-20.23 dB	-16.30 dB	-25.24 dB
VSWR	1.22	1.36	1.12
Impedance (Ohm)	56.5 - j8.31	48.8 + j15.4	54.7 – j3.36

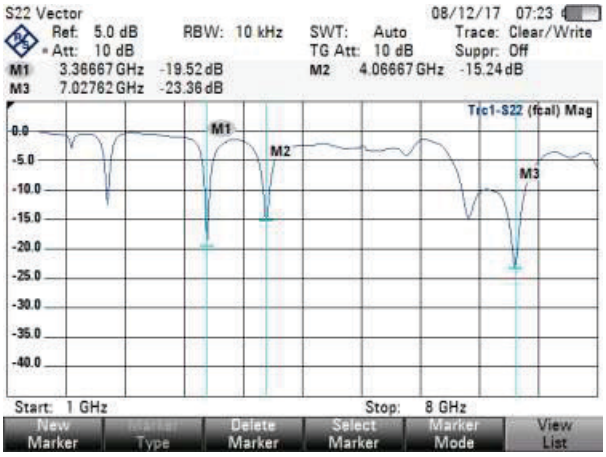

Fig. 4. Return Loss (RL) presenting triple bands

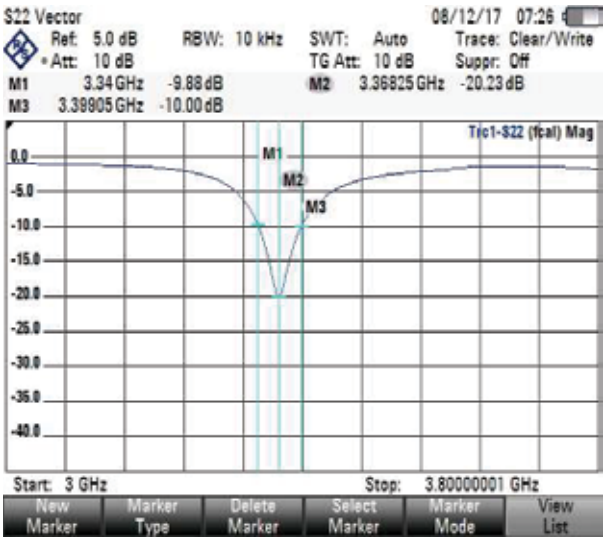

Fig. 5. Return loss (RL) of band 1

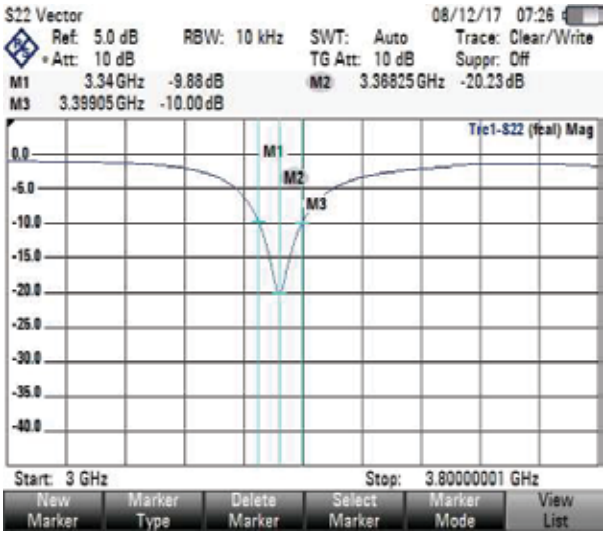

Fig. 6. VSWR' of band 1

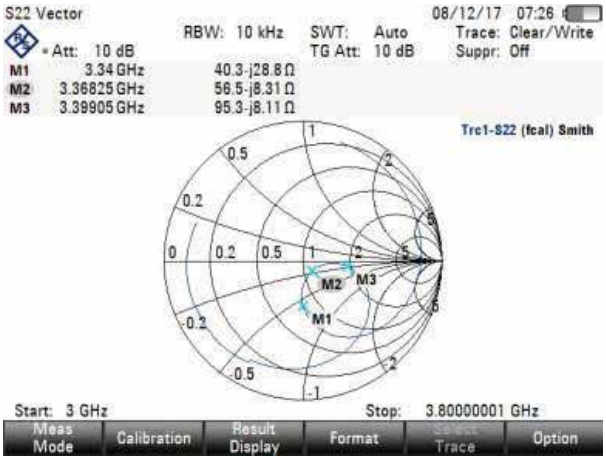

Fig. 7. Input impedance in band 1

independently elaborated and analyzed below.

4.1 DISCUSSION ON THE FIRST BAND

The band 1 resonates at 3.36GHz as depicted in Fig. 5 giving a -10 dB BW of 60 MHz whereas sustaining voltage standing wave ratio (VSWR) is under the standard level of 2 as presented in Fig. 6. M_1, M_2 and M_3 in Fig. 5 represent the initial, central and final frequencies of the first band which are 3.34GHz, 3.36GHz and 3.399 GHz respectively. The corresponding values of the voltage standing

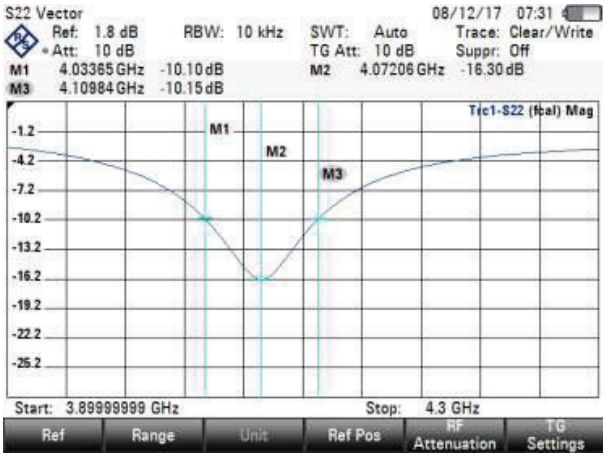

Fig. 8. Return Loss (RL) of band 2

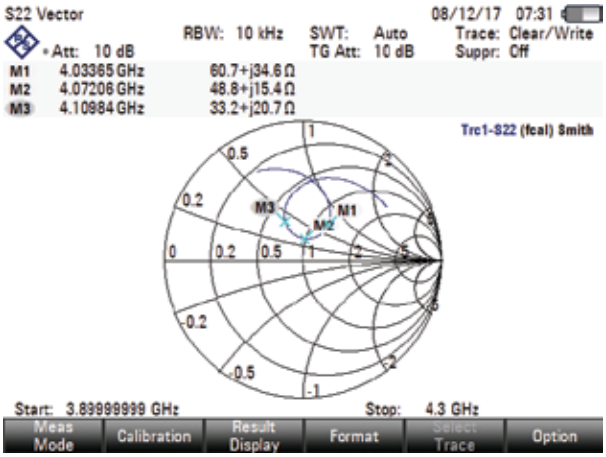

Fig. 10. Smith chart of band 2

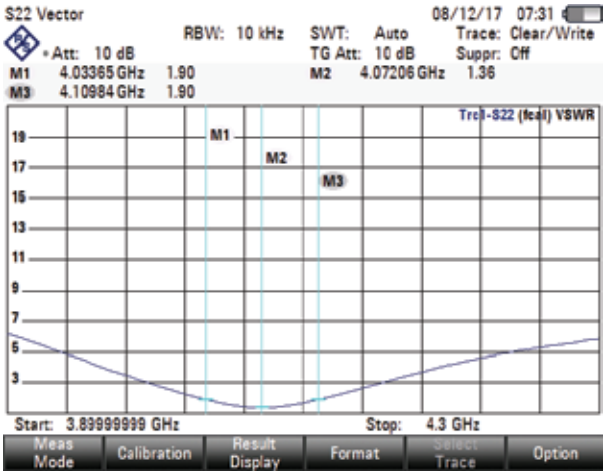

Fig. 9. 'VSWR' of band 2

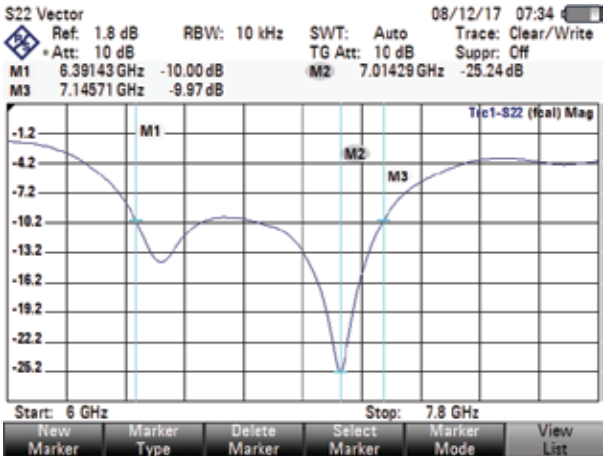

Fig. 11. Return Loss (RL) of band 3

wave ratios at the above mentioned frequencies are mentioned in Fig. 6 as 1.94, 1.22 and 1.92 respectively. Input Impedance of the antenna at central frequency is 56.5 - j8.31 Ω as presented in Fig. 7. This shows a good match of antenna with transmission line. The discussion on the results implies that this indigenous structure will work satisfactorily in the first band.

4.2 DISCUSSION ON THE SECOND BAND

Band 2 resonates at a frequency of 4.06GHz offering a -10 dB bandwidth of 76 MHz as given in Fig. 8. VSWR is displayed in Fig. 9 for band 2. The structure gives an acceptable ratio that guarantees the working of the fabricated design in band 2.M_1, M_2 and M_3 in Fig. 8 represent the initial, central and final frequencies of the 2nd band which are 4.033GHz, 4.072GHz and 4.109 GHz respectively. The corresponding values of the voltage standing wave ratios at the above mentioned frequencies aregiven in Fig.9 as 1.90, 1.36 and 1.90 respectively. The smith chart reveals the input impedance as 48.8 + j15.4 Ω at central frequency shown in Fig. 10, demonstrating a decent impedance match.

4.3 DISCUSSION ON THE THIRD BAND

Band 3 resonates at a frequency of 7.01 GHz. Its -10 dB bandwidth is 754MHz as shown in Fig. 11. M_1, M_2 and M_3 in Fig. 11 represent the initial, central and final frequencies of the third band which are 6.39GHz, 7.014GHz and 7.143 GHz respectively. The corresponding values of the voltage standing wave ratios at the above mentioned frequencies are given in Fig.12 as 1.92, 1.12 and 1.93 respectively. Input Impedance of the antenna at central frequency is 54.7-j3.36 Ω presenting a strong matching as demonstrated in Fig. 13. VSWR of band 3 is depicted in Fig. 12. The VSWR value rests under

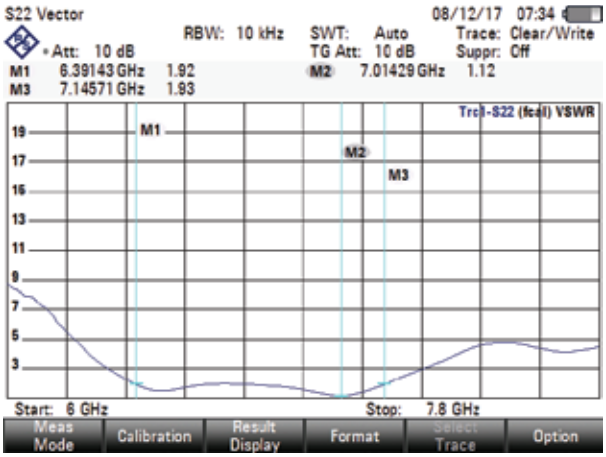

Fig. 12. 'VSWR' of band 3

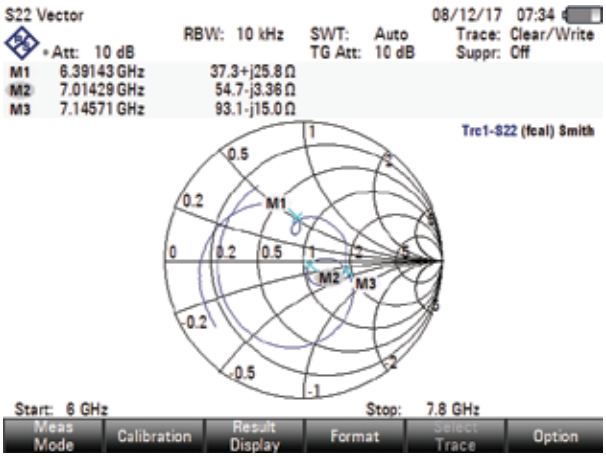

Fig. 13. Smith chart of band 3

Fig. 14. Front and back views of the fabricated antenna

Fig. 15. Pictorial view of the vector network analyzer

the tolerable range of 2 inside all the mentioned three bands. Figure 14 demonstrates front and back sight of the developed antenna.

5. CONCLUSION

In this work an indigenous hexagonal shaped patch antenna was implemented on FR-4 with overall dimensions of 61×48×1.6mm^3. An inverted C-shaped cut was etched on the patch to produce multiple resonances. Important parameters were measured using VNA. The hexagonal type antenna demonstrated three bands with center resonant frequencies of 3.36GHz, 4.06GHz and 7.01GHz with corresponding return losses of 20.23dB, 16.30dB and 25.24dB respectively. The achieved impedance bandwidths were 60MHz, 76MHz and 754MHz. VSWR in all the above mentioned three bands remains below 2. The antenna is a better

candidate for various government and military applications within S and C bands.

6. REFERENCES

1. Pei, J. & A.G. Wang. Miniaturized Triple-Band Antenna with a Defected Ground Plane for WLAN/ WiMAX Applications. *IEEE Antennas Wireless Propagation Letter.* 10, 298–301(2012).
2. Balanis, C.A. *Antenna Theory-Analysis*. 3rd edition, John Wiley & Sons (2005).
3. Garg, R., P. Bhartia, I. Bahl, A. Ittipiboon. *Microstrip antenna design handbook*. Artech House Antenna and Propagation Library, page number: 538(2001).
4. Kumar, G. & K.P. Ray. *Broadband microstrip antennas*. Artech House antennas and propagation library, page number: 14 (2003).
5. Anguera, J. & C. Puente. Dual-Frequency Broadband-Stacked Microstrip Antenna Using a Reactive Loading and a Fractal-Shaped Radiating Edge. *IEEE Antenna and Wireless Propagation Letter*. 6, 309-312 (2007).
6. Kingsley, N. Liquid Crystal Polymer: Enabling Next-Generation Conformal and Multilayer Electronics, Nickolas Kingsley. *Auriga Measurement Systems Lowell, MA Microwave Journal*, 188-200 (2008)
7. Harrington, R.F. Effect of antenna size on gain, bandwidth and efficiency. *J. Res. Nat. Bureau Stand*. 64D, 1 – 12 (1960).
8. Gupta, K.C. *Broadbanding Technique for Microstrip Patch Antennas- A Review*. Scientific Report no. 98, Electromagnetics Laboratory University of Colorado (1988).
9. Dwivedi, S., V. Mishra & Y.P. Kosta. Design and Comparative analysis of a Metamaterial included Slotted Patch Antenna with a Metamaterial Cover over Patch. *International Journal of Recent Technology and Engineering*. 1(6), 1-6 (2013).
10. Nordin, M.A.W., M.T. Islam & N. Misran. Design of a compact Ultra-Wideband metamaterial antenna based on the modified Split ring resonator and Capacitively Loaded Strips unit cell. *PIER*. 136, 157-173 (2013).
11. Ahmed, E.S. Multiband CPW-Fed Rectangular Ring Microstrip Antenna for Wireless Communications. *IEEE Jordan Conference, AEECT*, 185-190 (2011).
12. Bakariya, P.S. Proximity Coupled Multiband Microstrip Antenna for Wireless Applications. *IEEE Antennas and Wireless Propagation Letter*s, 646 - 649 (2013).
13. Kim, J.W. Compact Multiband Microstrip Antenna Using Inverted L and T-Shaped Parasitic Elements. *IEEE Antenna and Propagation Letters*. 12, 1299-1302 (2013).
14. Guptiet, A. Fractal Impact of Feeding Techniques on the Radiation Pattern of Modified Star Triangular Fractal. *NGCT, IEEE Conference*, 441-446 (2015).
15. Salamat, C.D. L-Probe Fed Multiband Microstrip Antennas with Slots. *IEEE Asia-Pacific Microwave Conference* (2008).
16. Basu, S., A. Srivastava & A. Goswami. Dual Frequency Hexagonal Microstrip Patch Antenna. *International Journal of Scientific and Research Publications*. 3(11) 1-9 (2013).
17. Roy,A., S. Bhunia, D.C. Sarkar & P.P. Sarkar. Slot Loaded Compact Microstrip Patch Antennafor Dual Band Operation. *Progress In Electromagnetics Research*. 73, 145–156 (2017).
18. Bhardwaj, M. & A. Kaur. A Tri-Band Microstrip Patch Antenna for Wireless Applications at 5.5, 6.3 And 6.8 GHz. *International Journal of Advanced Research in Electrical, Electronics and Instrumentation Engineering.* 3(6), 9834-9841 (2014).
19. Goyal, S. & B.S. Sidhu. A Compact Slotted Microstrip Patch Antenna for Multiband Applications. *International Journal of Scientific Research Engineering & Technology*. 3(7), 1059-1063 (2014).
20. Gufran, N., R. Saxena, M. Kumar & A.K. Jaiswal. Designing and Analyzing the Defected Ground Triple-Band Microstrip Patch Antenna. *International Research Journal of Engineering and Technology*, Volume: 03(07), 1439 -1445 (2016).
21. Humberto C. C., J.L.S. Fernandes, & A.S.S. Neto. Multi-frequency Microstrip Antenna Using Defected Ground Structures with Band-Notched Characteristics. *XXXV Simpósio Brasileiro De Telecomunicações E Processamento De Sinais* , 62-66 (2017).

Proceedings of the Pakistan Academy of Sciences:
A. Physical and Computational Sciences 55 (3): 53–65 (2018)

ISSN: 2518-4245 (print), 2518-4253 (online)

Pakistan Academy of Sciences

Research Article

Energy-Efficient TDMA based Clustering Scheme for WSN

Shakeel Ahmad[1*], Mohammad Haseeb Zafar[1,2], Majid Ashraf[1], Imran Khan[1], and Fazal Qudus Khan[2]

[1]Department of Electrical Engineering, University of Engineering and Technology, Peshawar, Pakistan
[2]Department of Information Technology Faculty of Computing and IT, King Abdul-Aziz University, Jeddah, KSA

Abstract: Wireless Sensor Networks (WSNs) are broadly deployed for civil and military purposes. WSN is a sensor network used to monitor physical and environmental conditions of a system such as a temperature, sound, and pressure. Sensors collect the data and send it to the desired destination such as base station. It consists of tiny nodes having very limited energy; once this energy ends then the node dies. Energy consumption is a major issue in these sensor networks. Hence, the focus of this research is to make these sensors cheap and energy-efficient. In order to gain optimized results, hundreds and thousands of nodes are deployed. To make the system more energy efficient, different routing techniques are used. In this paper, a new Efficient Time Division Multiple Access (TDMA)-based Clustering (ETC) Scheme for WSNs has been introduced which is more energy efficient than other schemes. ETC scheme uses clustering and TDMA by using hierarchy. In this hierarchy, nodes are divided into three levels, lower level nodes, medium level nodes and high energy nodes. Simulation results show that ETC has high energy efficiency, higher throughput and lower end-to-end delay. ETC results have been compared with existing schemes like Modified Low-Energy Adaptive Clusturing Hierarchy (MODLEACH) and Low-Energy Adaptive Clusturing Hierarchy (LEACH)-CCH. ETC showed better results than these schemes. ETC was 2.13% better than Low-Energy Adaptive Clusturing Hierarchy -CCH and Modified Low-Energy Adaptive Clusturing Hierarchy in case of throughput analysis. ETC had less energy consumption than Low-Energy Adaptive Clusturing Hierarchy-CCH and Modified Low-Energy Adaptive Clusturing Hierarchy. ETC showed $2.29*10^4$ joules of average energy consumption which was far better than Low-Energy Adaptive Clusturing Hierarchy-CCH which showed$1.16*10^5$ joules and Modified Low-Energy Adaptive Clusturing Hierarchywhich was $3.63*10^4$ joules. In the end-to-end delay, ETC show much better results as compared to Low-Energy Adaptive Clusturing Hierarchy-CCH and Modified Low-Energy Adaptive Clusturing Hierarchy. ETC showed $4.94*10^4$ seconds of an end-to-end delay which was far better than Low-Energy Adaptive Clusturing Hierarchy-CCH which shows $9*10^4$ seconds and Modified Low-Energy Adaptive Clusturing Hierarchy which was $6.66*10^4$ seconds. It is shown from the results that ETC has high stability period and higher throughput.

Keywords: WSN, ETC, LEACH-CCH, MODLEACH

1. INTRODUCTION

Wireless Sensor Networks (WSNs) consist of small tiny nodes also known as sensor nodes. These sensors are used to monitor physical and environmental conditions of a system such as a temperature, sound, and pressure etc. Hundreds and thousands of these small size nodes are deployed in the region of interest to sense an environment. These low-cost, low-power and multifunctional nodes sense the data from the environment and transmit the desired data to the sink node or base station [1, 2]. They have the ability to sense the data and process the desired data. Sensors sense the data from the environment and send it to the sink node or base station [3, 4]. Energy consumption during sensing and transmission of data is very high. So, to reduce this energy consumption efficient schemes are used [3, 4].

In order to avoid the problem of energy consumption and to achieve network scalability

Received: May 2018; Accepted: September 2018
* Corresponding Author: Shakeel Ahmad; shakeel3314@gmail.com

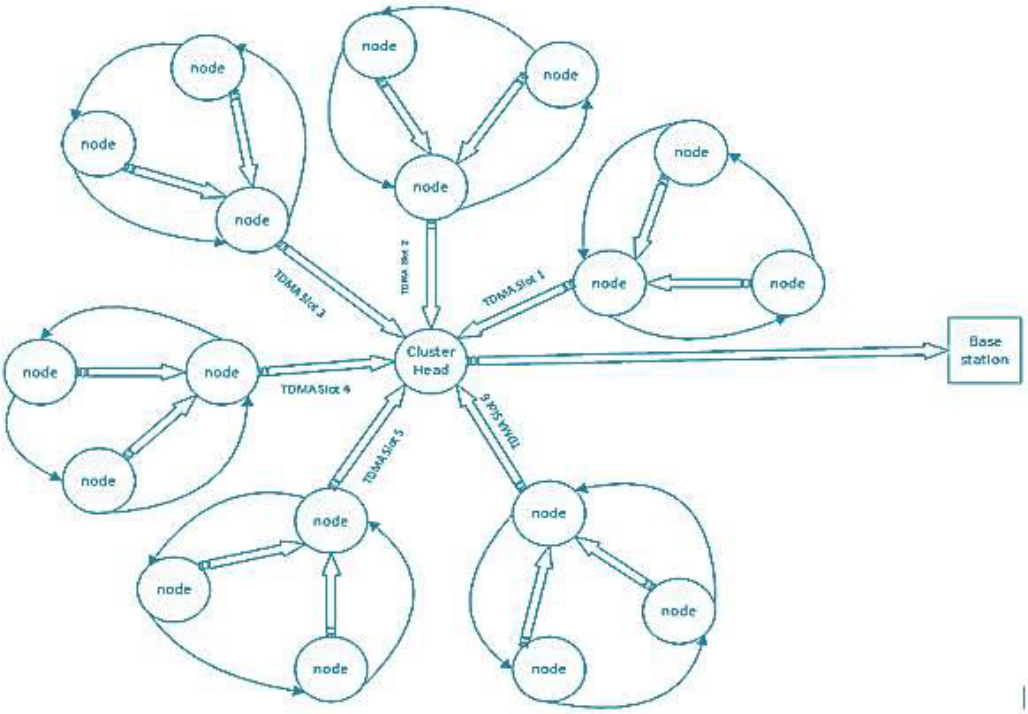

Fig. 1. Clustering in Wireless Sensor Networks (WSN)

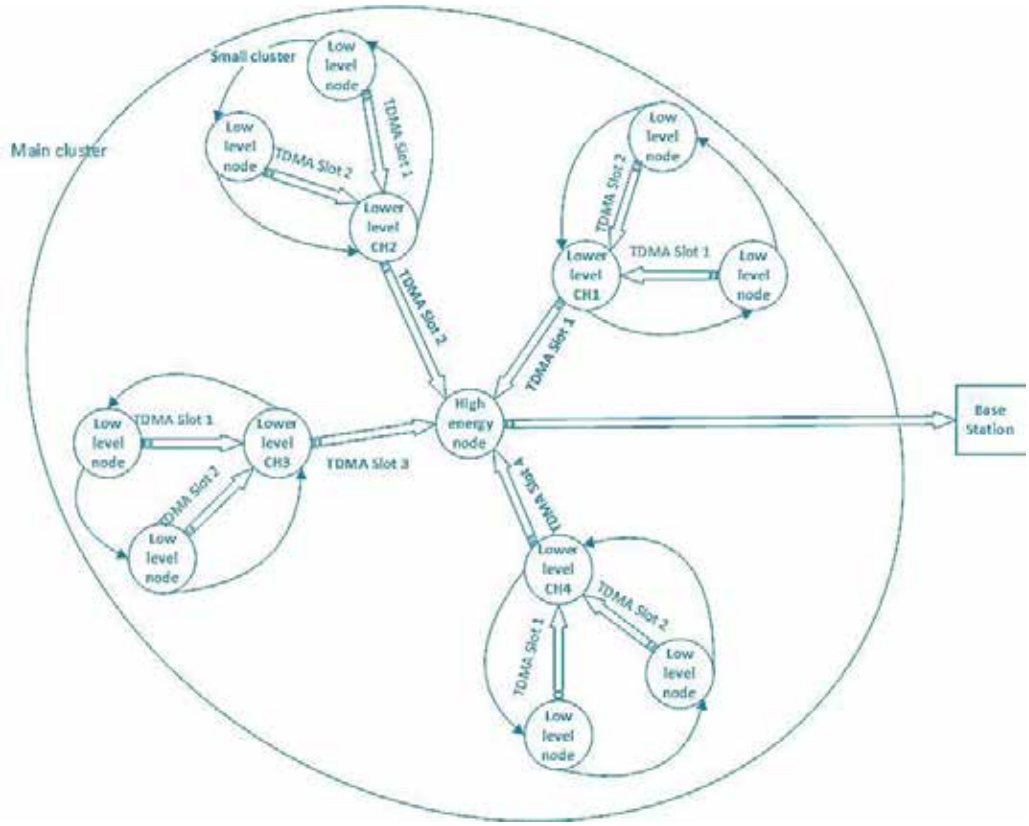

Fig. 2. TDMA based hierarchical clustering.

clustering technique are used. Clustering is also used because if all the nodes send their own data directly to the base station this will consume most of the energy of every node. The nodes which are far away from the base station require more energy to transmit which will result in the drainage of battery [4, 5]. The cluster chooses a leader known as CH. The CH may be randomly chosen through election or on the bases of the amount of the energy remaining in any node. The nodes which have higher energy are chosen as a CH [4, 5].

As shown in Figure 1, by making clusters only a few nodes communicate directly with the base station. This decreases energy consumption of other nodes. Clusters are made according to the nearest node. The node which requires less energy to transmit the data to the CH is taken in to cluster as a member. These nodes then send their data to the desired CH, not to the base station. CH makes a TDMA schedule for each node so they can send their data on their prescribed time and then remains OFF.

This scheduling helps nodes to save their energy and hence the lifetime of the system increases. This scheduling technique also helps to limit redundancy in coverage and prevent medium access collision [4, 5]. These CHs are randomly chosen for the short period of time and then the new CH is chosen. In this way, the whole energy load is distributed among all the nodes and hence the lifetime of the system increases eventually.

When CH receives data from all nodes, then data aggregation is done by the CH in order to decrease the number of packets. After this data is sent to the base station from where this data is sent to the end user. In data aggregation, the whole information is combined together which CH has received from all the nodes then the extra information is removed by enhancing the common signal and removing the noise. After data aggregation, all the information is sent to the base station. The following are the key features of network clustering:

- Load balancing
- Fault-tolerance
- Increased connectivity and reduced delay
- Minimal cluster count
- Maximal network longevity [5]

A number of simple clustering, clustering with TDMA and non-clustering schemes have been proposed which are summarized in Table 1.

2. PRPOSED SCHEME

We proposed an Energy Efficient TDMA based Clustering (ETC) Scheme for WSN which uses hierarchy (Figure 2). In this hierarchy three level nodes are used; Lower Level Nodes, Medium Level Nodes and High Energy Nodes. Low-level nodes are nodes within a small cluster of radius r equal to 1meter. They are always more than one node. Medium level nodes also called as low-level CH are elected on the basis of their residual energy. If two nodes have the same residual energy, then it should check the minimum distance between the main CH and nodes. The node which has less distance from the main CH is chosen as a medium level node or low-level CH. After selection of Low-level CH, the TDMA schedule is made for rest of the nodes and nodes send their data according to the TDMA schedule. The data which is collected from low-level nodes is sent to the high energy nodes or main CH through TDMA scheduling and main CH aggregates the data and sends it to the base station. In this hierarchy, load balancing on each node is used due to which network lifetime will be increased and energy consumption will be low. Flow Chart of TDMA base Hierarchical Clustering is shown in Figure 3.

2.1. First Order Radio Model

The advantage of the protocol depends on the radio characteristics like energy loss during transmission and receiving of data. LEACH assume a simple model that the radio dissipation is E_{elec} = 50 nJ/ bit to run the transmitter or receiver circuitry and $\in_{amp}$= 100 pJ/bit/m for the transmit amplifier. This would help to achieve an acceptable $\frac{E_b}{N_o}$ (Figure 4 and Table 2). In radio design these parameters are better than other state-of-the-art design parameters [1].

In this model, it is assumed that the r^2 energy loss is due to channel transmission. In order to transmit k-bit message at a distance d, then radio expansion is:

$$E_{Tx}\text{ (k, d)} = E_{Tx-elec}(k) + E_{Tx-amp}\text{(k, d)}$$

$$E_{Tx}\text{ (k, d)} = E_{elec}\text{* k+ } \in_{amp}\text{* k* } d^2 \quad (1)$$

Table 1. Routing Schemes for Wireless Sensor Networks (WSN)

Scheme Name	Parameters addressed	Methodology	Limitations
LEACH [1]	Energy efficiency	Clustering	Low stability time for 1st node
Improved LEACH [2]	Energy efficiency and energy conservation	Clustering	Does not concentrate on end to end delay
CBDR [3]	End to end delay, delivery ratio of data	Clustering	Have additional overheads and contains extra information for each node
REAC-IN [4]	Selection of CH and node isolation	Clustering	Limited energy efficiency
Energy Efficient Clustering [5]	Uniform energy dissipation, end to end delay	Clustering	Limited for single WSN
Multi-Hop LEACH Protocol [6]	Energy Efficiency. CH election	Clustering	Limited network scalability
MODLEACH [7]	CH formation, throughput, and energy efficiency	Clustering and TDMA	Calculation of routing load, CH replacement issue
H-LEACH [8]	Threshold and average energy dissipation	Clustering and TDMA	Assigning of TDMA slot is not efficient
Energy-aware Routing Protocol [9]	Network scalability, energy efficiency, CH formation	Clustering	Have more average energy dissipation
LEACH-CCH [10]	Network throughput and energy efficiency	Clustering and TDMA	Forming clusters based on predicting future node, limited radio transmission capability
Modified LEACH [11]	Energy efficiency	Clustering and TDMA	For lager network areas Modified LEACH is not much more efficient
TFM Tree Approach [12]	Energy efficiency and energy conservation	TDMA in tree-based approach	Extra information of each node is taken. Allocation of slots is not good
Hybrid MAC Algorithm [13]	Collision avoidance and reduction in allocation of slots	MAC base TDMA	End to end Delay is more
Multi-Channel TDMA Scheduling (MDT) [14]	On time packet delivery and end to end delay	Mathematical modeling using TDMA	Dedicated time slots and extra time slots consumes a lot of energy
TDMA Scheduling for Multi-Hop WSN [15]	Interference avoidance, end to end delay	Tree-based Mathematical modeling in TDMA	Does not guarantee short time scheduling
EETS [16]	Time synchronization and node synchronization	TDMA base mathematical modeling	Extra overhead problem
BS-MAC [17]	Packet delays, overhead reduction	Mathematical modeling using TDMA	Interference is more
IDeg-LO and IDeg-ReLO base TDMA Scheduling [18]	Latency and end to end delay	TDMA	Uses single metric which causes problem in case of interference
TDMA Time Synchronization Protocol for WSN [19]	Synchronization errors, latency, and bandwidth utilization	TDMA	Have more energy dissipation
TDMA MAC slot allocation [20]	Data collision and transmission delay	TDMA with Modeling	High latency
Packets Distribution in a Tree-Based Topology [21]	Packets distribution	Tree base	Tree base topology in which each node communicates with the sink node which consumes a lot of energy
Energy efficient mobile sink path strategy [22]	Latency and data aggregation	Mathematical modeling	Extra overhead information
Algorithm for the Maximum-lifetime Data Aggregation Tree Problem in WSN [23]	Transmission power and data aggregation	Tree base	Load balancing is not good
EERC-MAC [24]	Throughput and energy efficiency	Tree base modeling	For smaller network
TST Algorithm [25]	Optimization of path length, energy and computation costs in multicast of WSNs	Tree base	Only for static networks. Does not provide backup routing path

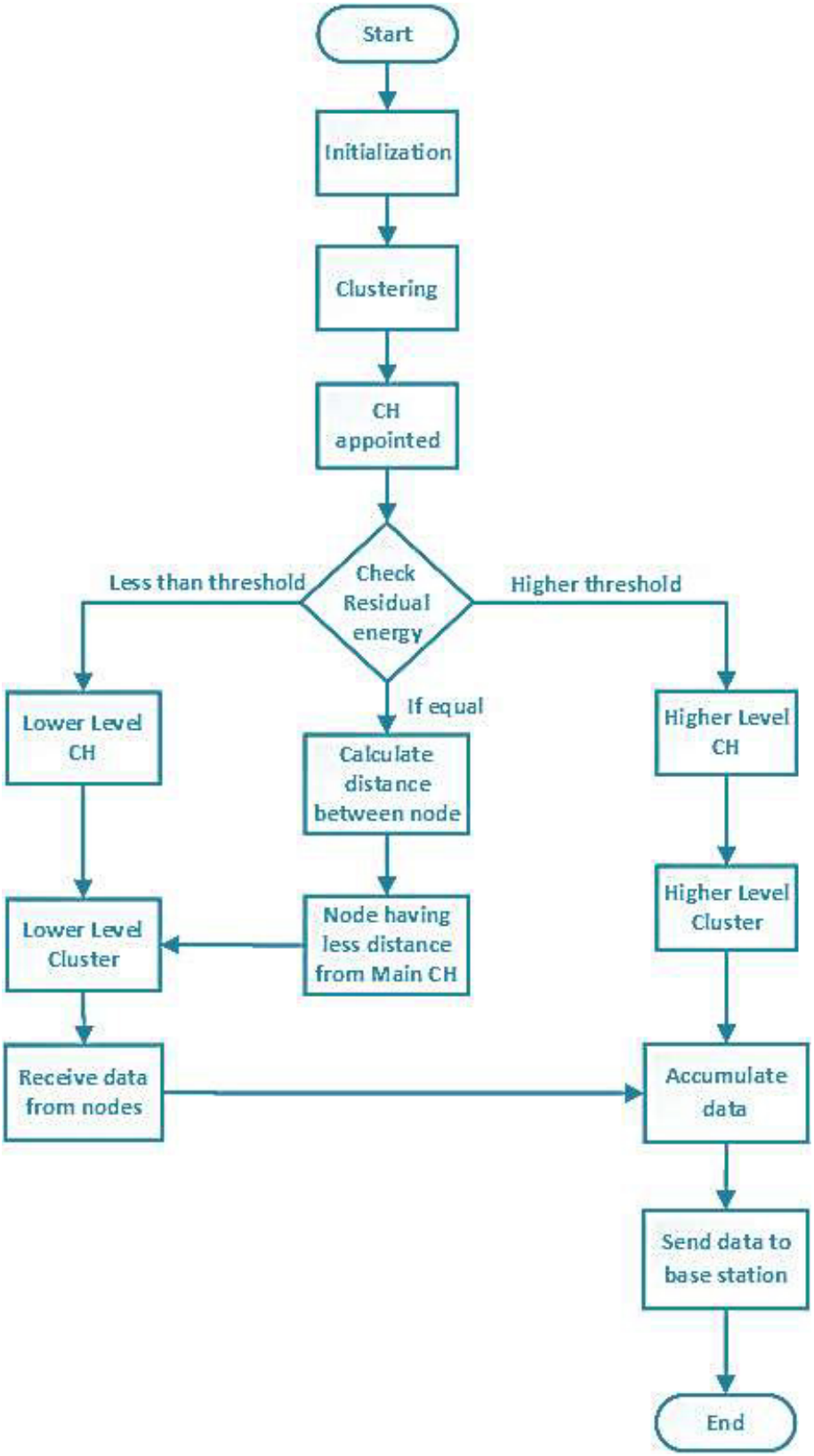

Fig. 3. Flow chart of TDMA based hierarchical clustering.

Table 2. Radio characteristics

Scheme Name	Parameters addressed
Transmitter Electronics ($E_{Tx\text{-}elec}$) Receiver Electronics ($E_{Rx\text{-}elec}$) $E_{Tx\text{-}elec} = E_{Rx\text{-}elec} = E_{elec}$	50 nJ/bit
Transmit Amplifier (E_{amp})	100 pJ/bit/m

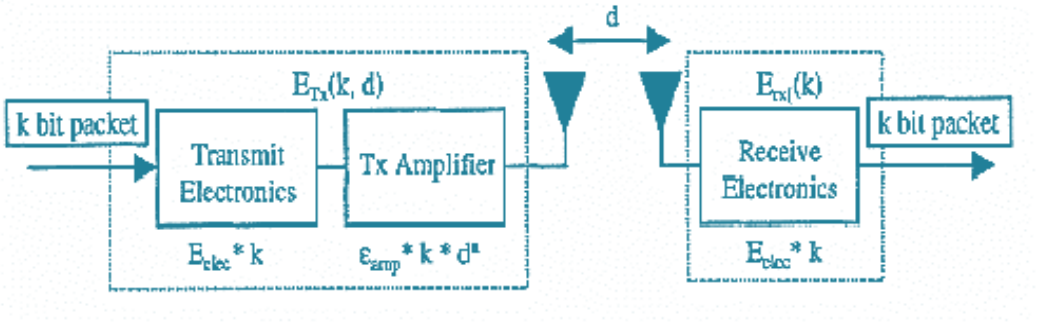

Fig. 4. First order radio model [1]

To receive a message, the equation we have is [1]:

$$E_{Rx}(k) = E_{Rx-elec}(k)$$

$$E_{Rx}(k) = E_{elec} * k \quad (2)$$

Receiving of the message for the above values of the parameter is not low cost. So, the protocol must decrease the number of operations for the transmission and receiving, and also decrease the distance for transmission of data [1].

An assumption is made that all the nodes require the same amount of energy to transmit the data from node A to node B or vice versa for the given SNR (Signal to Noise Ratio). Such a system is called asymmetric system or channel. The assumption is also made that all the nodes have always a data to send and that they send the data at a constant rate [1].

In the minimum energy routing protocol, the data is sent through intermediate nodes. These nodes act as routers. Different schemes use different methods to choose the routes through which data is being transmitted from source to destination. To determine these routes, some protocol considers the transmit energy and some neglects the dissipation of energy. If the intermediate nodes are chosen, then their transmit amplifier energy will be minimum [1].

$$E_{Tx}(k, d) = E_{elec} * k + \in_{amp} * k * d^2$$

So, to transmit the data from node A to node C if

$$E_{Tx}(k, d=d_{AB}) + E_{Tx}(k, d=d_{BC}) < E_{Tx}(k, d=d_{Ac}) \quad (3)$$

$$d_{AB}^2 + d_{BC}^2 < d_{AC}^2 \quad (4)$$

For the ETC routing scheme, data is sent through n low transmits of low energy rather than sending a data directly to the base station in one transmits. The whole transmission is divided into n transmits and n receives. It depends on the radio electronics and transmitter amplifier cost. The total energy of the system is greater in ETC as compared with the direct transmission. Consider a network where the nodes are at an equal distance from each other and are at the distance of r. If the energy expended is k-bit message and is at a distance of nr. So the equation one and two transform as[1]:

$$E_{direct} = E_{Tx}(k, d=n*r) = E_{elec} * k + \in_{amp} * k * (nr)^2$$

$$= k(E_{elec} + \in_{amp} * k * n^2 r^2) \quad (5)$$

Each node sends a message to the near node in ETC routing to send a data to the base station. The node which is at a distance of nr requires n transmission bits for r distance and receives n-1 which is far from the base station [1].

$$E_{MTE} = n * E_{Tx}(k, d=n*r) + (n-1) * E_{Rx}(k)$$

$$= n(E_{elec} * k + \in_{amp} * k * r^2) + (n-1) * E_{elec} * k$$

$$= k((2n-1)\ E_{elec} + \in_{amp} * nr^2) \quad (6)$$

So ETC routing requires more energy than direct communication.

$$E_{direct} < E_{MTE}$$

$$E_{elec} + \in_{amp} \; n^2 r^2 < (2n\text{-}1) \; E_{elec} + \in_{amp} * nr^2)$$

$$\frac{E_{elec}}{\in_{amp}} > \frac{r^2 n}{2} \quad (7)$$

2.2. Cluster Formation

In ETC, scheme selection of CH is improved. Residual energy is the main part of this scheme. CH is chosen on the bases of residual energy and the distance between the node and base station in case of the two nodes having the same energy. Each node has the same probability of being chosen as CH for the first round. But after the first round, residual energy is to be considered. The nodes which have higher residual energy is taken as CH [2]. The selection of CH also depends on the threshold value which can be measured as

$$T_r(n) = \frac{P}{1-P*(rmod\frac{1}{P})}[\delta P + (1\text{-}\delta P)\frac{E_{residual}}{E_o}] \quad \text{if n} \epsilon C$$

$$T_r(n) = 0 \qquad \text{otherwise} \quad (8)$$

Where P stands for the nodes which can be chosen as CHs and is the residual energy of the node and E_o is initial energy of the node before transmission. δ is the continuous number of rounds. After the cluster formation, the CH is chosen based the residual energy of the node and the distance between the base station and the node. The value of the λ plays an important and vital role in choosing of CH, where λ is [2]

$$\lambda = \frac{E_{residual}}{d_{toBS}} \quad (9)$$

Where is the distance between the CH and the base station. λ is calculated between all the CHs. The node which has the higher value of lambda is chosen as CH [2].

In this work, hierarchical clustering routing is used which means that after every round new clusters are made and new CHs are chosen. The new CHs after every round helps us to balance the energy load among all the nodes equally. This helps us in load management. A number of nodes are chosen after every round as CH. The threshold value is used for the deciding of selection of CHs in each round [2]. This threshold value is calculated as:

$$T_r(S_{(nrm)}) = \{\frac{P}{1-P_{nrm}*(rmod\frac{1}{P_{nrm}})} \quad \text{if S } \varepsilon \; G$$

$$T_r(S_{(nrm)}) = \{\; 0 \qquad \text{otherwise} \quad (10)$$

Where r is the number of current rounds and G is the number of nodes that have not been chosen as CH, for the $\frac{1}{P_{opt}}$ rounds.

2.2.1 For maximum number of CHs

The first order leach model is used for receiving energy expense E_{Rx} (l) and the transmission energy expanse E_{Tx} (l, d) of 1-bit message between two nodes and d is the distance between two nodes [2]. The mathematical equation is:

$$E_{Tx}(l, d) = \{\; l * E_{elec} + E_{fs} * d^2 * l \qquad \text{if d} \leq d_o$$

$$E_{Tx}(l, d) = \{\; E_{elec} * l + E_{amp} * d^4 * l \quad \text{if d} \geq d_o \quad (11)$$

$$E_{Rx}(l) = l * E_{elec} \quad (12)$$

Where E_{elec} is the energy of the each bit dissipated during the transmission and gathering of data from source to destination. For the distance between transmitter and receiver there are two types of models used, namely the two ray model and the free space model. The threshold distance do can be calculated by the following equation [2]:

$$d_o = \sqrt{\frac{E_{fs}}{E_{amp}}} \quad (13)$$

If d < d_o, free space model is used otherwise two ray model is used. In order to find the ideal number of cluster, the following formula is used:

$$k_{opt} = \sqrt{\frac{n}{2\pi}} \cdot \sqrt{\frac{E_{fs}}{E_{amp}}} \cdot \frac{M}{d^2} \quad (14)$$

The ideal probability of a node to be selected as CH is calculated as [2]:

$$P_{opt} = \frac{k_{opt}}{n} \quad (15)$$

Initially, the energy of the normal nodes and advanced nodes is calculated as [2]:

$$E_1 = E_o(1 + a) \quad (16)$$

Where is the energy of the normal nodes and is the

energy of advance nodes.

$$E_t = n.E_o(1\text{-P-k}) + n.\ P\ .E_o(1-a) \quad (17)$$

$$E_t = n.E_o(1+a) \quad (18)$$

This protocol is used to the likelihood of a node to be selected as CH in the current round. This weight is equal to the initial energy of the node. The node which is turned into CH once is heterogeneous. The probability of normal and advanced node into CH is calculated as[2]:

$$P_{nrm} = \frac{P_{opt}}{1+P.a} \quad (19)$$

$$P_{adv} = \frac{P_{opt}}{1+P.a+(1+a)} \quad (20)$$

3. RESULTS AND DISCUSSIONS

This environment is simulated and the field has been taken as (300,300). The deployment of the sink is at the center of the field which is (150,150). The initial energy of each node is taken as Eo=0.9. The nodes are divided into 3 categories, some nodes are taken as advance nodes, some are medium energy nodes and some are normal nodes. Simulations are conducted and then analysis of the performance of the different protocols has been compared with each other. Proposed protocol ETC is compared with LEACH-CCH and MODLEACH. The aim of this comparison and evaluation is to observe the different effect of different scenarios on the proposed protocol ETC with LEACH-CCH and MODLEACH. The different parameters used for simulating results are shown in Table 3.

3.1. Throughput Analysis

Throughput is a number of packets delivered successfully to the base station. As shown in Figure 5 and Table 4, ETC has achieved greater throughput than LEACH-CCH and MODLEACH because lower nodes send their data to medium nodes and medium nodes send their data to the main CH or high energy nodes. TDMA scheme is used for sending data which helps us to achieve higher throughput. A result of each protocol is shown in Table 4 which shows that packet delivery ratio of ETC is showing much better results as compared to LEACH-CCH and MODLEACH. At 500 rounds, all are delivering 100% packet delivery. But at 1500 round ETC shows 95% packet delivery, LEACH-CCH has 18% and NODLEACH has 79% packet delivery. At 2000 round ETC shows 64% of packet delivery which is far better than LEACH-CCH which is 9% and MODLEACH which is 44%. This is the result at the ideal position of our sink at x=150, y=150. According to Table 4 ETC is 2.13% better than the LEACH-CCH and MODLEACH is 1% and 1.9% respectively.

3.2. Stability Period Analysis

As shown in Figure 6 and Table 5, the stability period of ETC is much more than LEACH-CCH

Table 3. Simulation parameters

Area of deployment	**(x*y)**	**(300*300)**
Initial energy	Eo	0.9 J
Sink location	(x, y)	(150,150)
No of nodes	N	100
Probability of making CH	P	0.1
Maximum No rounds	Rmax	10000
Percentage of normal nodes	M	0.3
Alpha times advance nodes having great energy than normal nodes	A	3
Transmission energy	E_{tx}	50 n J
Receiving energy	E_{rx}	50 n J
Free space energy	E_{fs}	10 p J
Amplification energy	E_{mp}	0.0013 p J
Data aggregation energy	E_{DA}	5 n J

Table 4. Packet delivery ratio vs rounds. For the position of sink at x=150, y=150

Protocol	Rounds 500	1000	1500	2000	2500	3000	Average	Ratio
MODLEACH	100	100	79	44	31	30	64	1.9
LEACH-CCH	100	60	18	9	8	7	33.6	1
ETC	100	100	95	64	39	32	71.6	2.13

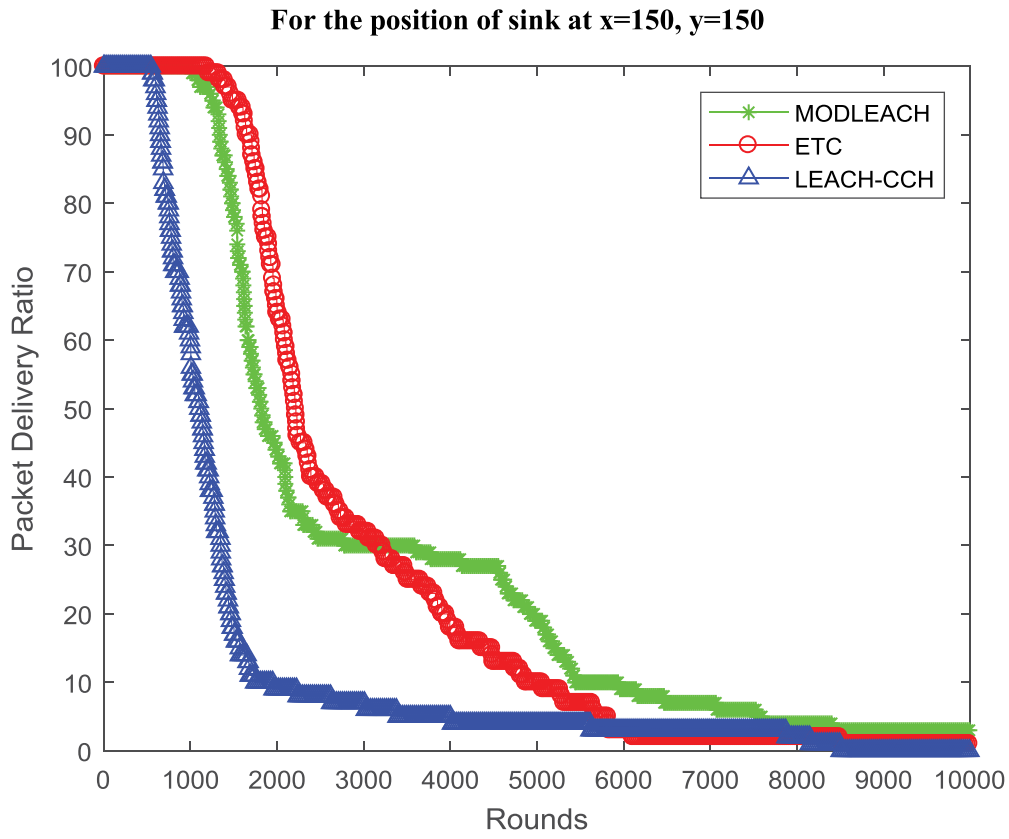

Fig. 5. Packet delivery ratio vs rounds

and MODLEACH. The reason is that data is transmitted through intermediate nodes. Level of nodes is divided into 3 levels like lower level nodes, medium level nodes and high energy nodes. So, data is sent only when needed. The simulation shows the number of nodes that are dead during transmission. If a node dies early it means that our protocol will work only for short period of time. A result of each protocol is shown in Table 5 which shows the number of dead nodes. Table 5 shows that ETC is showing much better results as compared to LEACH-CCH and MODLEACH. At 2000 round, ETC shows 32% of its nodes are dead which is far better than LEACH-CCH which shows 90% of dead nodes and MODLEACH which shows 63% of dead node. This is the result at the ideal position of our sink at x=150, y=150. But at 4000 round, these values change whereby, ETC shows 79% of its nodes are dead, LEACH-CCH shows 97% of dead nodes and MODLEACHshows72% of dead node.

3.3. Energy Efficiency Analysis

Energy efficiency of the system is how much the system is using energy for sending and receiving data. This energy consumption shows how much energy efficient is the protocol. Energy consumption, measured in joules is energy consumed or used during transmission of data it is always. There are 2 types of energies like initial energy and advance energy. Initial energy is 0.9 all the nodes have provided the same initial energy. The normal nodes are less energy as compared to advanced nodes. Advance nodes have greater energy which is a=3. A result of each protocol is

Table 5. Packet delivery ratio vs rounds. For the position of sink at x=150, y=150

Protocol	Rounds 2000	4000	6000	8000	10000	Average	Ratio
MODLEACH	63	72	91	97	98	84.5	1.04
LEACH-CCH	90	97	99	100	100	97.2	1.2
ETC	32	79	96	98	99	80.8	1

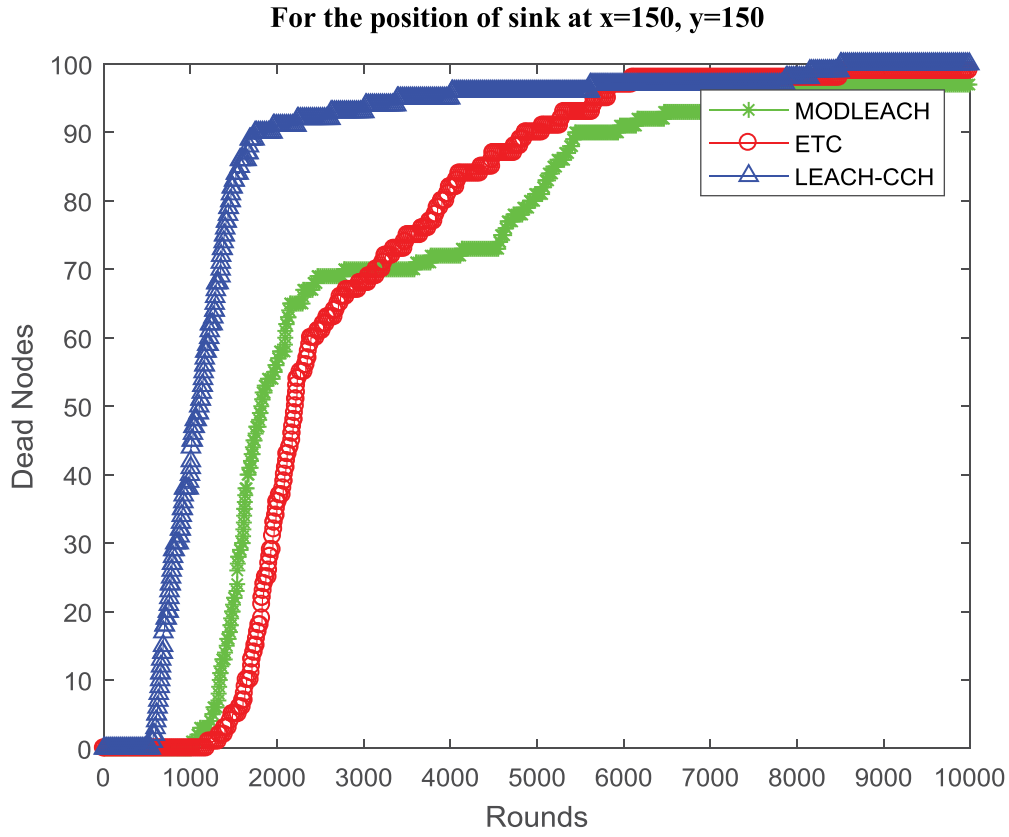

Fig. 6. Dead node vs rounds.

shown in Figure 7 and Table 6 which shows that average energy consumption in joules. Table 6 shows that ETC is showing much better results as compared to LEACH-CCH and MODLEACH. At 2000 round ETC shows $2.29*10^4$ joules of average energy consumption which is far better than LEACH-CCH which shows $1.16*10^5$ joules and MODLEACH which is $3.63*10^4$ joules. This is the result at the ideal position of our sink at x=150, y=150. But at 4000 round, these value change ETC shows $3.69*10^4$ joules of average energy consumption which is far better than LEACH-CCH which shows$1.32*10^5$ joules and MODLEACH which shows $5.06*10^4$ joules. As average energy consumption of ETC is less then LEACH-CCH and MODLEACH so the ETC is more energy efficient than all other protocols.

3.4. End to End Delay

End to end delay shows that how much time it takes to deliver the packets to the destination. Less the delay more efficient will be the protocol. For the ideal position of the sink at x=150, y=150,a result of each protocol is shown in Figure 8 and Table 7 which represent send to end delay. Table 7 shows that ETC is showing much better results as compared to LEACH-CCH and MODLEACH. ETC shows 49.4 milliseconds of end to end delay which is far better than LEACH-CCH which shows 90 milliseconds and MODLEACH which is $6.66*10^4$ seconds of end to end delay.

Table 6. Average energy consumption vs rounds. For the values of x=150, y=150

Protocol	Rounds 2000	4000	6000	8000	10000	Average	Ratio
MODLEACH	3.63	5.06	5.95	6.34	6.66	5.5	1.41
LEACH-CCH	11.6	13.2	13.5	13.6	13.7	13.1	3.3
ETC	2.29	3.69	4.35	4.67	4.93	3.9	1

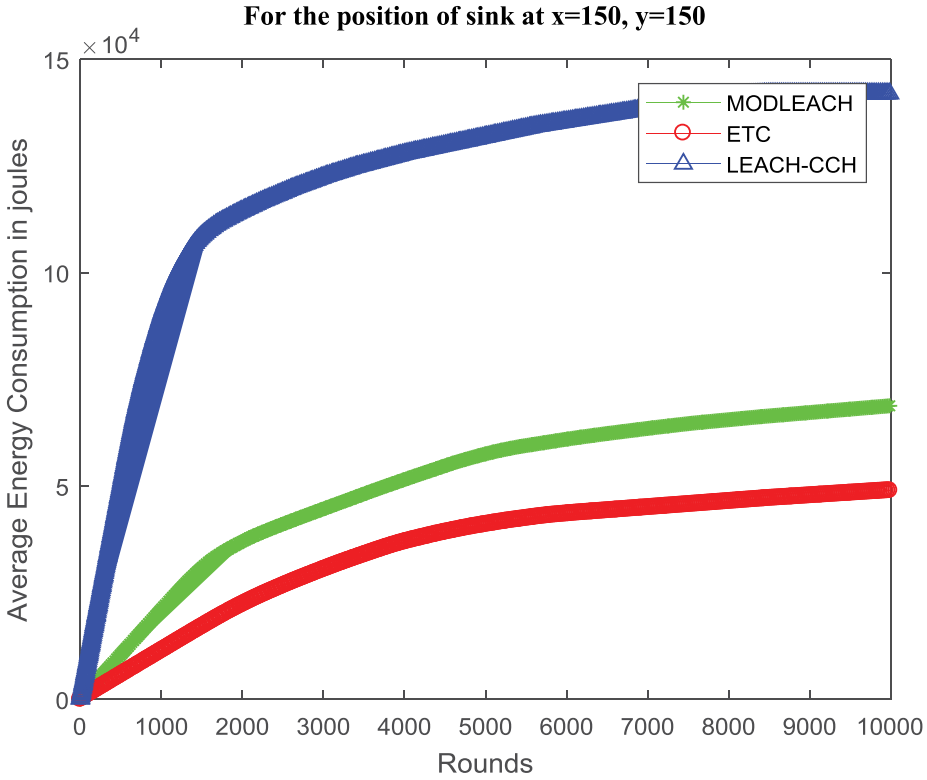

Fig. 7. Average energy consumption vs rounds.

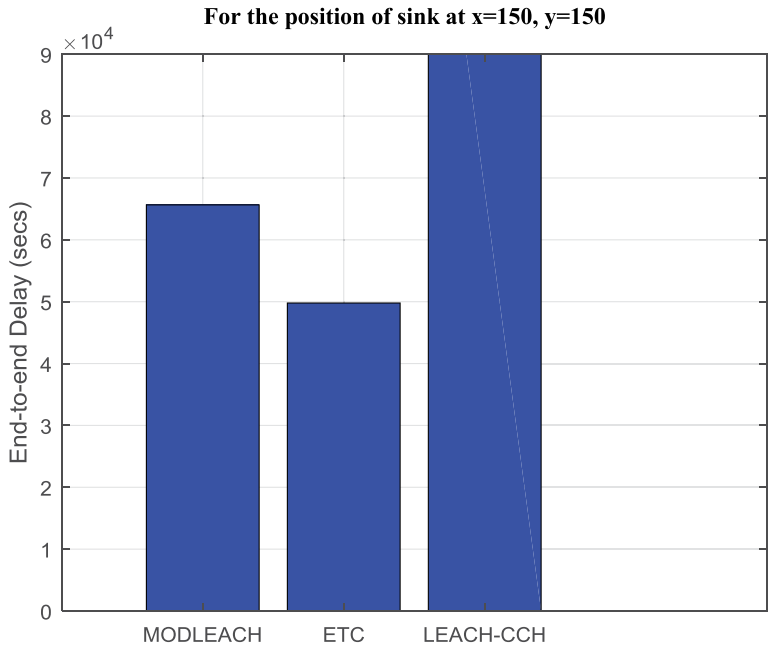

Fig. 8. End to end Delay.

Table 7. End to end Delay in seconds. For the position of sink at x=150, y=150

Protocol	Values
MODLEACH	66.6 msec
LEACH-CCH	90 msec
ETC	49.4 msec

4. CONCLUSION

An interest-based buffer management scheme is proposed in throw-boxes to increase the performance of the network. When the throw-box is full, we delete the data with high diffusion level instead of deleting the data with less popularity. The proposed scheme has good energy efficiency as compared to other routing protocols. This hybrid approach increases the delivery probability of the network by also delivering the data with less popularity. The overall average latency and overhead ratio are also decreased with this buffer management policy, and we also double-checked and prevented some critical data discrepancies. In future research, this buffer management scheme can be compared with other buffer management policies.

5. REFERENCES

1. Kaur, J, G. S. Gaba, R. Miglani & R. Pasricha. Energy efficient and reliable WSN based on improved Leach-R clustering techniques. *Indian Journal of Science and Technology* 16:1–6 (2015).
2. Imran & D. Singh. Energy-balance node-selection algorithm for heterogeneous wireless sensor networks.*Wiley ETRI Journal* 40:604–612 (2018).
3. Varma, GNS. Abhishek, G. A. K. Reddy, Y. R. Theja & T. A. kumar. Cluster Based multipath Dynamic Routing (CBDR) protocol for wireless sensor networks. *Indian Journal of Science and Technology* 8:17–22 (2015).
4. Leu, J.S, T. Chiang, Min-Chieh Yu & K. W. Su. Energy efficient clustering scheme for prolonging the lifetime of wireless sensor network with isolated nodes. *IEEE Communications Letters* 19:259–262 (2015).
5. Samantaray, A, G. Devi & R. S. Bal. The Energy Efficiency Clustering in Wireless Sensor Network. *Journal of Network Communications and Emerging Technologies* (JNCET) 6:86–92 (2016).
6. Sony, Chinchu T., C. P. Sangeetha & C. D. Suriyakala. Multi-hop LEACH protocol with modified cluster head selection and TDMA schedule for wireless sensor networks. *IEEE Global Conference on Communication Technologies* (GCCT),Thuckalay, India:539–543 (2015).
7. Mahmood, D, N. Javaid, S. Mahmood, S. Qureshi, A. M. Memon& T. Zaman. MODLEACH: a variant of LEACH for WSNs. *IEEE Eighth International Conference onBroadband and Wireless Computing, Communication and Applications* (BWCCA), Compiegne, France: 158 –163 (2013).
8. Razaque, A, S. Mudigulam, K. Gavini, F. Amsaad, M. A. Qader & G. S. Krishna. H-LEACH: Hybrid-low energy adaptive clustering hierarchy for wireless sensor networks. *IEEE Long Island Systems, Applications and Technology Conference* (LISAT), Farmingdale, NY, USA:1–4 (2016).
9. Goyal, R, S. Gupta& P. Khatri. Energy aware routing protocol over leach on wireless sensor network.*International Conference on Computing, Communication and Automation* (ICCCA), Noida, India:699–703 (2016).
10. Corn, J. & J. W. Bruce. Clustering algorithm for improved network lifetime of mobile wireless sensor networks.*IEEEInternational Conference on*, *Computing, Networking and Communications* (ICNC), Santa Clara, CA, USA: 1063–1067 (2017).
11. Sony, C.T., C. P. Sangeetha, & C. D. Suriyakala. Multi-hop LEACH protocol with modified cluster head selection and TDMA schedule for wireless sensor networks.*IEEE Global Conference on Communication Technologies* (GCCT), Thuckalay, India:539–543 (2015).
12. Bakshi, M., B. Jaumard, M. Kaddour & L. Narayanan. On TDMA scheduling in wireless sensor networks. *IEEE Canadian Conference on Electrical and Computer Engineering* (CCECE), Vancouver, BC, Canada:1–6 (2016).
13. Saraereh, O.A., I. Khan & B. M. Lee. An Efficient Neighbor Discovery Scheme for Mobile WSN. *IEEE Access* 7:4843-4855 (2018).
14. Lee, J, W. Jeong & B. C. Choi. A multi-channel timeslot scheduling algorithm for link recovery in wireless multi-hop sensor networks. In *IEEE2016 International Conference on Information and Communication Technology Convergence* (ICTC), Jeju, South Korea:871–876 (2016).
15. Sasaki, M, T. Furuta, U. K. A. I. Takamori & F. Ishizaki. TDMA scheduling problem avoiding interference in multi-hop wireless sensor networks. *Journal of Advanced Mechanical Design, Systems, and Manufacturing* 3:1–10 (2016).
16. Khedo, K. Kumar & D. Lobin. EETS: An Energy-Efficient Time Synchronization Algorithm for Wireless Sensor Networks. *International Journal of Advanced Research in Computer Science* 1:1–8 (2017).
17. Alvi, A. Naseem, S. H. Bouk, S. H. Ahmed, M. A.

Yaqub, N. Javaid & D. Kim. Enhanced TDMA based MAC protocol for adaptive data control in wireless sensor networks. *Journal of Communications and Networks* 17:247–255 (2015).

18. Louail, L, & V. Felea. Routing-aware TDMA scheduling for wireless sensor networks. *12th Annual Conference onWireless On-demand Network Systems and Services* (WONS), Cortina d'Ampezzo, Italy:1–8 (2016).
19. Lennvall, T, J. Å. berg, E. Hansen & K. Yu. A new wireless sensor network TDMA timing synchronization protocol.*IEEE 14th International Conference onIndustrial Informatics* (INDIN), Poitiers, France:606–611 (2016).
20. Chang, C. Lung & K. Y. Ho. Slot assignment for TDMA MAC in industrial wireless sensor network. *IEEE/ACIS 15th International Conference onComputer and Information Science* (ICIS), Okayama, Japan:1–5 (2016).
21. Akpakwu, G. A., Hancke G. P. & A. Mahfouz. Packets distribution in a tree-based topology Wireless Sensor Networks. *IEEE 14th International Conference on Industrial Informatics* (INDIN), Poitiers, France:1181–1184 (2016).
22. H. Salarian, K. W. Chin & F. Naghdy. Energy Efficient Mobile Sink Path Strategy for Wireless Sensor Network. *IEEE Transactions on Vehicular Technology*63:2407–2419 (2014).
23. Lin, H. Chun & W. Y. Chen. An Approximation Algorithm for the Maximum-lifetime Data Aggregation Tree Problem in Wireless Sensor Networks. *IEEE Transactions on Wireless Communications* 6:3787–3798 (2017).
24. Khalil, M. Ibrahim, M. A. Hossain, M. J. Haque & M. N. Hasan. EERC-MAC: Energy efficient Receiver Centric MAC protocol for Wireless Sensor network. *IEEE International Conference on*, *Imaging, Vision & Pattern Recognition* (icIVPR):1–5 (2017).
25. Gong, H, L. Fu, X. Fu, L. Zhao, K. Wang & X. Wang. Distributed Multicast Tree Construction in Wireless Sensor Networks. *IEEE Transactions on Information Theory* 63:280–296 (2017).

Proceedings of the Pakistan Academy of Sciences:
A. Physical and Computational Sciences 55 (3): 67–76 (2018)

ISSN: 2518-4245 (print), 2518-4253 (online)

Pakistan Academy of Sciences

Research Article

Spatial and Temporal Change Assessment in Land Surface Temperature of Lahore using GIS and Remote Sensing Techniques

Muhammad Nasar-u-Minallah*

Department of Geography, Govt. Postgraduate College Gojra, Pakistan

Abstract: This study is an attempt to evaluate Land Surface Temperature (LST) variations of Lahore, a metropolitan city of Pakistan. LST have wide-ranging application viz; global climate change, urban climate, evapotranspiration, hydrological cycle and environmental studies. Therefore, Spatio-temporal assessment of LST variation is becoming vital to recognize the contributing factors and corresponding magnitude of contribution to the variation using GIS and remote sensing techniques. This study employed the radiative transfer method in assessing Spatio-temporal LST change using multi-temporal imagery acquired by Landsat 5 TM and Landsat 8 TIRS satellite data, for the year 1990 and 2015, respectively. Thermal infrared images of Landsat satellite revealed its suitability in monitoring temporal change in LST. The results indicated that high mean LST was recognized in the areas of Shalamar town, Gulberg town, Data Ganj Baksh town and Ravi town. On the other hand, the low mean LST was observed in the areas of Aziz Bhatti town, Samanabad town, Wagha town and Iqbal town in 1990.The results further showed that the areas of Gulbarg town, Wagha town, Shalamar town, Ravi town, Nishter town and Iqbal town, had been warmer in the year 2015 than the year 1990. It was assessed that in the areas of Aziz Bhatti town, Nishtar town and Wagha town, there were no urbanization and urban development. Therefore the lowest LST was measured in the year 1990. However the expansion and urban development of Lahore in these areas increased surface radiant temperature and they reflect highest LST assessed in 2015. The present study explores the suitability of employing GIS and satellite remote sensing techniques in finding out the spatial and temporal temperature change to achieve accuracy in terms of urban planning, decision and policy making for sustainable urban environment of Lahore.

Keywords: LST, Temporal change, Heat Island, Urban warming, Landsat, Town, Lahore.

1. INTRODUCTION

Radiative temperature of land, generally recognized as Land Surface Temperature (LST) [1,2], is a significant parameter in the physics of land surface processes from local to global scales [3-5]. LST is controlled by land-atmosphere heat exchange and solar radiation [6]. It plays an important role in water and energy transfers between land surface and atmosphere [7]. Therefore, Spatio-temporal distribution of LST not only reveals the variations of climate factors but also recognizes the characteristics of land surface. A comprehensive understanding of spatial and temporal change assessment of LST variations is significant for a range of studies, comprising climatology, meteorology, vegetation and hydrology etc. [8].

The land surface temperature in urban areas is increasing gradually as a consequence of massive land use changes taking place due to urban expansion [9]. It has led to reduction in agricultural land and loss of vegetation and green area in cities around the world [9]. A number of studies indicate that the land surface temperature of cities is generally (1-6°C) higher than those of the adjacent rural areas. This phenomenon is named Urban Heat Island (UHI) [10, 11]. Since 1800, studies concerning the recognition of rising temperature phenomenon in urban areas have increased and it has significantly [12]. Several scholars [10-14] documented that temperature in urban areas varied from those of the nearby countryside, in line with the greenhouse effects produced by use of carbon fuelled machinery. The cities, in this regard, consume 60 to 80% of energy produced globally and are contributing to CO_2 emission with equal share [15]. This comes as no surprise

Received: April 2018; Accepted: September 2018
* Corresponding Author: Muhammad Nasar-u-Minallah; Nasarbhalli@gmail.com

that cities signify areas with higher density of population and center of human activities. Several contributing factors include, automobile, industry, heat generating human activities, thermodynamic capacities of material, structural geometry and impervious surfaces are responsible for trapping and re-radiation of heat in the atmosphere. These factors in turn change the environmental conditions that alter the near-surface atmospheric temperature over the urban areas. Urban built-up area and bare land can have a particularly high impact on LST [16]. LST has a positive relationship with built-up area and shows negative relationship with blue and green spaces and forest cover [17]. Major decrease in green area affects the equilibrium of energy and heat exchange, leading towards intensification of surface temperature and declinein evapotranspiration and precipitation simultaneously [18-19]. Not only the high density areas, but also buildings and their structures matter and impervious surfaces of complicated shapes also tend to increase the land surface temperature.

A number of techniques have been developed and adopted in the past to assess LST based on data obtained from meteorological stations [20]. Since the 1970s, satellite derived images and thermal infrared data have man advantages. Resultantly, most of the urban climate studies preferably utilized thermal data for regional LST analyses on different scales [21-24]. For instance, satellite remotely sensed data permits the acquisition of thermal data over a region and very large areas and also provides a lot of information. On the other hand, traditional method and direct measurements only provide point data. Another significant advantage of satellite remotely sensed data is that it is very economical and generally easy in acquiring thermal data, while direct measurement method is tremendously expensive and time consuming for the assessment of whole of the region where as thermal data from the satellite cover whole of the region and area of interest at same time. It is on this basis that GIS and remote sensing technology is adopted for the extraction of LST in the study area. This study aims at estimating spatial and temporal change assessment in land surface temperature of Lahore at town level. Therefore, there are two specific objectives of the present study. The first objective is to accomplish quantitative analysis to measure spatial and temporal change of land surface temperature of Lahore at town level for the year 1990 and 2015, using Landsat 5 (band 6) and Landsat 8 (band 10 and 11) thermal infrared data. The second objective is to make town wise LST map of Lahore for the year 1990 and 2015 using GIS and remote sensing techniques.

1.1. Study Area

The area selected for this study, Lahore, shown in Figure 1 is the capital city of punjab provice and second largest metroplitan city of Pakistan in term of population [25]. According to the provisional census report of 2017, Lahore population is about 11 million [26] and whole of the district Lahoreis declared an urbanized area [26]. Geographically the extent of Lahore is ranging from 31°-15' to 31°-43' N latitide and 74°-10' to 74°-39' E logitude (Figure 1) [25]. Lahore is surrounded by Sheikhupura district located in north and west, the two districts are separated by the river Ravi. It has Amritsar, a distrcit of India in the east while in the south, it has Kasur district of Pakistan [25]. Lahore covers an area of 1,772 km^2. The average elevation of district Lahore is about 217 m and characterized by a flate landscape [25]. Administratively, Lahore is divided into nine towns and Cantonment area [27]. Area wise, Iqbal town the largest town of Lahore, covers an area of 476.79km^2, while Shalamar town, the smallest town of Lahore, comprises an area of 26.88km^2 (Figure 1). Moreover, 80 percent of total area of Lahore district is occupied by 3 towns-Wagha town, Nishtar town and Iqbal town, while Shalamar town has the least area of about 15 Km^2 i.e. less than 1% of total area of the district. The area of the remaining five towns i.e. Samanabad town, Ravi town Gulberg town, Data Ganj Bukhsh town and Aziz Bhatti town occupies between 2 to 5 percent of the district area. Lahore has extreme climate with hotest weather in the months of May, June and July [25]. The mean minimum and maximum temperature for these months are 27.3 and 40.4 degree centigrades, respectively. The coldest months of the year are January and February. The minimum and maximum temperature for these months are 7.2 and 21.1degree centigrades, respectively [25].

2. MATERIAL AND METHODS

2.1. Data

Landsat satellite imagery was the primary source of

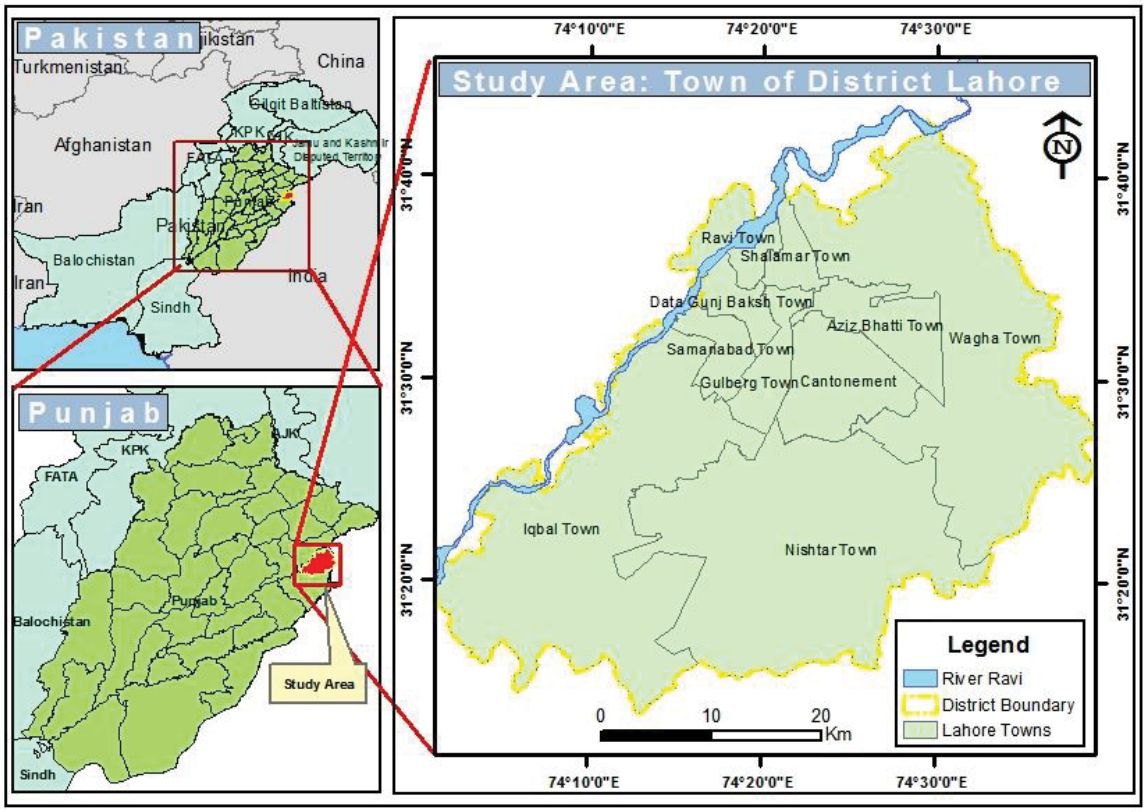

Fig. 1. Location Map of the study area (Lahore)

Table 1. Metadata of Landsat (5, and 8) Satellite Images

Date of Acquisition	Sensor	Bands	Spatial Resolution	Thermal Resolution	Path/Row
16 March 1990	TM	1-5 & 7	30m	-	149/38
		6	-	120m	
21 March 2015	OLI	1-8	30m	-	149/38
		Pan (9)	15m	-	
	TIRs	10 &11	-	100m	

data because of its temporal and spatial resolution and free availability. In total, two Landsat satellite images were collected for this research. Primary data was acquired through multi-source, multi-date and multi-sensor satellite images for the year 1990 and 2015 provided the data source for the Spatio-temporal change analysis of LST of the study area. Urban expansion and consequent change in temperature are assessed through Landsat 5/ TM, and Landsat 8/OLI_TIRs images for the year 1990 and 2015 respectively. These Landsat images were acquired and downloaded from U.S. Geological Survey database and from the site of http://landsat.usgs.gov/, according to the suitability and availability due to cloud cover (the acceptable cloud cover should not be more than 10%). The specifications and details of the acquired Landsat imagery are presented in Table 1. Global Land Cover Facility (GLCF) helps in understanding the environmental system deeply providing earth science data and its products. Satellite Remote Sensing (SRS) is, certainly, the most effective tool of monitoring, detection and estimation of temporal variation of temperature [28, 29].

2.2. Methodology

The overall research methodology of the present study is shown in Figure 2. Several studies have been accomplished on the relative hotness or "UHI effects" of metropolises to assess the air temperature using metrological data. Traditional

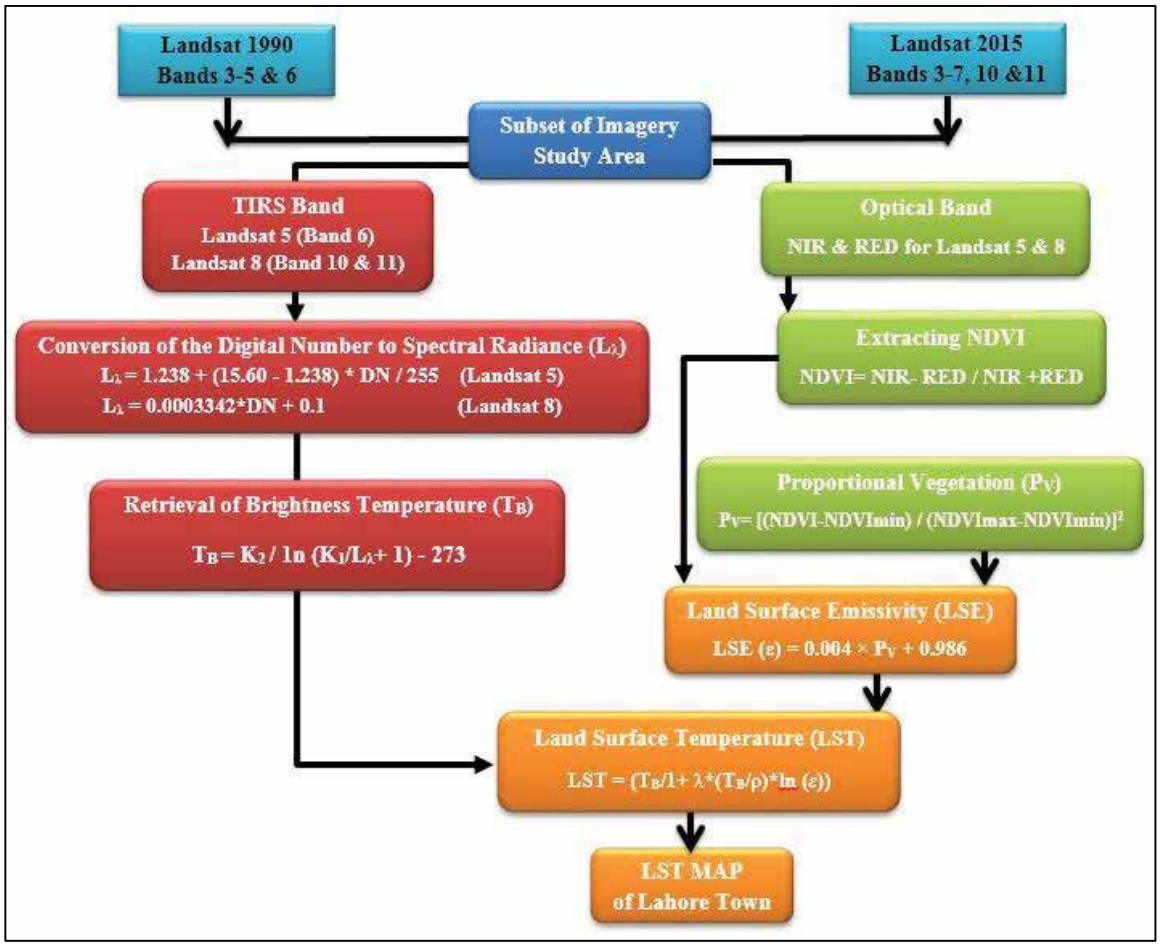

Fig. 2. Overall Methodology and Process of Land Surface Temperature Retrieval

techniques of obtaining data on temperature comprise direct observations using meteorological weather observatory. These measurements with high temporal resolution through weather observatory are expensive, time consuming and problematic for spatial interpolation as they have local and point coverage. Satellite sensors are capable of providing quantitative physical data at high temporal and spatial resolutions. A range of algorithms [30] has been established to estimate surface temperature from Landsat satellite 5/TM, 7/ETM+ and 8/TIRS imagery, such as single-channel method, mono-window algorithm [31] and radiative transfer method [32]. In the present study, the radiative transfer method is utilized to assess the spatiotemporal change in land surface temperature of Lahore. TIRS band 6 of Landsat 5/TM and TIRS band 10 and 11 of Landsat 8 were processed to retrieve the LST. Optical bands of Landsat-5 and 8 were analyzed to derive NDVI values to calculate land surface emissivity value to retrieve LST accurately. The detailed process and steps of retrieval of LST [33-36] are shown in Figure 2.

3. RESULTS AND DISCUSSION

The outcomes of this study reveal that the city of Lahore over the last few decades has experienced a rapid population and urban growth. The expansion of built-up areas in Lahore city has influenced the local climate. The urban climate of Lahore is affected not only by factors of global climate change in the South Asian region but indigenous factors also. The emission of CO_2 in particular, and greenhouse gases in general, contribute towards urban warming in Lahore. The significant variation in temperature trends of Lahore shows increase in temperature during various years. Moreover, land surface temperature is also progressively rising in Lahore. One of the leading causes is reduction in the vegetation and green area in the city. Lahore is undergoing rapid expansion of urban areas and it has caused formation of UHI. The UHI phenomenon

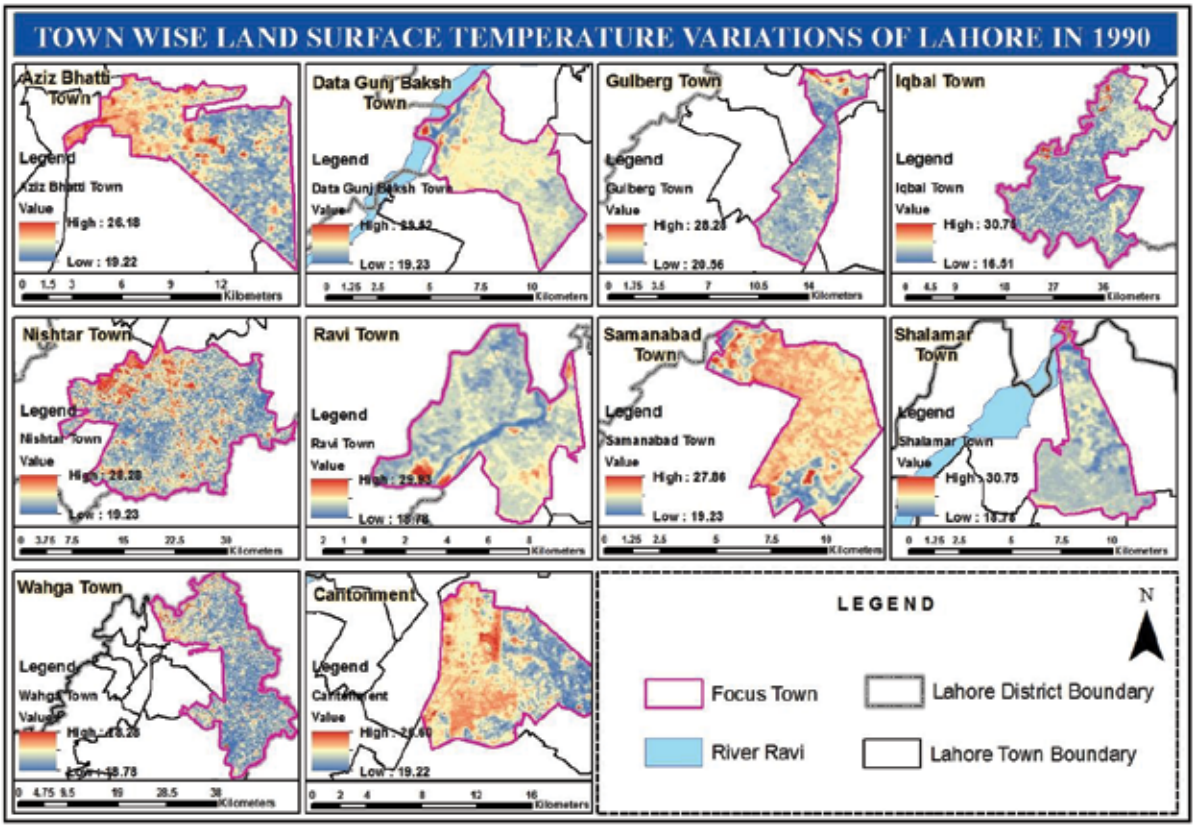

Fig. 3. Town wise comparison of land surface temperature of Lahore in 1990

requires the comprehensive analysis of LST spatial variations in order to investigate its mechanism and locate possible solution. Urban heat island effect in Lahore can be compared with the effects observed in the major cities on the globe like London [37], Beijing [38], Tokyo [39], Delhi [40] and Shanghai [41] and the contrast calls for modification in action plans to mitigate UHI effects.

The town wise comparative study of land surface temperature for the year 1990 and 2015 reflects the higher temperature with the extension of development going-on in the peri-urban regions. Some of the hot spots in the entire study region boast heat islands effects. The town wise LST mapof 1990, shows that high temperature areas were Shalamar town, Gulberg town, Data Ganj Baksh, Ravi, Nishtar and Iqbal town, as given in Figure 3. The mean LST variation between towns was 24.77°C to 23.63°C (Figure 5). Whereas, town wise LST map of March 1990, as shown in Figure 3, exhibits that low land surface temperature areas were Wagha town, Samanabad town, Aziz Bhatti town and Cantonment of Lahore. The mean land surface temperature variation of these towns was 22.71°C to 23.53°C (Figure 5).

For comparison, LST was also assessed for March 2015, as shown in Figure 4. According to the estimation, 1.98°C LST has increased in last 25 years. According to the town wise LST map of 2015, high temperature areas were Gulbarg town, Wahga town and Cantonment as shown in Figure 4. It is observed as per Figure 4 that Gulbarg town, Wahga town, Ravi town, Nishtar town, Iqbal town, Shalamar town and Cantonment were warmer in the year March 2015 than the year March 1990. LST observed in these towns ranged from 25.17°C to 27.85°C (Figure. 5). It is worth mentioning that in the area of Aziz Bhatti town, Nishtar town and Wagha town, there were no urbanization and development. Therefore the lower temperature was experienced in the year 1990, it ranged from 22.71°C to 23.76°C. However the expansion and urbanization of Lahore in these areas increased temperature in 2015, it ranged from 25.41°C to 26.14°C as compared to 1990 (Figure 5).

In the conclusion of the present research, the LST variations are examined and it is showed that there is a significant change in the land use

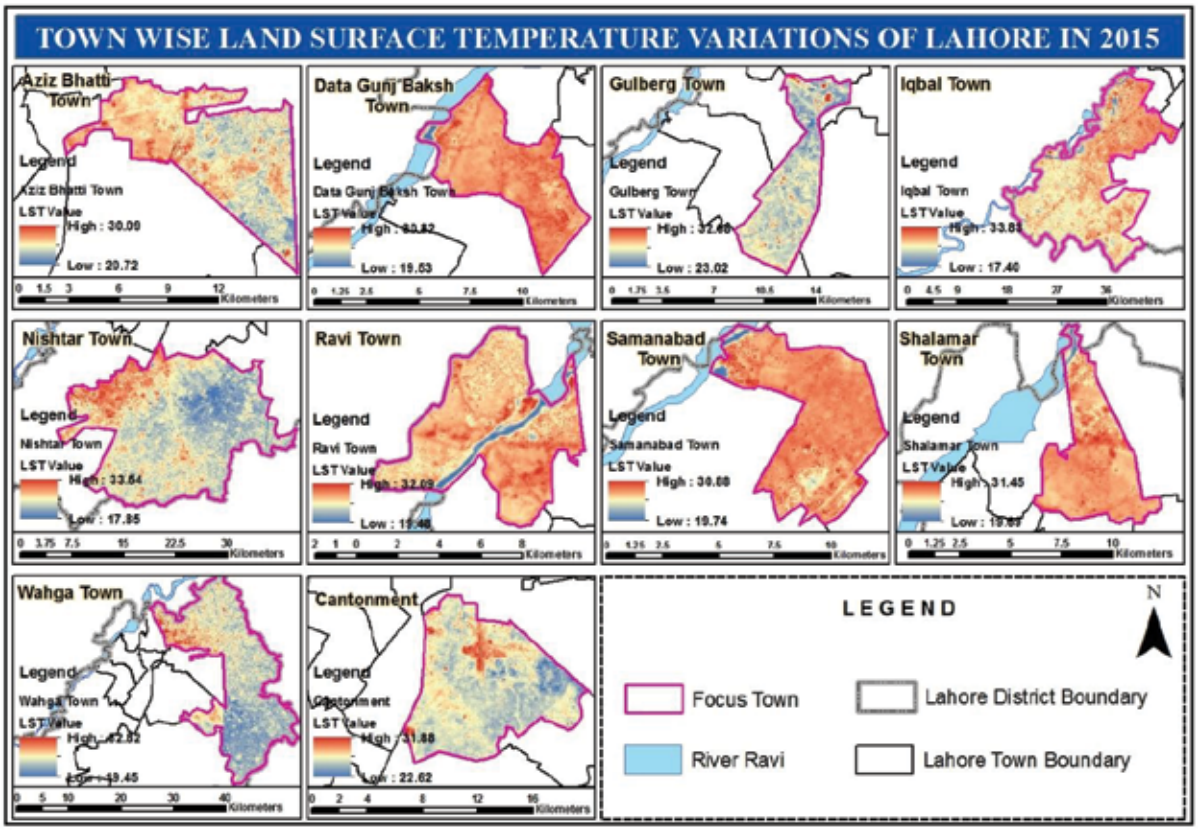

Fig. 4. Town wise comparison of land surface temperature of Lahore in 2015

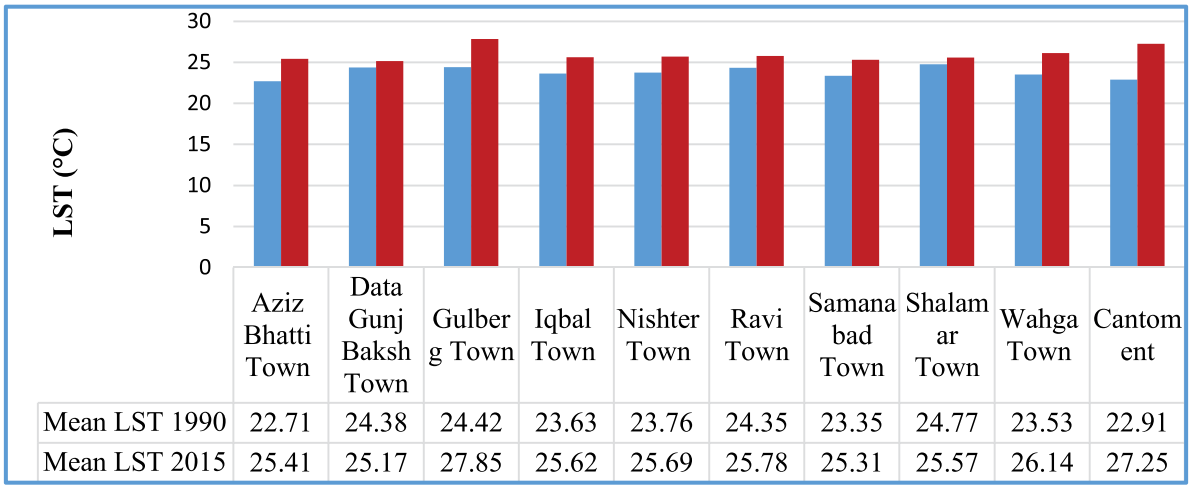

	Aziz Bhatti Town	Data Gunj Baksh Town	Gulberg Town	Iqbal Town	Nishter Town	Ravi Town	Samanabad Town	Shalamar Town	Wahga Town	Cantonment
Mean LST 1990	22.71	24.38	24.42	23.63	23.76	24.35	23.35	24.77	23.53	22.91
Mean LST 2015	25.41	25.17	27.85	25.62	25.69	25.78	25.31	25.57	26.14	27.25

Fig. 5. Town wise trends of land surface temperature of Lahore in 1990 and 2015

in terms of temperature comparisons as displayed in Figure 3 and 4. The reduction of the diversity of species and damage to the eco-system can be attributed to the conversion of natural vegetation and consumption of the cultivated land into built-up area. The built-up areas comprise buildings, pavements, parking lots, roads and respective infrastructure. All these building materials and concrete contribute towards the increase in land surface temperature of Lahore. In built up land, the highest temperature is recorded, followed closely by the vacant land, while the temperature is less

in the areas with water bodies and vegetation as shown in Figure 3 and 4. Similarly, transportation and the combustion of the vehicles add to more air pollution, creating health issues and contributing towards smog problem. The growing number of industries in Lahore has also been a contributing factor in increasing land surface temperature. The process of intensification of land surface temperature of Lahore is gradual, but persistent. One of the major issues in intensification is the reduction in green area in the city. It is significant to note that the consumption of the cultivated land and green spaces has been transformed into built-up areas and impervious surfaces, resulting in increased temperature in Lahore. The assessment of environmental conditions and measures for the policy making for the protection of the environment can be carried out by considering the above mentioned factors.

4. CONCLUSION

The study has shown the usefulness of GIS techniques and remote sensing data in assessing spatiotemporal LST variation in different towns of Lahore between 1990 and 2015. The land surface temperature of Lahore is increasing gradually as a consequence of massive land use changes taking place due to urban expansion. The study also confirmed that the urban development had increased LST in study area by 1.98°C within 25 years. The expansion of built-up areas in Lahore has influenced the local climate. In most of the densely populated and industrial areas of Lahore has high temperature is being experienced. It is significant to note that the cultivated land and green spaces had been transformed into built-up areas and eventually in impervious surfaces, resulting in increase in temperature of Lahore. One of the leading causes is reduction in the agricultural land and greenarea in the city. Finally, the combination of RS and GIS techniques has demonstrated that it is an effective and efficient methodology for analyzing and monitoring patterns of land use change and its effect on land surface temperature. Moreover, the present research shows that the integration of proportionate urban built-up area and greenery spaces can provide a significant measure to reduce urban heat island effect in Lahore. The conclusions drawn from the study signify that the development and the maintenance of green spaces are critical in sustainable urban environment and reduction of adverse effects of increased LST on the urban dwellers. These measures can reduce the urban warming and related effects of the climate change.

5. REFERENCES

1. Fu, P. & Q. Weng. A time series analysis of urbanization induced land use and land cover change and its impact on land surface temperature with Landsat imagery. *Remote Sensing of Environment*175:205-214 (2016).
2. Liu, X., B. H. Tang & Z. L. Li. Evaluation of Three Parametric Models for Estimating Directional Thermal Radiation from Simulation, Airborne, and Satellite Data. *Remote Sensing* 10(420): 1-18 (2018).
3. Li, Z. L., B. H.Tang, H.Wu, H. Ren, G. Yan, Z.Wan & J. A. Sobrino.Satellite-derived land surface temperature: Current status and perspectives. *Remote Sensing of Environment*131: 14-37 (2013).
4. Chatterjee, R., N.Singh, S.Thapa, D. Sharma & D. Kumar. Retrieval of land surface temperature (LST) from Landsat TM6 and TIRS data by single channel radiative transfer algorithm using satellite and ground-based inputs. *International Journal of Applied Earth Observation and Geoinformation*58: 264-277 (2017).
5. Chen, Y., S. B. Duan, H. Ren, J. Labed & Z. L. Li.Algorithm development for land surface temperature retrieval: Application to Chinese Gaofen-5 Data. *Remote Sensing* 9: 161 (2017).
6. Manzo-Delgado, L., R. Aguirre-Gómez & R. Alvarez.Multitemporal analysis of land surface temperature using NOAA-AVHRR: preliminary relationships between climatic anomalies and forest fires. *International Journal of Remote Sensing*25: 4417-4424 (2004).
7. Jin, M., R. Dickinson & A. Vogelmann. A comparison of CCM2–BATS skin temperature and surface-air temperature with satellite and surface observations. *Journal of Climate*10: 1505-1524 (1997).
8. Xu, Y., Y. Shen & Z. Wu. Spatial and temporal variations of land surface temperature over the Tibetan Plateau based on harmonic analysis. *Mountain Research and Development*33: 85-95 (2013).
9. Kumar, K. S., P. U. Bhaskar & Padmakumari, K. Estimation of land surface temperature to study urban heat island effect using Landsat ETM+ image. *International journal of Engineering Science and technology*4: 771-778 (2012).
10. Gabler, R. E., J. F.Petersen, L. Trapasso & D. Sack. *Physical geography*. Nelson Education, (2008).
11. Voogt, J. A. & T. R. Oke. Thermal remote sensing of

urban climates. *Remote sensing of environment*86: 370-384 (2003).
12. Howard, L. *The Climate of London: deduced from Meteorological observations, made at different places in the neighborhood of the metropolis*. Vol. 1 (W. Phillips, sold also by J. and A. Arch), (1818).
13. Harwood IV, J. W. *Delineation and GIS Mapping of Urban Heat Islands Using Landsat TM Imagery*, Kent State University, (2008).
14. James, M. & C. Mundia. Dynamism of land use changes on surface temperature in Kenya: a case study of Nairobi City. *International Journal of Science and Research*3: 38-41 (2014).
15. Kern, K. & G. Alber. Governing climate change in cities: modes of urban climate governance in multi-level systems. (2008).
16. Zhou, W., G. Huang & M. L. Cadenasso. Does spatial configuration matter? Understanding the effects of land cover pattern on land surface temperature in urban landscapes. *Landscape and urban planning*102: 54-63 (2011).
17. Sun, Q., J. Tan & Y. Xu. An ERDAS image processing method for retrieving LST and describing urban heat evolution: a case study in the Pearl River Delta Region in South China. *Environmental Earth Sciences*59: 1047-1055 (2010).
18. Guillevic, P., R. Koster, M. Suarez, L. Bounoua, G. Collatz, S. Los & S. Mahanama.Influence of the Interannual variability of vegetation on the surface energy balance—A global sensitivity study. *Journal of Hydrometeorology* 3: 617-629 (2002).
19. Meng, C., Z. L.Li., X.Zhan, J. Shi & C. Liu. Land surface temperature data assimilation and its impact on evapotranspiration estimates from the Common Land Model. *Water Resources Research*45: (2009).
20. Akinbode, O., A. Eludoyin & O. Fashae. Temperature and relative humidity distributions in a medium-size administrative town in southwest Nigeria. *Journal of environmental management*87: 95-105 (2008).
21. Akhoondzadeh, M. & M. Saradjian. Comparison of land surface temperature mapping using MODIS and ASTER images in semi-arid area. *The International Archives of the Photogrammetry, Remote Sensing and Spatial Information Sciences*37: 873-876 (2008).
22. Alavipanah, S., C. B. Komaki, R. M. Karimpour, M. Sarajian, F. G. R. Savaghebi & E. Moghimi. Land surface temperature in the Yardang region of Lut Desert (Iran) based on field measurements and Landsat thermal data.*Journal of Agricultural Science Technology* 9: 287-303(2007).
23. Oluseyi, I. O. & A. J. Olusegun. Managing land use transformation and land surface temperature change in Anyigba Town, Kogi State, Nigeria. *Journal of Geography and Geology* 3: 77-85 (2011).
24. Rajeshwari, A. & N. Mani. Estimation of land surface temperature of Dindigul district using Landsat 8 data. *International Journal of Research in Engineering and Technology*3: 122-126 (2014).
25. GoP. District Census Report of Lahore 1998. *Islamabad: Population Census Organization, Statistics Division. Govt. of Pakistan.* (2000).
26. GoP. Provisional summary results of 6th population and housing census-2017. *Population Census Organization, Statistics Division. Govt. of Pakistan.* (2017).
27. Rana, I. A. &S. S. Bhatti. Lahore, Pakistan–Urbanization challenges and opportunities. *Cities*72: 348-355 (2018).
28. Foody, G. M. Status of land cover classification accuracy assessment. *Remote sensing of environment*80: 185-201 (2002).
29. Alrababah, M. & M. Alhamad. Land use/cover classification of arid and semi-arid Mediterranean landscapes using Landsat ETM. *International journal of remote sensing* 27: 2703-2718 (2006).
30. Avdan, U. & G. Jovanovska. Algorithm for automated mapping of land surface temperature using LANDSAT 8 satellite data. *Journal of Sensors* 2016: 1-18 (2016).
31. Jiménez-Muñoz, J. C. & J. A. Sobrino. A generalized single-channel method for retrieving land surface temperature from remote sensing data. *Journal of Geophysical Research: Atmospheres* 108:1-12 (2003).
32. Qin, Z., Karnieli, A. & P. Berliner. A mono-window algorithm for retrieving land surface temperature from Landsat TM data and its application to the Israel-Egypt border region. *International journal of remote sensing*22: 3719-3746 (2001).
33. Bustos, E. & F. J. Meza. A method to estimate maximum and minimum air temperature using MODIS surface temperature and vegetation data: application to the Maipo Basin, Chile. *Theoretical and Applied Climatology*120: 211-226 (2015).
34. Ding, H. & A. J. Elmore.Spatio-temporal patterns in water surface temperature from Landsat time series data in the Chesapeake Bay, USA. *Remote Sensing of Environment*168: 335-348 (2015).
35. Fu, B. & I. Burgher. Riparian vegetation NDVI dynamics and its relationship with climate, surface water and groundwater. *Journal of Arid Environments*113: 59-68 (2015).
36. Sobrino, J. A., J. C. Jiménez-Muñoz.&L. Paolini. Land surface temperature retrieval from Landsat TM 5. *Remote Sensing of environment*90: 434-440 (2004).
37. Kolokotroni, M., I. Giannitsaris & R. Watkins. The effect of the London urban heat island on building summer cooling demand and night ventilation strategies. *Solar Energy*80: 383-392 (2006).
38. Liu, W., C.Ji, J.Zhong, X. Jiang & Z. Zheng.

Temporal characteristics of the Beijing urban heat island. *Theoretical and Applied Climatology*87: 213-221 (2007).
39. Fujibe, F. Urban warming in Japanese cities and its relation to climate change monitoring. *International Journal of Climatology*31: 162-173 (2011).
40. Mohan, M., Y.Kikegawa, B.Gurjar, S.Bhati & N. R. Kolli. Assessment of urban heat island effect for different land use–land cover from micrometeorological measurements and remote sensing data for megacity Delhi. *Theoretical and applied climatology*112: 647-658 (2013).
41. Chen, L., R. Jiang & W. N. Xiang. Surface heat island in Shanghai and its relationship with urban development from 1989 to 2013. *Advances in Meteorology* 2016:1-15 (2016).

Proceedings of the Pakistan Academy of Sciences:
A. Physical and Computational Sciences 55 (3): 77–84 (2018)

ISSN: 2518-4245 (print), 2518-4253 (online)

Pakistan Academy of Sciences

Research Article

Stringency Criterion for Modality Tests

Rana Muhammad Imran Arshad[1], Farrukh Jamal[2*], Muhammad Akbar Ali Shah[3] Gamze Ozel[4], and Shahina Imran[5]

[1]Department of Statistics Govt., S.E. College, Bahawalpur
[2]Department of Statistics Govt., S.A. Postgraduate. College, Dera Nawab Sahib
[3]Department of Statistics, The Islamia University of Bahawalpur
[4]Department of Statistics, Hacettepe University, Ankara, Turkey
[5]Department of Economics Govt., S. E. College, Bahawalpur

Abstract: Different techniques in the field of multimodality testing have aimed at different goals. In this study, we compare four nonparametric modality tests kernel density estimation test or Silverman Bandwidth test proposed by Silverman [13], Hartigan DIP test proposed by Hartigan and Hartigan [8], proportional mass test by Cavallo and Ringobon [4] and excess mass test by Muller and Sawitzki [12]. The most stringent test is found for different sample sizes 50, 100, 200 when only only μ_2 , μ_2 and σ^2_2 , μ_2 and α are considered period.

Keywords: Multimodality, Modality tests, Stringent test, Nonparametric test, Hypothesis tests, Period

1. INTRODUCTION

A stringency criterion is used to measure the performance of hypothesis tests. This criterion provides a unified view of optimality properties of tests. In most of the situations, size and power of any test are very useful for the comparison of different tests. However, in some situations this approach does not provide a satisfactory conclusion. Assume that there are two tests T_1 and T_2 for comparison of modality. These two tests can be compared on the basis of stringency criteria. For some alternatives,T_1 may be more powerful as compared to T_2 and for some other alternative situations, T_2 test may be more powerful as compared to T_1. To solve this type of problem, a technique has been introduced by Zaman [15] to compare the tests of modality. The approach of Zaman [15] is based on the density function of parametric assumption but this study discusses only non-parametric modality tests. There is no possible way to calculate most stringent test by the approach of likelihood ratio test when null and alternative hypotheses are tested. A modified method of Zaman [15] has been used in this study for estimating more stringent test by taking the minimum value of maximum difference between Maximum Power Approximation (MPA) and the power of different alternatives. Most of the nonparametric modality tests are developed for testing modality. The present study explores the following most popular tests only in univariate case:

(1) Kernel Density Estimation Test or Silverman Bandwidth Test proposed by Silverman [13].
(2) Hartigan Dip Test proposed by Hartigan and Hartigan [8].
(3) Proportional Mass Test by Cavallo and Ringobon [4].
(4) Excess Mass Test by Muller and Sawitzki [12].

Now-a-days these tests are used to measure modality of the distribution. These four tests are very useful measures to test the homogeneity and heterogeneity in the data. Most of the researcher applied these tests in different fields of life especially in economics, Bianchi [1] used modality tests to test the convergence by two nonparametric techniques (a) bootstrap multimodality (b) nonparametric density estimation tests, in a cross-

Received: February 2018; Accepted: September 2018
* Corresponding Author: Farrukh Jamal; drfarrukh1982@gmail.com

section annual per capita GDP at constant US dollar of 119 countries. Cavallo and Ringobon [4] applied different theories of price stickiness having different implications of the distributions of price changes. Chen et al. [2] anticipated a modified likelihood ratio test for homogeneity in the finite mixture models. This criterion has never been used to test modality tests on the basis of stringency criterion. It also estimates the most stringent test. This research measures the modality tests on the basis of stringency for estimating best and worst test.

2. METHODOLOGY

Step-wise procedure for testing modality to compare the four tests under Stringency Criteria;

1. Find out critical values for each test of modality by Monte Carlo simulation technique.
2. The Power curve is drawn for each test of modality by plotting different alternatives along x-axis and Power of that test along y-axis. Let

   $P\left(L_{\pi i}{}^{h}\right)$ is denoted by different alternatives and

   $P\left(L^{*}_{\pi_j}{}^{h}\right)$ is denoted by the Power of test.
3. For the deduction of the Approximated Power Envelope (APE), this study plots the different alternatives along X-axis and the Maximum Power Approximation (MPA) along Y-axis.
4. Short comings have been detected by each test through measuring maximum difference between the Power Curve and Maximum Power Approximation (MPA) and approximated Power Envelope has also been developed with the maximum difference. The short coming of the modality tests is given as

   $$S_C\left(L_{\pi_h}\right)=\left[\text{Max}\left\{P^{*}\left(L_{\pi j}{}^{h}\right)\text{-}P\left(L_{\pi i}{}^{h}\right)\right\}\right],$$

   where $P^{*}\left(L_{\pi j}{}^{h}\right)$ is denoted by MPA and $P\left(L_{\pi i}{}^{h}\right)$ is denoted by Power of different alternatives.
5. The most stringent test is identified by taking the minimum value of maximum differences between Maximum Power Approximation (MPA) and the Power of different alternatives. The function for most stringency test of this research is given as

   $$M_S\left(L_{\pi_h}\right)=\text{Min}\left[\text{Max}\left\{P^{*}\left(L_{\pi j}{}^{h}\right)\text{-}P\left(L_{\pi i}{}^{h}\right)\right\}\right],$$

   where $M_S\left(L_{\pi_h}\right)$ is denoted by most stringent test.
6. Steps 1 to 5 have been repeated for different sample sizes 50, 100, 200 when only μ_2 , μ_2 and σ_2^2 ,μ_2 and α are varying and finally found the most σ stringent test.

3. IDENTIFICATION OF MOST STRINGENT TEST

For identification of most stringent test from each test of modality, first we subtract the power of each test from the Maximum Power Approximation (MPA) then we take the value of maximum of these differences that is called short comings of the tests and finally get the minimum value of that maximum difference at different alternatives and different sample sizes. A test that has minimum short coming is called most stringent test. The "**Max"** is used for the maximum value of the short comings and **"MPA**" is used for the maximum power approximation. All of these results at different alternatives and different sizes are given in the Tables 1 to 9.

The results of sample size 50 has shown the shortcoming of Silverman that has minimum value from those maximum shortcomings. So Silverman test is the most stringent test because of minimum shortcoming. The shortcomings of the four tests at sample size 100 produced the maximum values of these shortcomings and concluded that the minimum value of that maximum is the most stringent test. So Silverman is the most stringent test because of minimum shortcoming. The shortcomings of the four tests at sample size 200 are an estimate then finding the maximum values of these shortcomings and finally concluded that the minimum value of that maximum is the most stringent test. So PM test is the most stringent test because of minimum shortcoming. The shortcomings of the four tests at sample size 50 calculated and found the maximum values of these shortcomings and finally concluded that the minimum value of that maximum is the most stringent test. So Silverman test is the most stringent test because of minimum shortcoming. The shortcomings of the four tests at sample size 100 calculated and found the maximum values of these shortcomings and finally concluded that the minimum value of that maximum is the most stringent test. So Silverman test is also the most

Table 1. Comparison of most stringent test for sample size is 50 and only μ_2 is varying.

Short comings of various test at sample size 50				
MPA	**Hartigan DIP test**	**Silverman test**	**PM test**	**EM test**
11.3	6.25	0	7.3	5.5
44	34.86	0	33	34.8
97.4	67.31	0	87.4	67.6
100	23.8	0	88	26.2
100	3.08	0	81	2.1
100	0.27	0	58	0.1
100	0.02	0	47	0
100	0.01	0	47	0
100	0	0	51	0
Max	67.31	0	88	67.6

Table 2. Comparison of most stringent test for sample size is 100 and only μ_2 is varying.

Short comings of various test at sample size 100				
MPA	**Hartigan DIP test**	**Silverman test**	**PM test**	**EM test**
20	14.61	13	0	15.9
15	9.6	0	7	10.6
24	7.38	0	7	7.3
100	16.69	0	84	16.9
100	0.1	0	90	0.1
100	0	0	84	0
100	0	0	59	0
100	0	0	54	0
100	0	0	37	0
Max	16.69	13	90	16.9

Table 2. Comparison of most stringent test for sample size is 200 and only μ_2 is varying.

Short comings of various test at sample size 200				
MPA	**Hartigan DIP test**	**Silverman test**	**PM test**	**EM test**
98	92.88	86	0	91.9
94	88.98	61	0	90.1
95	74.22	47	0	73.8
100	2.5	0	3	2.5
100	0	0	2	0
100	0	0	9	0
100	0	0	5	0
100	0	0	0	0
100	0	0	0	0
Max	92.88	86	9	91.9

Table 4. Comparison of most stringent test for sample size is 50 when μ_2 and σ^2_2 arevarying.

Short comings of various test at sample size 50				
MPA	**Hartigan DIP test**	**Silverman test**	**PM test**	**EM test**
7	0.96	4	0	2.2
35	29.56	0	24	29.3
78	71.17	0	64	69.6
88	78.94	0	64	77.6
90	75.97	0	59	77
91	73.39	0	56	75.7
96	75.71	0	52	73.7
100	76.43	0	44	73.4
100	73.5	0	42	73.3
Max	78.94	4	64	77.6

Table 5. Comparison of most stringent test for sample size is 100 when μ_2 and σ^2_2 arevarying.

Short comings of various test at sample size 100				
MPA	**Hartigan DIP test**	**Silverman test**	**PM test**	**EM test**
15.6	9.91	0	6.3	10.5
57.4	46.07	0	55.7	48.5
98.9	31.25	0	97.9	34.4
100	0.14	0	100	0.1
100	0	0	100	0
100	0	0	99.9	0
100	0	0	99.7	0
100	0	0	99.4	0
100	0	0	99.3	0
Max	46.07	0	100	48.5

Table 6. Comparison of most stringent test for sample size is 200 when μ_2 and σ^2_2 arevarying.

Short comings of various test at sample size 200				
MPA	**Hartigan DIP test**	**Silverman test**	**PM test**	**EM test**
17	11.43	0	6.9	10.8
67	62.98	0	63.21	63
91	86.37	0	81.24	85.2
100	89.61	0	95.28	88.6
100	81.04	0	97.27	81.7
100	70.76	0	90.33	70.6
100	59.56	0	73.01	60.6
100	51.84	0	54.54	50
100	44.02	0	47.46	49.1
Max	89.61	0	97.27	88.6

Table 7. Comparison of Most Stringent Test for sample size is 50, when μ_2 and α are varying.

Short comings of various test at sample size 50				
MPA	**Hartigan DIP test**	**Silverman test**	**PM test**	**EM test**
6.5	1.75	3.5	3.5	0
11	5.26	0	9	5.5
21	6.28	0	16	5.9
67	5.44	0	54	2
95.6	0.2	6.6	62.6	0
99.8	0	4.8	61.8	0.1
99.9	0	2.9	47.9	0.2
100	0.85	1	54	0
100	0.06	0	73	0.3
Max	6.28	6.6	73	5.9

Table 8. Comparison of Most Stringent Test for sample size is 100, when μ_2 and α are varying.

Short comings of various test at sample size 100				
MPA	**Hartigan DIP test**	**Silverman test**	**PM test**	**EM test**
21	15.88	14	0	16.9
15	9.98	0	11	10.6
24	3.22	0	19	7.3
100	2.5	0	94	16.9
100	0	0	87	0.1
100	0	0	78	0
100	0	0	66	0
100	0	0	58	0
100	0	0	87	0
Max	15.88	14	94	16.9

Table 9. Comparison of Most Stringent Test for sample size is 200, when μ_2 and α are varying.

Short comings of various test at sample size 200				
MPA	**Hartigan DIP test**	**Silverman test**	**PM test**	**EM test**
99.6667	94.2767	87.6667	0	93.5667
94	88.6	61	0	90.1
87	70.38	39	0	65.8
100	16.69	0	6	2.5
100	0.1	0	2.6667	0
100	0	0	3	0
100	0	0	2	0
100	0	0	0.6667	0
100	0	0	0.6667	0
Max	94.2767	87.6667	6	93.5667

stringent test because of minimum shortcoming. The shortcomings of the four tests at sample size 200 calculates and finds the maximum values of these shortcomings and finally concludes that the minimum value of that maximum is the most stringent test. So Silverman test is the most stringent test because of minimum shortcoming. These short- comings of the four tests at sample size 50 calculated and estimated the maximum values of these shortcomings and finally concluded that the minimum value of that maximum is the most stringent test. In this table the shortcomings of Hartigan Dip test, Excess mass Test and Silverman test are looking very close, but Excess Mass test is the most stringent test because of minimum shortcoming. It may occur due to random fluctuation of the density. The short- comings of the four tests at sample size 100 are estimated and found the maximum values of these shortcomings and finally concluded that the minimum value of that maximum is the most stringent test. The shortcomings of Hartigan Dip test, Excess Mass Test and Silverman test are looking very close but Silverman test has the minimum shortcoming, so it is the most stringent test. These shortcomings of the four tests at sample size 200 also calculated and then found the maximum values of these shortcomings and finally conclude that the minimum value of that maximum is the most stringent test. The shortcomings of PM test have the minimum shortcoming, so it is the most stringent test.

4. CONCLUSION

It is concluded from Tables 1 to 3, when only μ_2 is varying the shortcomings of the four tests at sample size 50 and 100, the Silverman is the most stringent test because of minimum short coming. But the shortcomings of PM test for all four tests at sample size 200 are least, so the PM test is most stringent due to large bumps and large sample size. From Tables 4 to 6 the shortcomings of the four tests at sample sizes 50,100 and 200, when are varying, it is concluded that the Silverman test is the most stringent test because of minimum short coming and small bumps. From Tables 7 to 9 when μ_2 and σ^2_2 are varying at sample size 50 , the short comings of Hartigan DIP test, Excess Mass Test and Silverman test are looking very close but Excess Mass test is the most stringent test because of minimum shortcoming. It may occur due to random fluctuation of the density. The shortcomings of the four tests at sample size 100 Silverman test is looking the most stringent test due to large bumps. At sample size 200 it is found that the shortcomings of PM test has the minimum value, so it is the most stringent test due to large sample size and large bumps. Finally it is concluded that the Silverman test is the most stringent test as compared to the other tests except in the large samples and large bumps.

5. ACKNOWLEDGMENTS

The authors would like to thank the Editor-in-Chief, and the referees for constructive comments which greatly improved the paper.

6. REFERENCES

1 Bianchi. Testing for convergence: evidence from nonparametric multimodality tests. *Journal of Applied Econometrics* 12 (4): 393-409 (1997).

2 Chen, A., Chen, J. & Kalbfleisch, J. A modified likelihood ratio test for homogeneity in finite mixture models. *Journal of the Royal Statistical Society: Series B* 63: 19–29(2001).

3 Cheng. & Hall . Calibrating the Excess Mass and Hartigan Dip Test Tests of Modality. *Journal of the Royal Statistical Society, Series B* 60: 579-590 (1998).

4 Cavallo, A. & Rigobon, R. The Distribution of the size of price changes, *NBER Working Paper No. 16760*, 1-40(1910).

5 Fisher. &Marron. Mode testing via the excess mass estimate. *Biometrica* 88: 499–517 (2001).

6 Hall. & York. On the calibration of Silverman's test for multimodality. *Statist.Sinica*11: 515–536 (2001).

7 Hartigan . Algorithm AS217: Computation of the Hartigan Dip Test statistic to test for unimodality. *Journal of Applied Statistics*34: 320–325(1985).

8 Hartigan. &Hartigan. The Hartigan Dip Test of unimodality. *The Annals of Statistics*13(1): 70-84 (1985).

9 Henderson . Modes, Weighted Modes and Calibrated Modes: Evidence of Clustering Using Modality *Tests. Journal of Applied Econometrics forthcoming* (2006).

10 Hall. & York. On the Calibration of Silverman's Test for Multimodality. *Statistica Sinica* 11: 515-536 (2001).

11 Hall & OOI. Attributing a Probability to the Shape of a Probability Density. *The Annals of Statistics* 32 (5): 2098-2123 (2004).

12 Mueller & Sawitzki. Excess mass estimates and tests for multimodality.*The Journal of the Acoustical*

*Society of America*86: 738 -746(1991).

13 Silverman. *Some properties of a test for multimodality based on kernel density estimates in J. F. C. Kingman and G. E. H. Reuter (eds), Probability, Statistics, and Analysis,* Cambridge University Press, Cambridge (1983).

14 Silverman. *Density Estimation for Statistics and Data Analysis, Monographs on Statistics and Applied Probability.* 26, Chapman and Hall, London (1986).

15 Zaman A. *Statistical Foundations for Econometrics Techniques*. Academic Press, London (1996).

Proceedings of the Pakistan Academy of Sciences
Instructions for Authors

Aims and Scope: *Proceedings of the Pakistan Academy of Sciences* is official journal of the Academy, published quarterly, in English. This open access journal publishes research papers in *Engineering Sciences & Technology, Life Sciences, Medical Sciences, and Physical Sciences*. State-of-the-art reviews (~20 pages, supported by recent references) summarizing R&D in a particular area of science, especially in the context of Pakistan, and suggesting further R&D are also considered. Manuscripts undergo double-blind review. Authors are not required to be Fellows or Members of the *Pakistan Academy of Sciences* or citizens of Pakistan.

Manuscript Format

Manuscript may contain **Abstract, Keywords, INTRODUCTION, MATERIALS AND METHODS, RESULTS, DISCUSSION (or RESULTS AND DISCUSSION), CONCLUSIONS, ACKNOWLEDGEMENTS and REFERENCES** *and any other information that the author(s) may consider necessary.* The Manuscript sections must be numbered, i.e., **1. INTRODUCTION, 2. MATERIALS AND METHODS,** and so on.

Manuscripts, in *Times New Roman*, 1.5-spaced (but single-space the Tables), with line numbering and one-inch margins on all sides on A-4 size paper, should not exceed 20 pages including Tables and Figures. Number manuscript pages throughout. The text (in **Font Size 11,** except for the sections mentioned in **Font Size 10)** must be typed in a single column across the paper width. All Tables and Figures must be placed after the text, i.e., after REFERENCES section.

(a) **Title** of the article **(**Capitalize initial letter of each main word; font size 16; **bold**), max 160 characters (no abbreviations or acronyms), depicting article's contents; (b) Author' first name, middle initial and last name (font size 12, **bold**), and professional affiliation (i.e., each author's Department, Institution, Mailing address and Email; but no position titles) (font size 12); (c) Indicate the corresponding author with *; (d) **Short running title**, max 50 characters (font size 10).The **next Page** should start with **Title** of the Article, followed by entire manuscript. **Headings and Subheadings** (font size 11): All flush left

LEVEL-1: **ALL CAPITAL LETTERS; bold**

Level-2: **Capitalize each main word; bold**

Level-3: Capitalize each main word; Bold, Italic

Level-4: *Run-in head*; *Italics*, *in the normal paragraph position. Capitalize the initial word only and end in a colon (i.e., :)*

Abstract (font size 10; max 250 words)**:** Must be self-explanatory**,** stating rationale, objective(s), methodology, main results and conclusions of the study. Abbreviations, if used, must be defined on first mention in the Abstract as well as in the main text. Abstract of review articles may have variable format.

Keywords (font size 10)**:** Three to eight keywords**,** depicting the article.

INTRODUCTION: Provide a clear and concise statement of the problem, citing relevant recent literature, and objectives of the investigation.

MATERIALS AND METHODS: Provide an adequate account of the procedures or experimental details, including statistical tests (if any), in a concise manner but sufficient enough to replicate the study.

RESULTS: Be clear and concise with the help of appropriate Tables, Figures and other illustrations. Data should not be repeated in Tables and Figures, but must be supported with statistics.

DISCUSSION: Provide interpretation of the RESULTS in the light of previous relevant studies, citing published references.

ACKNOWLEDGEMENTS (font size 10)**:** In a brief statement, acknowledge financial support and other assistance.

REFERENCES (font size 10)**:** Cite references in the text **by number only** in **square brackets**, e.g. "Brown et al [2] reported ..." or "... as previously described [3, 6–8]", and list them in REFERENCES section, in the order of citation in the text, Tables and Figures (not alphabetically). Only published (and accepted for publication) journal articles, books, and book chapters qualify for REFERENCES.

List of REFERENCES must be prepared as under:

a. **Journal Articles** *(Name of journals must be stated in full)*

1. Golding, I. Real time kinetics of gene activity in individual bacteria. *Cell* 123**:** 1025–1036 (2005).
2. Bialek, W. & S. Setayeshgar. Cooperative sensitivity and noise in biochemical signaling. *Physical Review Letters* 100**:** 258–263 (2008).
3. Kay, R.R. & C.R.L. Thompson. Forming patterns in development without morphogen gradients: differentiation and sorting. *Cold Spring Harbor Perspectives in Biology* 1: doi: 10.1101/cshperspect.a001503 (2009).

b. **Books**

4. Luellen, W.R. *Fine-Tuning Your Writing*. Wise Owl Publishing Company, Madison, WI, USA (2001).
5. Alon, U. & D.N. Wegner (Ed.). *An Introduction to Systems Biology: Design Principles of Biological Circuits*. Chapman & Hall/CRC, Boca Raton, FL, USA (2006).

c. **Book Chapters**

6. Sarnthein, M.S. & J.D. Stanford. Basal sauropodomorpha: historical and recent phylogenetic developments. In: *The Northern North Atlantic: A Changing Environment.* Schafer, P.R. & W. Schluter (Ed.), Springer, Berlin, Germany, p. 365–410 (2000).
7. Smolen, J.E. & L.A. Boxer. Functions of Europhiles. In: *Hematology, 4th ed*. Williams, W.J., E. Butler & M.A. Litchman (Ed.), McGraw Hill, New York, USA, p. 103–101 (1991).

Tables, with concise but self-explanatory headings must be numbered according to the order of citation (like **Table 1**, **Table 2**). Round off data to the nearest three significant digits. Provide essential explanatory footnotes, with superscript letters or symbols keyed to the data. Do not use vertical or horizontal lines, except for separating column heads from the data and at end of the Table.

Figures may be printed in two sizes: column width of 8.0 cm or page width of 16.5 cm; number them as **Fig. 1**, **Fig. 2**, … in the order of citation in the text. Captions to Figures must be concise but self-explanatory. Laser printed line drawings are acceptable. Do not use lettering smaller than 9 points or unnecessarily large. Photographs must be of high quality. A scale bar should be provided on all photomicrographs.

Declaration: Provide a declaration that: (i) the results are original; (ii) the same material is neither published nor under consideration elsewhere; (iii) approval of all authors has been obtained; and, (iv) in case the article is accepted for publication, its copyright will be assigned to *Pakistan Academy of Sciences*. Authors must obtain permission to reproduce, where needed, copyrighted material from other sources and ensure that no copyrights are infringed upon.

Reviewers: Authors may suggest four relevant reviewers, two local and two from scientifically advanced countries.

Manuscripts must be submitted in Microsoft Word (.doc or .docx format; **pdf** files not acceptable). Figures can be submitted in Word format, TIFF, GIF, JPEG, EPS, PPT.

Manuscripts may be submitted as email attachment at the following email address. In case of any difficulty while submitting your manuscript, please get in touch with:

Editor-in-Chief
Pakistan Academy of Sciences
3-Constitution Avenue, G-5/2, Islamabad, Pakistan
Email: editor@paspk.org
Tel: +92-51-920 7140
Website: www.paspk.org

PROCEEDINGS
OF THE PAKISTAN ACADEMY OF SCIENCES:
A. Physical and Computational Sciences

CONTENTS

Volume 55, No. 3, September 2018 **Page**

Case Study

Research Articles

PAKISTAN ACADEMY OF SCIENCES, ISLAMABAD, PAKISTAN

HEC Recognized, Category Y; PM&DC Recognized

Website: www.paspk.org